/SEMI-ANALYTICAL EVALUATION OF THE SCATTERING SOURCE TERM IN DISCRETE-ORDINATES TRANSPORT CALCULATIONS/

by

JOEL MARK RISNER

B.S., Kansas State University, 1983

A MASTER'S THESIS

submitted in partial fulfillment of the

requirements for the degree

MASTER OF SCIENCE

Department of Nuclear Engineering

KANSAS STATE UNIVERSITY
Manhattan, Kansas

1986

Approved by:

Major Professor

TABLE OF CONTENTS

TABLE OF CONTENTS (Continued)

LIST OF FIGURES

LIST OF FIGURES (Continued)

LIST OF TABLES

1. INTRODUCTION

One of the most important areas of study in engineering and physics is that branch of statistical mechanics known as transport theory. A wide variety of physical phenomena involve particle transport processes. The radiant energy transfer in a stellar atmosphere, the number of particles emerging from a radiation shield, and the power distribution in a nuclear reactor are all governed by the distribution of particles which interact stochastically with the atoms of the host medium. The determination of such distributions is the central problem of transport theory.[1-3]

The solution of this problem becomes much more difficult when the scattering processes involved are anisotropic. Anisotropic scattering is encountered in a wide range of transport phenomena such as Compton scattering of gamma photons,[4] light transmission through clouds and hazes,[5,6] multigroup neutron transport with fine-energy-group structures,[7] and elastic electron-nuclear scattering.[8]

Scattering anisotropy can result from several factors. Consider, for example, the elastic scattering of neutrons. When viewed in the center-of-mass coordinate system, such scattering is isotropic for low-energy neutrons. At neutron energies above $\sim$0.1 MeV, scattering generally becomes anisotropic, with the scattering cross section usually being forward peaked.[9]

Scattering anisotropy is also induced by the transition from the center-of-mass coordinate system to the laboratory coordinate system, which is the frame of reference most often used in transport calculations. Scattering which is isotropic in the center-of-mass

system becomes forward peaked in the lab system. While this effect is not significant for heavy nuclei (in which case there is little difference between the two systems), it is very important for light nuclei.[9]

Use of the multigroup approximation of the energy variable in the transport equation introduces group-to-group scattering (or transfer) cross sections which are often nonzero over only a limited range of scattering angles. This limited angular support is a direct consequence of the constraints for energy and momentum conservation.[7] Such anisotropy becomes more severe as finer multigroup structures are used.

The traditional method of treating anisotropic scattering in transport calculations has been to expand the angular dependence of the scattering cross section in a finite series of Legendre polynomials. Such an expansion is mathematically convenient to use because the Legendre polynomials obey an "addition theorem"[2] which allows significant analytical simplification of the scattering source term in the transport equation. This method is accurate if a sufficiently high order expansion is used. However, a highly anisotropic cross section often requires a very high order expansion to represent the cross section accurately. Use of a prematurely truncated Legendre expansion often introduces spurious oscillations in the approximated cross section. These oscillations in turn can produce unrealistic fluctuations in the calculated angular fluxes, and may, in fact, even lead to estimates of negative angular fluxes.[10]

The failure of the Legendre expansion method to produce physically realistic angular fluxes occurs only in problems which are characterized

by highly anisotropic angular fluxes as well as by highly anisotropic scattering. Although the degree of anisotropy in the angular flux is seldom known *a priori*, problems with anisotropic sources and vacuum boundary conditions as well as anisotropic scattering can be expected to yield anisotropic flux distributions, especially near the sources and boundaries.[23]

To avoid the problem of negative fluxes, many alternative methods of cross section approximation have been proposed. One of the simplest remedies, which is known as the transport approximation, is to replace an anisotropic scattering cross section that is highly peaked in the forward direction by an isotropic component and a forward-scattered component.[11] The forward-scattered component is most simply represented by a delta function. Although this transport approximation can provide good accuracy for problems which are characterized by only a small degree of anisotropy,[12] it often gives poor results for highly anisotropic problems.[11,12]

Razani[13] proposed a modified transport approximation in which singly-scattered particles are accounted for exactly and the effect of higher-order scattering is treated by the transport approximation. He found that, for radiation transport through homogeneous slabs, the error in the transport approximation was considerably reduced by using this modified transport approximation. Lathrop[12] examined an extended transport approximation, obtained by adjusting the coefficients of a P_1 (i.e., first order Legendre) approximation. He applied this method to several neutron transport problems and found it to be more accurate than

the delta-function transport approximation, but not as accurate as higher order standard Legendre expansions. Bell *et al.*[14] examined the extended transport approximation for higher order Legendre expansions and concluded that it was an effective method for neutron transport problems.

Attia and Harms[15] used a partial-range Legendre polynomial expansion of the scattering cross section. While this representation yields more accurate cross section fits than a standard full-range expansion, it does not lend itself readily to use in discrete-ordinates transport codes. Pearlstein[16] proposed an expansion of the scattering cross section in terms containing quadratic Bessel functions. He found that such an expansion accurately modeled scattering cross sections for a variety of elements with fewer terms than a standard Legendre expansion required. However, the use of quadratic Bessel functions is mathematically inconvenient, and it has not been established whether such an expansion would be feasible in discrete-ordinates calculations.

Carter and Forest[17] utilized a step function representation of the scattering cross section in Monte Carlo transport calculations. Takeuchi[18] assumed a step function approximation of the scattering cross section with respect to the lethargy mesh, and a step function approximation of the angular flux with respect to both the angular mesh and the lethargy mesh. These approximations were utilized in the PALLAS computer code, which numerically solves the integral form of the transport equation.

A more direct approach to avoid the use of Legendre polynomial cross section expansions is to use a transfer matrix whose elements are

the exact cross sections for transfer from one discrete direction to another. While this possibility had been considered in the 1960's,[19] it was not fully developed at that time due to the associated requirement of large computer memories. Odom,[20] who finally implemented this technique in plane-geometry, discrete-ordinates neutron transport calculations, referred to it as the "exact kernel" method. He found that the exact kernel method provides accurate angular fluxes even for highly anisotropic problems.

Mikols[21] reduced the computational effort of calculating exact kernel cross sections by assuming a triangular representation of group-to-group neutron transfer cross sections. He also developed the "order of angular coverage" concept for determination of the minimum order of numerical quadrature required for accurate transport calculations.

Ryman[22] applied the exact kernel technique to discrete-ordinates gamma photon transport problems. He showed that the exact kernel technique yields far more accurate results for such problems than does the standard Legendre expansion. He also developed a semi-analytical technique for rapid evaluation of exact kernel cross sections.

Hong[23] applied the exact kernel method to neutron inelastic scattering. He developed an exact kernel, discrete-ordinates transport code which is applicable to plane, spherical, cylindrical, and two-angle plane geometries. He also introduced a method to evaluate the scattering source term using piecewise polynomial approximations for the angular flux and the transfer cross section.

While the exact kernel technique offers greater accuracy than the Legendre expansion method, it has the disadvantage of being incompatible with standard discrete-ordinates transport codes. Because these standard codes almost always are based on Legendre polynomial expansions, they would require modification in the scattering source term calculation in order to utilize exact kernel cross sections. Beranek and Conn[24] suggested a method by which a discrete transfer cross section expansion can be utilized in standard discrete-ordinates transport codes. This method involves the generation of pseudo-Legendre expansion coefficients which will reproduce the exact kernel cross sections for scatter between any discrete directions of the quadrature set used. However, the number of expansion coefficients required to reproduce all the exact kernel cross sections increases rapidly with the quadrature order, rendering this method impractical for highly anisotropic problems.

In this work, the method suggested by Hong for the semi-analytical evaluation of the scattering source term is developed more fully and is applied to several transport problems. This new method is more accurate for highly anisotropic problems than is the conventional Legendre expansion method. In addition, the new method eliminates the problem of angular coverage encountered in exact kernel transport calculations.

In Chapter 2 a general development of the multigroup, discrete-ordinates transport equations is presented. Evaluation of the scattering source term is discussed for both the Legendre expansion method and the exact kernel method. In Chapter 3, the approximated scattering kernel method is developed. This semi-analytical evaluation

of the scattering source term utilizes piecewise polynomial expansions of the transfer cross section and the angular flux. Use of these polynomial expansions allows the integration of the scattering source term to be performed analytically, thereby obviating the need for numerical quadrature.

In Chapter 4, the approximated scattering kernel method is applied to several slab albedo problems. The results are compared to those obtained using the exact kernel and Legendre expansion methods. Finally, the conclusions reached from these problems, as well as suggestions for further study, are presented in Chapter 5.

2. SOLUTION OF THE TRANSPORT EQUATION BY THE DISCRETE-ORDINATES METHOD

2.1 The Transport Equation

The transport of neutral particles (e.g., neutrons and photons) through a host medium is described by the linearized Boltzmann equation. This equation, which neglects particle-particle interactions, is a linearized form of the equation derived by Boltzmann more than a century ago in his study of the kinetic theory of gases. The derivation of the linearized Boltzmann equation (hereafter referred to as "the transport equation") can be found in many texts (see, for example, Refs. 1 and 2) and will not be repeated here.

In this work, we are concerned only with steady-state transport through a homogeneous, non-multiplying slab for cases in which the particle flux density possesses azimuthal symmetry. Thus we seek solutions of the steady-state, one-dimensional transport equation, which can be written as

$$\mu \frac{\partial}{\partial x} \Phi(x,E,\mu,\psi) + \sigma(E)\Phi(x,E,\mu,\psi) = Q(x,E,\mu,\psi)$$

$$+ \int_0^{\infty} dE' \int_{-1}^{1} d\mu' \int_0^{2\pi} d\psi' \; \sigma_s(E' \to E, \vec{\Omega}' \cdot \vec{\Omega}) \; \Phi(x,E',\mu',\psi'), \qquad (2.1)$$

where

μ = the cosine of the polar angle between a particle's velocity vector and the positive x-axis (see Fig. 2.1),

x = the distance travelled into the slab,

E = the particle's energy,

ψ = the azimuthal angle between the z-axis and the projection of the particle's velocity vector onto the slab face,

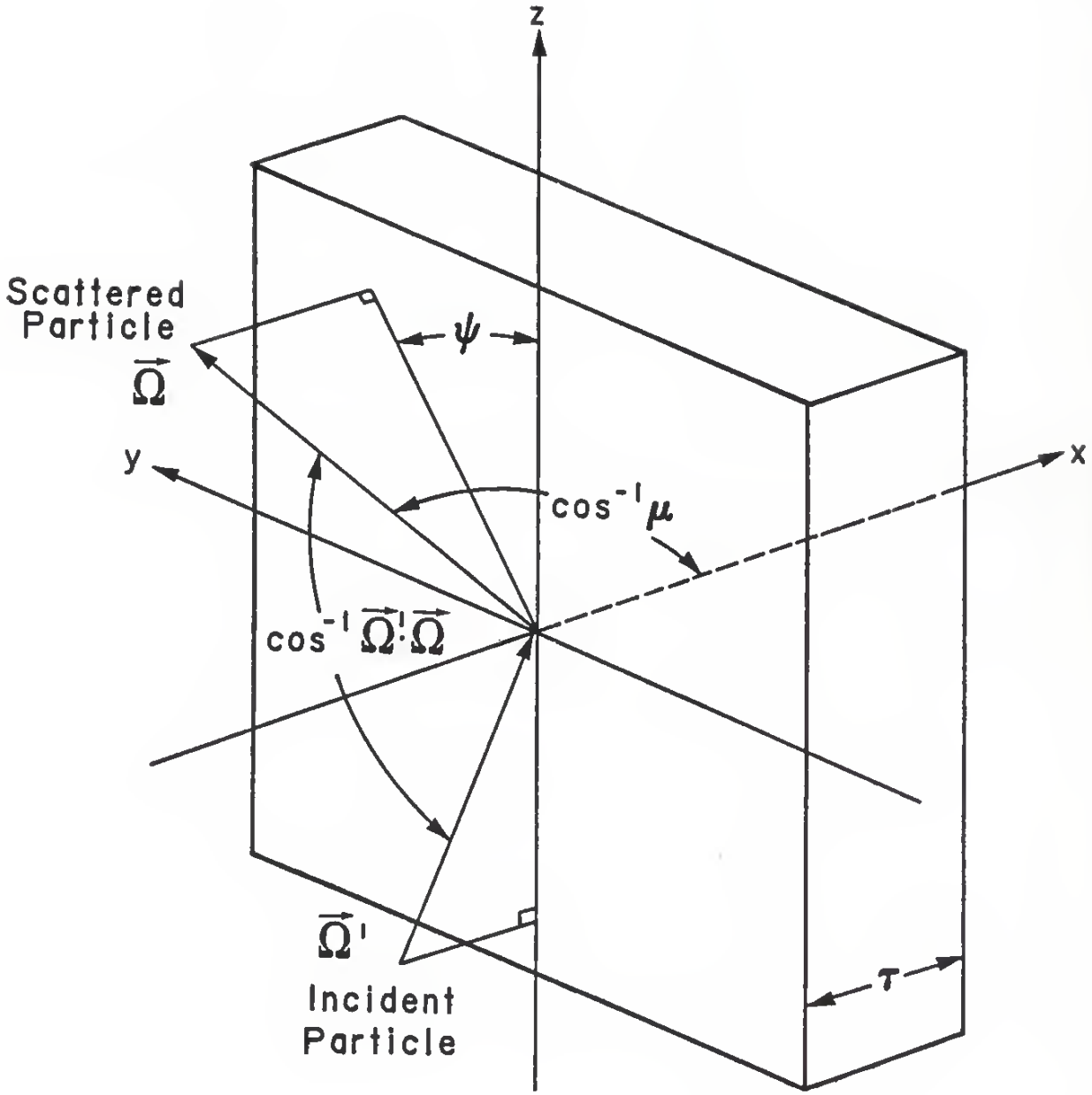

Fig. 2.1. The coordinate system for particle transport in a slab. The slab dimensions in the Y and Z directions are assumed to be infinite.

Φ = the angular flux density,

σ = the total macroscopic cross section,

Q = extraneous (flux-independent) sources,

σ_s = the macroscopic scattering cross section,

and

$\vec{\Omega}$ = a unit vector in the direction of particle travel.

The medium is assumed to be isotropic so that σ_s is rotationally invariant (i.e., σ_s depends on $\omega \equiv \vec{\Omega}'\cdot\vec{\Omega}$, not on $\vec{\Omega}'$ and $\vec{\Omega}$ individually).

In terms of the incident particle direction $\vec{\Omega}'(\mu',\psi')$ and final particle direction $\vec{\Omega}(\mu,\psi)$, the cosine of the scattering angle is given by[2]

$$\omega \equiv \vec{\Omega}'\cdot\vec{\Omega} = \mu\mu' + (1-\mu^2)^{\frac{1}{2}}\,(1-\mu'^2)^{\frac{1}{2}}\cos\phi \tag{2.2}$$

where ϕ is the difference in the azimuthal angles of the vectors $\vec{\Omega}'$ and $\vec{\Omega}$ (i.e., $\phi = \psi'-\psi$).

For azimuthally symmetric problems, one often solves for the azimuthally integrated flux density. Integration of Eq. (2.1) over the azimuthal angle ψ yields the transport equation for the azimuthally integrated flux density, viz.:

$$\mu\frac{\partial}{\partial x}\Phi(x,E,\mu) + \sigma(E)\Phi(x,E,\mu) = Q(x,E,\mu)$$

$$+ \int_0^\infty dE' \int_{-1}^{1} d\mu' \int_0^{2\pi} d\psi\ \sigma_s(E'\to E,\omega)\ \Phi(x,E',\mu'), \tag{2.3}$$

where

$$\Phi(x,E,\mu) \equiv \int_0^{2\pi} d\psi\ \Phi(x,E,\mu,\psi) \tag{2.4}$$

and

$$Q(x,E,\mu) \equiv \int_0^{2\pi} d\psi \; Q(x,E,\mu,\psi) \; . \tag{2.5}$$

Due to the dependence of ω on $\cos\phi = \cos(\psi'-\psi)$, the azimuthal integral over all ψ on the right hand side of Eq. (2.3) can equivalently be replaced by an integral over all ψ' or ϕ. Because we are concerned only with the change in azimuthal angle upon scattering, we will find it most convenient to work with the variable ϕ, and thus Eq. (2.3) is rewritten as

$$\mu \frac{\partial}{\partial x} \Phi(x,E,\mu) + \sigma(E)\Phi(x,E,\mu) = Q(x,E,\mu)$$

$$+ \int_0^{\infty} dE' \int_{-1}^{1} d\mu' \int_0^{2\pi} d\phi \; \sigma_s(E'\rightarrow E,\omega) \; \Phi(x,E',\mu') \; . \tag{2.6}$$

Even in this simplified form, the transport equation is much too complex to solve analytically for realistic geometries. Thus it is common practice to introduce further approximations such as discretizing the energy, angular, and/or spatial variables. By using such approximations, one is left with sets of algebraic equations rather than an integrodifferential equation. The resulting algebraic equations lend themselves readily to numerical solution techniques.

2.2 Energy Approximations for the Transport Equation

2.2.1 The Multigroup Transport Equations

The energy dependence of Eq. (2.6) is commonly approximated by employing the multigroup method. This formulation is accomplished by

discretizing the energy variable into G contiguous energy groups, as shown schematically below:

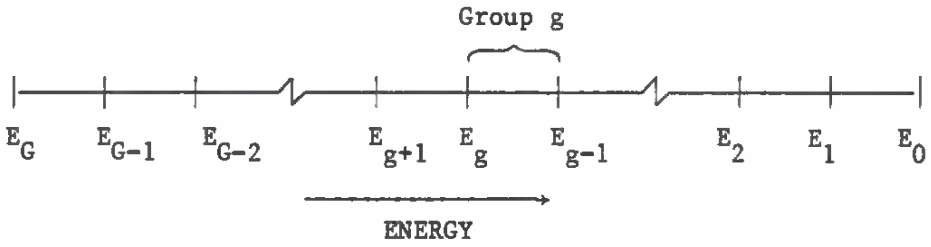

The standard multigroup convention, which will be followed in this work, is to index the energy groups such that the group index g increases with decreasing energy. The energy level E lies within group g if $E_g < E \leq E_{g-1}$.

To derive the multigroup equations, we first define the group angular flux density and group extraneous source as

$$\Phi_g(x,\mu) \equiv \int_{E_g}^{E_{g-1}} dE\ \Phi(x,E,\mu) \tag{2.7}$$

and

$$Q_g(x,\mu) \equiv \int_{E_g}^{E_{g-1}} dE\ Q(x,E,\mu)\ . \tag{2.8}$$

Upon integrating Eq. (2.6) over energy group g and replacing the integration over energy in the scattering source term by a sum of integrals over all the energy groups, we obtain the following multigroup equations:

$$\mu \frac{\partial}{\partial x} \Phi_g(x,\mu) + \sigma_g \Phi_g(x,\mu) = Q_g(x,\mu)$$

$$+ \sum_{g'=1}^{G} S_{g'\to g}(x,\mu) \quad , \qquad g = 1,\ldots , G \tag{2.9}$$

where the group total cross section is defined by

$$\sigma_g \equiv \frac{\int_{E_g}^{E_{g-1}} dE\ \sigma(E)\ \Phi(x,E,\mu)}{\int_{E_g}^{E_{g-1}} dE\ \Phi(x,E,\mu)} , \tag{2.10}$$

the scattering source is defined by

$$S_{g'\to g}(x,\mu) \equiv \int_{-1}^{1} d\mu' \int_{0}^{2\pi} d\phi\ \sigma_{g'\to g}(\omega)\ \Phi_{g'}(x,\mu') , \tag{2.11}$$

and the group-to-group scattering cross section is defined by

$$\sigma_{g'\to g}(\omega) \equiv \frac{\int_{E_g}^{E_{g-1}} dE \int_{E_{g'}}^{E_{g'-1}} dE'\ \sigma_s(E'\to E,\omega)\ \Phi(x,E',\mu)}{\int_{E_g}^{E_{g'-1}} dE'\ \Phi(x,E',\mu)} . \tag{2.12}$$

The evaluation of the group cross sections through the use of Eqs. (2.10) and (2.12) presupposes knowledge of the angular flux density, which is not known until the transport equation itself is solved. This problem is usually circumvented by assuming that the energy dependence of the flux is separable from the spatial and angular dependence, i.e.,

$\Phi(x,E,\mu) \cong W(E)\ \Psi(x,\mu)$. With this assumption, Eq. (2.10) can be rewritten as

$$\sigma_g \equiv \frac{\int_{E_g}^{E_{g-1}} dE\ \sigma(E)\ W(E)}{\Delta_g} , \tag{2.12}$$

where

$$\Delta_g \equiv \int_{E_g}^{E_{g-1}} dE\ W(E) . \tag{2.13}$$

In a similar manner, Eq. (2.12) can be rewritten as

$$\sigma_{g'\to g}(\omega) \equiv \frac{1}{\Delta g'} \int_{E_g}^{E_{g-1}} dE \int_{E_{g'}}^{E_{g'-1}} dE'\ W(E')\ \sigma_s(E'\to E,\omega) . \tag{2.14}$$

For very fine energy meshes, the weight function W(E) is often assumed to be constant over each energy group. For broader energy meshes, a variety of approximations have been used. For example, in neutron transport in fission reactors, one often uses a fission spectrum for W(E) in the MeV range, a 1/E spectrum in the epithermal range, and a Maxwellian spectrum in the thermal energy region.[25]

2.2.2 The One-Speed Transport Equation

In many particle transport problems, the particles are assumed to be characterized by a single energy. This assumption is a simplification of the multigroup equations in that only one energy group need be utilized. The resulting equation is known as the "one-speed" or "one-group" transport equation. It is also referred to as the "constant cross-section approximation", since if the cross sections are postulated

to be independent of energy, the one-speed equation results. Although this treatment may seem rather crude, it actually has a great deal of practical application,[1,26] and is the basis of most analytical studies of the transport equation.

The one-speed transport equation can be derived quite simply from the multigroup equations. Let us first write the multigroup equations in the following form (cf. Eqs. (2.9) and (2.11)):

$$\mu \frac{\partial}{\partial x} \Phi_g(x,\mu) + \sigma_g \Phi_g(x,\mu) = Q_g(x,\mu)$$

$$+ \sum_{g'=1}^{G} \int_{-1}^{1} d\mu' \int_{0}^{2\pi} d\phi \; \sigma_{g' \to g}(\omega) \; \Phi_{g'}(x,\mu') \;, \; g = 1,\ldots, G. \quad (2.15)$$

Since we are considering only one energy group, we can drop the group subscripts and delete the summation over the incident energy groups in the scattering source term to obtain the one-speed transport equation, viz.:

$$\mu \frac{\partial}{\partial x} \Phi(x,\mu) + \sigma\Phi(x,\mu) = Q(x,\mu) + \int_{-1}^{1} d\mu' \int_{0}^{2\pi} d\phi \; \sigma_s(\omega) \; \Phi(x,\mu'). \quad (2.16)$$

It is often convenient to recast the transport equation into dimensionless form. To do so we express distances in terms of the collision mean-free-path length, also referred to as the "optical thickness". We define this dimensionless distance as

$$z \equiv \sigma x \quad (2.17)$$

so that

$$\frac{\partial}{\partial x} = \sigma \frac{\partial}{\partial z} . \tag{2.18}$$

Eq. (2.16) can now be rewritten as

$$\mu\sigma \frac{\partial}{\partial z} \Phi(z,\mu) + \sigma\Phi(z,\mu) = \sigma Q(z,\mu) + \int_{-1}^{1} d\mu' \int_{0}^{2\pi} d\phi \; \sigma_s(\omega) \; \Phi(z,\mu'), \tag{2.19}$$

where

$$\Phi(z,\mu) \equiv \Phi(x(z),\mu) \tag{2.20}$$

and

$$Q(z,\mu) \equiv \frac{Q(x(z),\mu)}{\sigma} . \tag{2.21}$$

Equation (2.19) can be simplified by expressing the differential scattering cross section $\sigma_s(\omega)$ as the product of the total scattering cross section σ_s and a scattering distribution function $f_s(\omega)$, viz.:

$$\sigma_s(\omega) \equiv \sigma_s \; f_s(\omega) , \tag{2.22}$$

where $f_s(\omega)$ is normalized to unity, i.e.,

$$\int_{4\pi} d\Omega \; f_s(\omega) = 1 . \tag{2.23}$$

Substitution of Eq. (2.22) into Eq. (2.19) yields

$$\mu\sigma \frac{\partial}{\partial z} \Phi(z,\mu) + \sigma\Phi(z,\mu) = \sigma Q(z,\mu) + \sigma_s \int_{-1}^{1} d\mu' \int_{0}^{2\pi} d\phi \; f_s(\omega) \; \Phi(z,\mu') \tag{2.24}$$

or, in dimensionless form,

$$\mu \frac{\partial}{\partial z} \Phi(z,\mu) + \Phi(z,\mu) = Q(z,\mu) + c \int_{-1}^{1} d\mu' \int_{0}^{2\pi} d\phi \; f_s(\omega) \; \Phi(z,\mu') \; , \qquad (2.25)$$

where c, the "mean number of secondary particles emitted per collision," is given by

$$c \equiv \frac{\sigma_s}{\sigma} \; . \qquad (2.26)$$

2.3 The Discrete-Ordinates Equations

2.3.1 Angular Discretization

The angular dependence on the transport equation is commonly approximated by the discrete-ordinates method. In this method, the angular variable μ is discretized into a set of N discrete directions $\{\mu_i\}$ at which the angular flux is to be evaluated. The scattering source term is evaluated by numerical quadrature where the μ_i values are the quadrature ordinates. The set of corresponding quadrature weights is denoted by $\{w_i\}$. With this approximation, Eq. (2.9) can be rewritten as

$$\mu_i \frac{\partial}{\partial x} \Phi_g(x,\mu_i) + \sigma_g \; \Phi_g(x,\mu_i) = Q_g(x,\mu_i)$$

$$+ \sum_{g'=1}^{G} S_{g' \to g}(x,\mu_i) \; , \; i = 1,\ldots, N; \;\; g = 1,\ldots, G \qquad (2.27)$$

where

$$S_{g' \to g}(x,\mu_i) \equiv \sum_{j=1}^{N} w_j \int_{0}^{2\pi} d\phi \; \sigma_{g' \to g}(\omega) \; \Phi_{g'}(x,\mu_j) \; . \qquad (2.28)$$

Equations (2.27) and (2.28) represent one form of the discrete-ordinates transport equations.

The evaluation of the group-to-group scattering source $S_{g' \to g}(x,\mu_i)$ of Eq. (2.28) is dependent upon the method used to express the group-to-group scattering cross section. Two of these methods, the Legendre polynomial expansion method and the exact kernel method, will be examined in sections 2.4 and 2.5. A new method of evaluating the scattering source, which is the subject of this work, will be examined in Chapters 3 and 4. This alternative method is based on direct evaluation of Eq. (2.11) by analytical integration.

The accuracy which can be obtained in solving the discrete-ordinates equations when Eq. (2.28) is used to evaluate the scattering source term is largely dependent on the quadrature set used.[2] In general, one would like to use a set which is large enough to describe adequately the angular detail in the fluxes, yet small enough that excessive computational effort is not required. The choice of such an optimum set is typically problem dependent, especially when anisotropic scattering is involved. Failure to choose an appropriate quadrature set can lead to serious errors in the calculation of the angular fluxes.[27]

Unfortunately, there is no standard procedure for choosing *a priori* an adequate set. The choice is usually made on the basis of experience or trial and error. However, as a general rule, the following criteria should be met:[1]

(1) *Projection Invariance*. For one-dimensional slab geometry with azimuthal symmetry, the discrete directions $\{\mu_i\}$ should be symmetric

about $\mu = 0$. However, if one knows that the angular flux is peaked near a certain direction μ_j, it may be advantageous to tailor a nonsymmetric quadrature set with several discrete directions clustered near μ_j.[28]

(2) *Positivity of the scalar flux.* The scalar flux

$$\Phi_g(x) = \int_{-1}^{1} d\mu\ \Phi_g(x,\mu) \cong \sum_{i=1}^{N} w_i\ \Phi_g(x,\mu_i)$$

should be always positive. Choosing the $w_i > 0$ will ensure positivity of the scalar flux (provided the angular flux values are positive).

(3) *Accurate Evaluation of Angular Integrals.* The scalar flux and scattering source should be evaluated accurately with a minimum of quadrature ordinates and weights.

Two commonly used quadrature sets for one-dimensional geometries are the Gaussian quadrature set and the Lobatto quadrature set. Values of the ordinates and weights of these quadrature sets for various values of N can be found in Ref. 29. Because the angular flux is discontinuous at a plane interface at $\mu = 0$,[2] odd order quadrature sets are not used in plane geometry transport calculations (since they contain a quadrature ordinate at $\mu = 0$). In order to avoid this possible discontinuity, one can split up the angular integration range into two parts, $-1 \leq \mu < 0$ and $0 < \mu \leq 1$, and perform Gaussian quadrature separately over each sub-range. This approach is known as the double P_N (or DP_N) method. In plane-geometry transport problems, the DP_N method has often been found to give numerical results which are superior to those obtained from a standard full-range expansion.[2]

2.3.2 Spatial Discretization

For some simple cases (e.g., a one-group problem with isotropic scattering and no extraneous sources), the discrete-ordinates equations (2.27) can be solved analytically. This approach was used by Wick and Chandrasekhar in the original development of the discrete-ordinates method.[25] However, for most realistic transport problems, Eqs. (2.27) are too difficult to solve analytically and hence must be solved numerically.

One method of effecting a numerical solution of Eqs. (2.27) is to form a set of finite-difference equations by discretizing the spatial variable x into a set of spatial nodes $\{x_k\}$. Let the left boundary be denoted by x_1 and the right boundary by x_{K+1} (see Fig. 2.2). The spatial derivative of the flux is then approximated by a finite difference scheme, viz.:

$$\frac{\partial}{\partial x}\,\Phi_g(x_{k+\frac{1}{2}},\mu_i) \cong \frac{\Phi_g(x_{k+1},\mu_i) - \Phi_g(x_k,\mu_i)}{\Delta_{k+\frac{1}{2}}} \quad , \tag{2.29}$$

where

$$x_{k+\frac{1}{2}} \equiv \frac{x_k + x_{k+1}}{2} \tag{2.30}$$

and

$$\Delta_{k+\frac{1}{2}} \equiv x_{k+1} - x_k \quad . \tag{2.31}$$

We thus obtain the finite difference form of the multigroup discrete-ordinates equations as

$$\frac{\mu_i}{\Delta_{k+\frac{1}{2}}} [\phi_g(x_{k+1},\mu_i) - \phi_g(x_k,\mu_i)] + \sigma_g \phi_g(x_{k+\frac{1}{2}},\mu_i)$$

$$= q_g(x_{k+\frac{1}{2}},\mu_i) \ , \ k = 1,\ldots, K; \quad i = 1,\ldots, N; \quad g = 1,\ldots, G \qquad (2.32)$$

where the group total source q_g is defined by

$$q_g(x_{k+\frac{1}{2}},\mu_i) \equiv Q_g(x_{k+\frac{1}{2}},\mu_i) + \sum_{g'=1}^{G} S_{g'\to g}(x_{k+\frac{1}{2}},\mu_i) \ . \qquad (2.33)$$

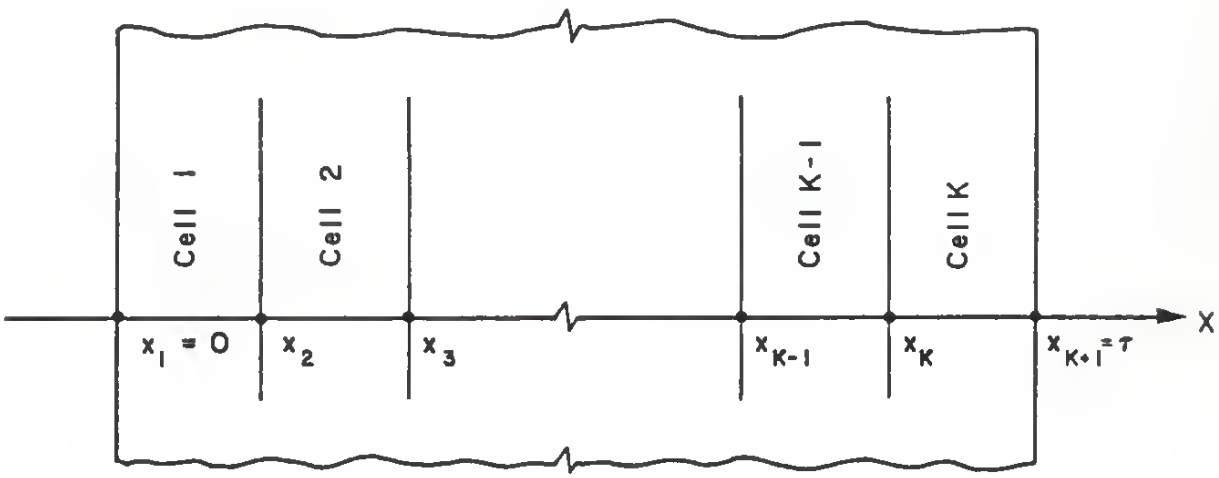

Fig. 2.2. Spatial discretization of a one-dimensional slab.

2.3.3 Solution of the Spatially Discretized Discrete-Ordinates Equations

Before the set of equations represented by Eq. (2.32) can be solved, it is necessary to reduce the number of unknowns by assuming a relation between the cell-edged fluxes and cell-centered fluxes. The most commonly used method is the diamond difference scheme which uses

$$\Phi_g(x_{k+\frac{1}{2}},\mu_i) = \frac{\Phi_g(x_k,\mu_i) + \Phi_g(x_{k+1},\mu_i)}{2} . \qquad (2.34)$$

Substitution of Eq. (2.34) into Eq. (2.32) yields

$$\frac{\mu_i}{\Delta_{k+\frac{1}{2}}} [\Phi_g(x_{k+1},\mu_i) - \Phi_g(x_k,\mu_i)] + \frac{\sigma_g}{2} [\Phi_g(x_k,\mu_i) + \Phi_g(x_{k+1},\mu_i)]$$

$$= q_g(x_{k+\frac{1}{2}},\mu_i), \; k = 1,\ldots, K; \quad i = 1,\ldots, N; \quad g = 1,\ldots, G \qquad (2.35)$$

which represents K x N x G equations in K x N x G unknowns, $\Phi_g(x_k,\mu_i)$. (The incident flux densities at the outer surfaces of the slab, x_1 and x_{K+1}, are assumed known from the boundary conditions.)

Equation (2.35) can be solved for $\Phi_g(x_{k+1},\mu_i)$ in terms of $\Phi_g(x_k,\mu_i)$ as

$$\Phi_g(x_{k+1},\mu_i) = \frac{\left(1 - \frac{\sigma_g \Delta_{k+\frac{1}{2}}}{2\mu_i}\right) \Phi_g(x_k,\mu_i) + \frac{\Delta_{k+\frac{1}{2}}}{\mu_i} q_g(x_{k+\frac{1}{2}},\mu_i)}{1 + \frac{\sigma_g \Delta_{k+\frac{1}{2}}}{2\mu_i}} \qquad (2.36)$$

or for $\Phi_g(x_k,\mu_i)$ in terms of $\Phi_g(x_{k+1},\mu_i)$ as

$$\Phi_g(x_k,\mu_i) = \frac{\left(1 + \frac{\sigma_g \Delta_{k+\frac{1}{2}}}{2\mu_i}\right) \Phi_g(x_{k+1},\mu_i) - \frac{\Delta_{k+\frac{1}{2}}}{\mu_i} q_g(x_{k+\frac{1}{2}},\mu_i)}{1 - \frac{\sigma_g \Delta_{k+\frac{1}{2}}}{2\mu_i}} . \qquad (2.37)$$

These two results permit the evaluation of the angular flux densities at all the spatial nodes by starting at one of the slab surfaces (where the incident flux is known) and sweeping inward through the spatial mesh

along the direction of particle travel. Equation (2.36) must be used for $\mu_i > 0$ and Eq. (2.37) for $\mu_i < 0$. This procedure minimizes the accumulation of roundoff errors.[1]

The number of spatial nodes and the number of discrete ordinates are not independent of each other. From examination of Eqs. (2.36) and (2.37), it is seen that to ensure the positivity of the left-hand side of each equation, the following condition must be met:

$$\left| \frac{\sigma_g \Delta_{k+\frac{1}{2}}}{2\mu_i} \right| \leq 1 \tag{2.38}$$

Thus, the maximum cell width $\Delta_{k+\frac{1}{2}}$ is constrained by the smallest cosine of the polar angle (i.e., the value of μ_i closest to zero). As more discrete directions are used, the minimum $|\mu_i|$ becomes smaller, and hence the number of spatial nodes required for positivity of the computed fluxes increases.

The solution of the discrete ordinates equations is complicated by the fact that the source term $q_g(x_{k+\frac{1}{2}},\mu_i)$ is dependent on the unknown flux $\Phi_g(x_{k+\frac{1}{2}},\mu_i)$ (except for a purely absorbing medium, in which case $\sigma_{g'\to g}(\omega)$ is zero). The usual method of solving the discrete ordinates equations is thus to employ an iterative scheme in which the source term is approximated more accurately with each iteration. The procedure is as follows:

(1) Estimate the initial source term $q_g(x_{k+\frac{1}{2}},\mu_i)$ at each spatial cell midpoint using any reasonable source distribution.

(2) Solve for the angular flux densities using Eqs. (2.36) and (2.37) as appropriate.

(3) Calculate the cell-centered fluxes using Eq. (2.34).

(4) Reconstruct the source terms using Eqs. (2.33) and (2.28).

(5) Repeat steps (2) - (4) until the computed flux densities converge.

The rate of convergence of this iterative process depends on both the nature of the scattering involved and the thickness of the slab. For the extreme case of no scattering (σ_s=0) the method converges in a single iteration. As the amount of scattering increases, so in general will the number of iterations required for convergence.[1] For optically thick slabs with values of the scattering ratio c close to unity, convergence is extremely slow.[30]

Because of the need to reduce computational time (and hence cost) in discrete ordinates calculations, various methods have been developed to accelerate the convergence of the iterative routine. Some of the more common methods are reviewed in Ref. 31. The method used in this work is a simple overrelaxation (SOR) scheme which is implemented as follows.

Consider the calculation of the scattering source terms $S_{g'\to g}(x_{k+\frac{1}{2}},\mu_i)$ for iteration $\nu+1$. These values, denoted by $S^{\nu+1}_{g'\to g}(x_{k+\frac{1}{2}},\mu_i)$, can be expressed as a vector functional of the previous iterate scattering source values,[20] i.e.

$$S^{\nu+1}_{g'\to g}(x_{k+\frac{1}{2}},\mu_i) = f\left[\left\{S^{\nu}_{g'\to g}(x_{k+\frac{1}{2}},\mu_i)\right\}\right] . \qquad (2.39)$$

It has been found[20] that convergence may be accelerated by calculating a modified source term, viz.:

$$S^{\nu+1}_{g'\to g}(x_{k+\frac{1}{2}},\mu_i) = [I+\delta^{\nu}]\, f\left(\left\{S^{\nu}_{g'\to g}(x_{k+\frac{1}{2}},\mu_i)\right\}\right) - [\delta^{\nu}]\left\{S^{\nu}_{g'\to g}(x_{k+\frac{1}{2}},\mu_i)\right\} \tag{2.40}$$

where [I] is the identity matrix and $[\delta^{\nu}]$ is a diagonal matrix defined by

$$[\delta^{\nu}] = d^{\nu}[I]. \tag{2.41}$$

The quantity d^{ν} is a scalar between 0 and 1 which may vary with the iteration number.

Ryman[22] obtained good acceleration results by setting d^{ν} initially to some small value ($\cong$0.1) and multiplying it by a constant ($\cong$1.1) with each iteration until an upper limit ($\cong$0.2) was reached. This procedure was found to provide good results in this work as well.

Having developed the multigroup discrete-ordinates equations and described the method by which they are solved, we now turn our attention to the evaluation of the scattering source term.

2.4 Evaluation of the Scattering Source Term by the Legendre Expansion Method

The accuracy which can be obtained in the solution of the discrete ordinates equations is dependent on, among other factors, the accuracy obtained in the evaluation of the scattering source term. In Section 2.3.1 it was mentioned that the evaluation of the scattering source term is dependent upon the method used to express the group-to-group

scattering cross section. In the next two sections, we will examine two of these methods.

The most widely used method is to represent the angular dependence of the scattering cross section by a truncated Legendre polynomial expansion, i.e.,

$$\sigma_{g'\to g}(\omega) = \sum_{\ell=0}^{L} \left(\frac{2\ell+1}{4\pi}\right) \sigma_{\ell,g'\to g} \, P_\ell(\omega) \ , \tag{2.42}$$

where the expansion coefficients are given by

$$\sigma_{\ell,g'\to g} = 2\pi \int_{-1}^{1} d\omega \, \sigma_{g'\to g}(\omega) \, P_\ell(\omega) \tag{2.43}$$

and P_ℓ is the Legendre polynomial of order ℓ.

Application of the addition theorem for Legendre polynomials[25] to Eq. (2.42) yields

$$\sigma_{g'\to g}(\omega) = \sum_{\ell=0}^{L} \left(\frac{2\ell+1}{4\pi}\right) \sigma_{\ell,g'\to g} \left\{P_\ell(\mu) \, P_\ell(\mu') + 2 \sum_{m=1}^{\ell} \frac{(\ell-m)!}{(\ell+m)!} \, P_\ell^m(\mu) \, P_\ell^m(\mu') \cos(m\phi)\right\} \ , \tag{2.44}$$

where the P_ℓ^m are associated Legendre polynomials of the first kind. Upon insertion of Eq. (2.44) into Eq. (2.28), the terms containing $\cos(m\phi)$ vanish upon integration over ϕ. The result is

$$S_{g'\to g}(x,\mu_i) = \frac{1}{2} \sum_{j=1}^{N} w_j \sum_{\ell=0}^{L} (2\ell+1) \, \sigma_{\ell,g'\to g} \, P_\ell(\mu_i) \, P_\ell(\mu_j) \, \Phi_{g'}(x,\mu_j). \tag{2.45}$$

Equation (2.45) can also be expressed in terms of the angular flux moments as

$$S_{g'\to g}(x,\mu_i) = \sum_{\ell=0}^{L} \left(\frac{2\ell+1}{4\pi}\right) P_\ell(\mu_i)\, \sigma_{\ell,g'\to g}\, \Phi_{\ell,g'}(x), \qquad (2.46)$$

where the moments of the flux are given by

$$\Phi_{\ell,g'}(x) = 2\pi \int_{-1}^{1} d\mu\, \Phi_{g'}(x,\mu)\, P_\ell(\mu). \qquad (2.47)$$

While Eqs. (2.45) and (2.46) provide convenient methods for the evaluation of the scattering source term, they suffer from a serious drawback. A low order expansion of two to nine terms (typically used in reactor physics calculations) may fail to model the scattering cross section adequately . This is particularly true when highly anisotropic scattering is involved. Such anisotropic scattering is common in neutron transport problems involving elastic scattering from light elements and with very fine energy group structures. As an example, consider the hydrogen multigroup scattering cross section of Fig. 2.3. The eighth-order Legendre expansion is seen to exhibit oscillatory behavior, with the cross section expansion actually having negative values over portions of the ω range. The use of such an expansion can lead to the calculation of oscillatory and even negative flux values.[20] While the use of higher order expansions could mitigate this problem, the extra computational effort involved often makes such an approach unfeasible.

In spite of this drawback, the Legendre expansion method is widely used and, in most situations, provides satisfactory results. For many

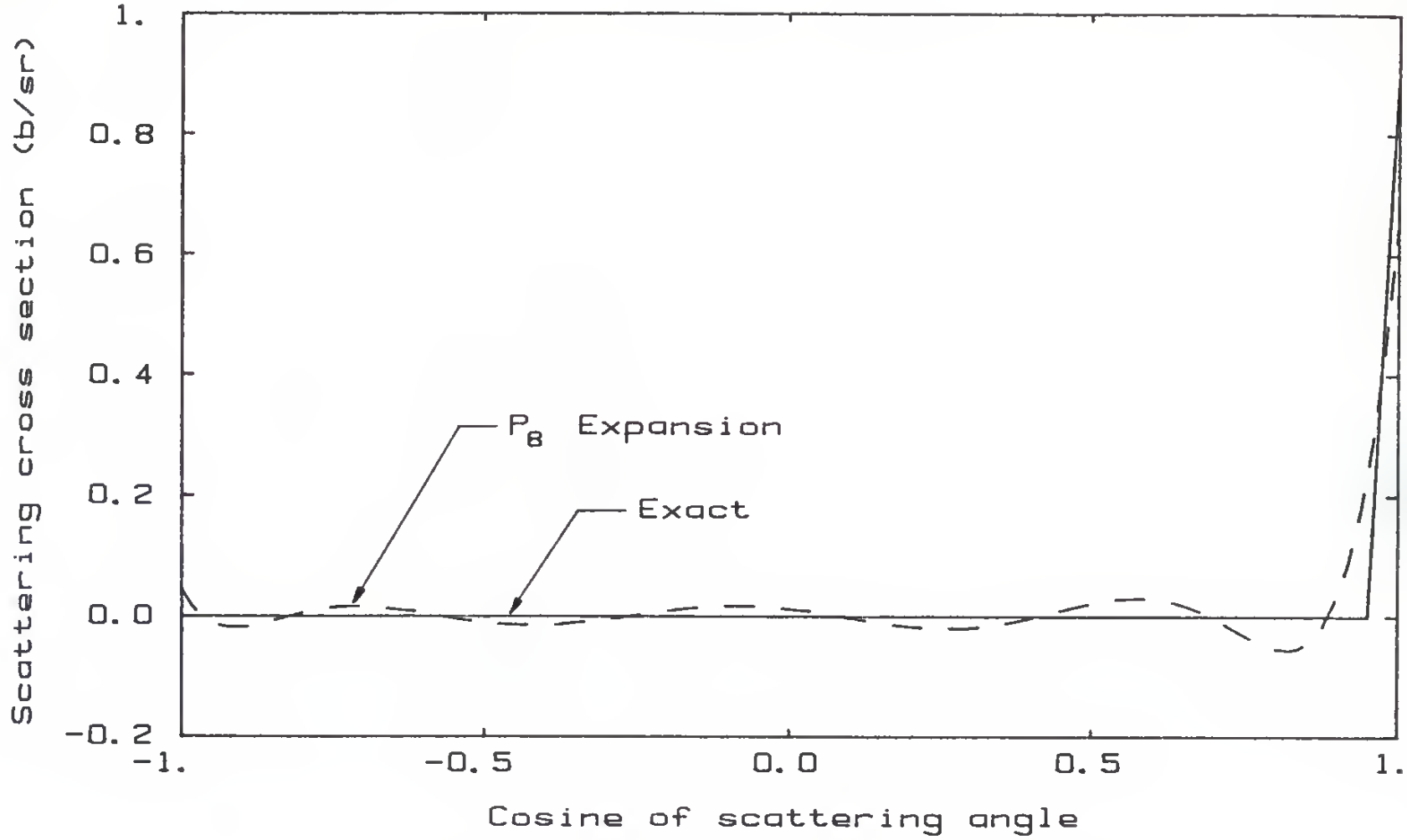

Fig. 2.3. The scattering cross section for a Hydrogen DLC/2 group 20 to 20 transfer, as calculated exactly and by an eighth-order Legendre expansion. The energy limits for group 20 of the DLC/2 energy structure are 2.2313 - 2.019 MeV.

situations in which the scattering cross sections would appear to require a very accurate angular description, low-order Legendre expansions are often justified if the angular flux is not highly anisotropic or if only angularly integrated quantities (e.g., scalar fluxes) are of interest. Only for those problems in which both the angular flux and the scattering cross sections are highly anisotropic is it necessary to resort to a more accurate method, such as the exact kernel technique.[20]

2.5 Evaluation of the Scattering Source Term by the Exact Kernel Method

For problems in which the Legendre expansion method produces inaccurate or nonphysical fluxes, more accurate results can be obtained by using a non-expansion method. This method, referred to by Odom as the "exact kernel" method, involves the use of a transfer matrix composed of scattering cross sections for every μ_j to μ_i transfer. Use of the exact kernel method guarantees positivity of the computed fluxes (provided Eq. (2.38) is satisfied) and has been shown to provide accurate results for both neutron[20,21,23] and gamma photon[22] transport problems.

The exact kernel form of the scattering source term is simply

$$S_{g'\to g}(x,\mu_i) = \sum_{j=1}^{N} w_j \, \sigma_{g'\to g}(\mu_j\to\mu_i) \, \Phi_{g'}(x,\mu_j), \tag{2.48}$$

where $\sigma_{g'\to g}(\mu_j\to\mu_i)$ is the exact kernel cross section for transfer from polar direction μ_j to polar direction μ_i. Comparison of Eqs. (2.28) and (2.48) shows that the exact kernel cross section is defined as

$$\sigma_{g'\to g}(\mu_j\to\mu_i) \equiv \int_0^{2\pi} d\phi\ \sigma_{g'\to g}(\omega(\mu_i,\mu_j,\phi)) \ , \tag{2.49}$$

where $\omega(\mu,\mu',\phi)$ is given by Eq. (2.7). Due to the dependence of $\sigma_{g'\to g}(\omega)$ on $\cos\phi$, which is symmetric about π in the interval $[0, 2\pi]$, Eq. (2.49) can also be written as

$$\sigma_{g'\to g}(\mu_j\to\mu_i) = 2\int_0^{\pi} d\phi\ o_{g'\to g}(\omega). \tag{2.50}$$

Several techniques have been developed to facilitate the evaluation of Eq. (2.50). These techniques include restriction of the azimuthal integration range and the use of low-order piecewise polynomial approximations for $o_{g'\to g}(\omega)$. The method used to evaluate exact kernel cross sections for the transport calculations performed in this work is presented in Sec. 3.2.1. For more information on the evaluation and use of exact kernel cross sections, the interested reader is referred to Refs. 22 and 23.

Although the exact kernel method does provide more accurate results in problems with a high degree of anisotropy than does the Legendre expansion method, it does have drawbacks. The most obvious of these is the problem of cross section storage. In the Legendre expansion method, the only cross section terms required are the L + 1 expansion coefficients for an L'th order cross section expansion. In the exact kernel method, however, it is necessary to store an N x N matrix of cross section values (N being the number of discrete ordinates). For transport problems involving a large number of discrete ordinates and/or many energy groups, it is easy to see that the number of exact kernel

cross sections required becomes very large. While this storage requirement is a disadvantage of the exact kernel method, it has become less of a problem as larger computers and fast access peripheral storage devices have been developed.

Another problem associated with the exact kernel method is that of angular redistribution of scattered particles. This problem can best be illustrated by considering a highly anisotropic scattering cross section which is nonzero only over a small portion of the scattering range $\omega \in [-1,1]$ (cf. Fig. 2.3). For such a cross section, many of the exact kernel cross sections $\sigma(\mu_j \to \mu_i)$ will be identically zero. Whether or not a particular exact kernel cross section is nonzero depends upon the spacing between adjacent μ_i values of a discrete-ordinates quadrature set. If the spacing between these values is too large, particles traveling in direction μ_j will never scatter into other directions. This inability of particles to redistribute angularly remains even after multiple scatters.

In order to ensure that angular redistribution can occur, it is necessary to have at least one nonzero value of $\sigma(\mu_j \to \mu_i)$ for some $i \neq j$. For this condition to be met, Mikols[27] has shown that there must exist at least one polar quadrature ordinate $\theta_i \equiv \cos^{-1} \mu_i$ such that

$$\beta_{min} \leq \theta_i \leq \beta_{max} . \tag{2.51}$$

The values of β_{min} and β_{max} are dependent upon the nonzero range of the scattering cross section, as well as upon the initial particle direction $\theta_j \equiv \cos^{-1} \mu_j$. In particular, consider a cross section which is nonzero only over the range $[\omega_{min}, \omega_{max}]$. The angles β_{min} and β_{max} are given by

$$\beta_{min} = \begin{cases} \max[(\theta_j - \theta_{max}), 0] , & \theta_j \geq \theta_{min} , \\ \theta_{min} - \theta_j , & \theta_j < \theta_{min} , \end{cases} \tag{2.52}$$

and

$$\beta_{max} = \begin{cases} \min[(\theta_j + \theta_{max}), \pi] , & \theta_j + \theta_{min} \leq \pi , \\ 2\pi - \theta_j - \theta_{min} , & \theta_j + \theta_{min} > \pi , \end{cases} \tag{2.53}$$

where $\theta_{max} \equiv \cos^{-1} \omega_{min}$ and $\theta_{min} \equiv \cos^{-1} \omega_{max}$.

The fundamental concern when choosing a discrete-ordinates quadrature set for exact kernel transport calculations is whether or not the set can "completely model" scattering transfers within a group and to the next lower group.[27] The term "completely model" refers to the ability of a quadrature set to produce at least one nonzero value of $\sigma(\mu_j \rightarrow \mu_i)$, with $i \neq j$, for all μ_j values of the quadrature set. This is referred to as first-order coverage of a quadrature set. In the same manner, n'th-order coverage is that coverage which permits transfer from μ_j to at least n different μ_i values. In general, a quadrature set which provides first-order coverage is sufficient for transport calculations. While larger quadrature sets (with a higher order of coverage) may provide some increase in accuracy, they do so at the cost of increased computational effort. On the other hand, if the quadrature set is so coarse that not even first-order coverage is achieved, the exact kernel method yields very poor results.

In the next chapter, a new method of evaluating the scattering source term is introduced. This new method avoids the angular coverage problem of the exact kernel method, and also provides better accuracy for highly anisotropic problems than does the Legendre expansion method.

3. DEVELOPMENT OF AN APPROXIMATED SCATTERING KERNEL FOR SEMI-ANALYTICAL EVALUATION OF THE SCATTERING SOURCE TERM

In the previous chapter, two methods for evaluating the scattering source term of Eq. (2.28) were summarized -- the Legendre expansion method and the exact kernel method. For problems characterized by highly anisotropic fluxes and scattering cross sections, the Legendre expansion method can lead to the calculation of inaccurate and even unphysical fluxes. The exact kernel technique provides much more accurate results, but can suffer from angular redistribution problems.

In the next two chapters we will examine a method based on the analytical evaluation of the scattering source term of Eq. (2.11). This method, which we will refer to as the "approximated scattering kernel" method, will be seen to provide better accuracy than the Legendre expansion method, and to alleviate the angular redistribution problem of the exact kernel method for highly anisotropic problems.

3.1 Approximations for the Scattering Source

In Chapter 2 it was shown that the group-to-group scattering source for a direction μ is given by

$$S_{g'\to g}(\mu) = \int_{-1}^{1} d\mu' \int_{0}^{2\pi} d\phi\ \sigma_{g'\to g}(\omega)\ \Phi_{g'}(\mu'), \qquad (3.1)$$

where the spatial variable has been dropped for simplicity of notation. Due to the dependence of $\sigma_{g'\to g}(\omega)$ on $\cos\phi$, which is symmetric about π in the interval $[0, 2\pi]$, Eq. (3.1) can be rewritten as

$$S_{g'\to g}(\mu) = 2 \int_{-1}^{1} d\mu' \int_{0}^{\pi} d\phi\ \sigma_{g'\to g}(\omega)\ \Phi_{g'}(\mu'). \qquad (3.2)$$

In order to evaluate Eq. (3.2) analytically, it is first necessary to assume a functional form for both the group-to-group scattering cross section and the angular flux density. In this section, we will examine approximations which often represent the shape of $\sigma_{g'\to g}(\omega)$ and $\Phi_{g'}(\mu')$ more accurately than the traditional Legendre polynomial expansions.

3.1.1 Approximation of the Scattering Cross Section

In previous studies of transport calculations involving anisotropic scattering, it has been shown that the angular range of the scattering cross section $\sigma_{g'\to g}(\omega)$ is naturally divided into subregions bounded by at most four breakpoints ω_i, $i = 1, \ldots, 4$, such that $-1 \leq \omega_1 \leq \omega_2 \leq \omega_3 \leq \omega_4 \leq 1$.[21-23] The values ω_1 and ω_4 represent the minimum and maximum cosine of the scattering angle, respectively, for which scattering is permissible within the constraints of energy and momentum conservation for transfer from group g' into group g. Thus the scattering cross section $\sigma_{g'\to g}(\omega)$ is zero for $\omega<\omega_1$ or $\omega>\omega_4$. For anisotropic scattering, the interval $[\omega_1, \omega_4]$ over which $\sigma_{g'\to g}(\omega)$ is nonzero is often only a small portion of the entire range $[-1,1]$ (cf. Fig. 2.3).

In general, the breakpoints in the scattering cross section can be expressed as[23]

$$\omega_1 = [[-1, S(E_g, E_{g'-1}), 1]] , \tag{3.3}$$

$$\omega_2 = [[-1, S(E_{g-1}, E_{g'-1}), 1]] , \tag{3.4}$$

$$\omega_3 = [[-1, S(E_g, E_{g'}), 1]] , \tag{3.5}$$

and

$$\omega_4 = [[-1,\ S(E_{g-1},\ E_{g'}),\ 1]] \ , \tag{3.6}$$

where the notation $[[a,x,b]] = \max[a,\min(x,b)]$, i.e., $= x$ if $a < x < b$, $= b$ if $x \geq b$, or $= a$ if $x \leq a$. The function $S(E,E')$, which is obtained from scattering kinematics, gives the relationship among the initial and final particle energies and the cosine of the scattering angle. For elastic scattering of neutrons from a nucleus of mass number A, this relationship is given by[2]

$$\omega = S(E,E') \equiv \frac{1}{2}\left[(A+1)\sqrt{\frac{E}{E'}} - (A-1)\sqrt{\frac{E'}{E}}\right] \ , \tag{3.7}$$

while for Compton scattering of photons[25]

$$\omega = S(E,E') \equiv 1 - \frac{m_o c^2}{E} + \frac{m_o c^2}{E'} \ , \tag{3.8}$$

where $m_o c^2$ is the rest mass energy of the electron (0.511 MeV).

Under certain conditions, the four breakpoints defined by Eqs. (3.3) - (3.6) are not all distinct. For energy group structures equally spaced in lethargy [$u = \ln(E_{g-1}/E_g)$] or Compton wavelength [$\lambda = (m_o c^2/E)$], ω_2 and ω_3 coalesce. For such a group structure we can define three distinct breakpoints as

$$\omega_1 = [[-1,\ S(E_g,\ E_{g'-1}),\ 1]] \ , \tag{3.9}$$

$$\omega_2 = [[-1,\ S(E_{g-1},\ E_{g'-1}),\ 1]] = [[-1,\ S(E_g,\ E_{g'}),\ 1]] \ , \tag{3.10}$$

and

$$\omega_3 = [[-1,\ S(E_{g-1},\ E_{g'}),\ 1]] \ . \tag{3.11}$$

For within-group scattering (e.g., one-speed transport problems), ω_2, ω_3, and ω_4 are coincident at $\omega = 1$. We can thus define two distinct breakpoints as

$$\omega_1 = [[-1, S(E_g, E_{g'-1}), 1]] , \tag{3.12}$$

and

$$\omega_2 = 1 . \tag{3.13}$$

The utility of the ω_1 breakpoints lies in the fact that the shape of the scattering cross section is usually very smooth in each ω subrange and can generally be well modeled by piecewise, low-order polynomials between the breakpoints.[23] Such piecewise polynomial fits are generally far superior to traditional full-range Legendre polynomial expansions (see, for example, Fig. 2.3). In particular, piecewise linear fits have been shown to be a good approximation for neutron elastic scattering cross sections involving fine-energy-group structure or scattering from light elements,[7] while piecewise quadratic fits have been shown to provide good results for Compton scattering of gamma photons.[22] In this work we will consider both piecewise linear and piecewise quadratic models for the scattering cross section. We can represent a general model for both cases as

$$\sigma_{g'\to g}(\omega) = \sum_{k=1}^{k_{max}} \sigma^k_{g'\to g}(\omega) \tag{3.14}$$

where

$$\sigma^k_{g'\to g}(\omega) = \begin{cases} a_k\omega^2 + b_k\omega + c_k & , \quad -1 \le \omega_k \le \omega \le \omega_{k+1} \le 1 \\ 0 & , \quad \text{otherwise} \end{cases} \tag{3.15}$$

and k_{max} is one less than the number of distinct breakpoints in the scattering cross section.

Given the values of the cross section at the breakpoints, it is a simple matter to compute the coefficients of Eq. (3.15) for a linear fit. In the case of a quadratic fit, it is necessary to know the cross section at one additional point in each subdomain. A convenient point to use is the midpoint of each subdomain.

For a quadratic fit the coefficients are given by[22]

$$a_k = D_1/D \ , \tag{3.16}$$

$$b_k = D_2/D \ , \tag{3.17}$$

and

$$c_k = D_3/D \ , \tag{3.18}$$

where

$$D = \omega_k^2[\omega_{k+\frac{1}{2}} - \omega_{k+1}] - \omega_{k+\frac{1}{2}}^2[\omega_k - \omega_{k+1}] + \omega_{k+1}^2[\omega_k - \omega_{k+\frac{1}{2}}] \ , \tag{3.19}$$

$$D_1 = \sigma_k[\omega_{k+\frac{1}{2}} - \omega_{k+1}] - \sigma_{k+\frac{1}{2}}[\omega_k - \omega_{k+1}] + \sigma_{k+1}[\omega_k - \omega_{k+\frac{1}{2}}] \ , \tag{3.20}$$

$$D_2 = \omega_k^2[\sigma_{k+\frac{1}{2}} - \sigma_{k+1}] - \omega_{k+\frac{1}{2}}^2[\sigma_k - \sigma_{k+1}] + \omega_{k+1}^2[\sigma_k - \sigma_{k+\frac{1}{2}}] \ , \tag{3.21}$$

and

$$D_3 = \omega_k^2[\omega_{k+\frac{1}{2}}\,\sigma_{k+1} - \omega_{k+1}\,\sigma_{k+\frac{1}{2}}] - \omega_{k+\frac{1}{2}}^2[\omega_k\,\sigma_{k+1} - \omega_{k+1}\,\sigma_k]$$

$$+ \omega_{k+1}^2[\omega_k\,\sigma_{k+\frac{1}{2}} - \omega_{k+\frac{1}{2}}\,\sigma_k] \ . \tag{3.22}$$

In Eqs. (3.19) through (3.22) $\omega_{k+\frac{1}{2}}$ is the cosine of the scattering angle at the midpoint of the k'th subdomain and σ_k, $\sigma_{k+\frac{1}{2}}$, and σ_{k+1} are the cross section values at ω_k, $\omega_{k+\frac{1}{2}}$, and ω_{k+1}, respectively.

For a piecewise linear fit the coefficients of Eq. (3.15) are given by

$$a_k = 0 \quad , \tag{3.23}$$

$$b_k = \frac{\sigma_{k+1} - \sigma_k}{\omega_{k+1} - \omega_k} \quad , \tag{3.24}$$

and

$$c_k = \frac{\omega_{k+1}\,\sigma_k - \omega_k\,\sigma_{k+1}}{\omega_{k+1} - \omega_k} \quad . \tag{3.25}$$

3.1.2 Approximation of the Angular Flux

The second approximation needed to evaluate the scattering source term of Eq. (3.2) is a representation of the angular flux density. Perhaps the simplest approximation is to represent the angular flux by a series of straight lines between the discrete ordinates $\{\mu_i\}$. This approximation was the basis of Carlson's original S_N method.[2] In this work, we will utilize this approximation and also generalize it to higher-order, piecewise polynomial fits.

In particular, consider a set of (NM + 1) discrete ordinates $\{\mu_i\}$, where $\mu_1 = -1$ and $\mu_{NM+1} = 1$. We can divide this set into M segments of N + 1 discrete ordinates each. Let the ordinates at the boundaries of each segment be denoted by $\bar{\mu}_j$, j = 1,..., M + 1, where $\bar{\mu}_j = \mu_{(j-1)N+1}$.

In each of the M segments, the angular flux can be approximated by an N'th order polynomial through the N + 1 ordinates in that segment. In particular, the flux in the j'th segment can be approximated by an N'th order Lagrange polynomial as

$$\Phi_g(\mu) = \sum_{i=jN-N+1}^{jN+1} L_i(\mu)\, \Phi_g(\mu_i) \quad , \quad \bar{\mu}_j \leq \mu \leq \bar{\mu}_{j+1} \tag{3.26}$$

where

$$L_i(\mu) \equiv \prod_{\substack{k=jN-N+1 \\ k\neq i}}^{jN+1} \frac{\mu-\mu_k}{\mu_i-\mu_k} \quad , \quad \bar{\mu}_j \leq \mu \leq \bar{\mu}_{j+1} \ . \tag{3.27}$$

The angular expansion of Eq. (3.26) may be extended to the whole range $\mu \in [-1,1]$ as

$$\Phi_g(\mu) = \sum_{i=1}^{NM+1} L_i(\mu)\ \Phi_g(\mu_i) \quad , \quad -1 \leq \mu \leq 1 \tag{3.28}$$

where the full range Lagrange polynomials are defined by

$$L_i(\mu) \equiv \sum_{j=1}^{M} \left\{ \prod_{\substack{k=jN-N+1 \\ k\neq i}}^{jN+1} \frac{\mu-\mu_k}{\mu_i-\mu_k} \right\} H([\mu_i-\bar{\mu}_j][\bar{\mu}_{j+1}-\mu_i]) \ . \tag{3.29}$$

In Eq. (3.29) $H(x)$ is the unit step function [i.e. $H(x) = 0$, $x < 0$; $H(x) = 1$, $x \geq 0$], so that $L_i(\mu)$ vanishes unless μ and μ_i belong to the j'th segment.

3.2 Decomposition of the Source Integrals

Having developed explicit piecewise polynomial approximations for the scattering cross section and the angular flux density, we now consider the resulting form of the scattering source term of Eq. (3.2). With the piecewise quadratic approximation for $\sigma_{g'\to g}(\omega)$ of Eqs. (3.14) and (3.15), the scattering source term can be written as

$$S_{g'\to g}(\mu) = 2 \int_{-1}^{1} d\mu' \int_{0}^{\pi} d\phi \sum_{k=1}^{k_{max}} \sigma^k_{g'\to g}(\omega)\ \Phi_{g'}(\mu') \tag{3.30}$$

or, equivalently,

$$S_{g'\to g}(\mu) = \sum_{k=1}^{k_{max}} S^k(\mu) \ , \tag{3.31}$$

where

$$S^k(\mu) \equiv 2 \int_{-1}^{1} d\mu' \int_{0}^{\pi} d\phi \ \sigma^k_{g'\to g}(\omega) \ \Phi_{g'}(\mu'). \tag{3.32}$$

The integration of Eq. (3.32) can be performed analytically using the piecewise polynomial approximations for $\sigma_{g'\to g}(\omega)$ and $\Phi_{g'}(\mu')$. In order to carry out the integration, it is first necessary to decompose the integration ranges of μ' and ϕ into subranges, in each of which the integrands assume a distinct functional form.

In Sec. 3.1.1 it was noted that $\sigma^k_{g'\to g}(\omega)$ is zero outside the interval $[\omega_k, \omega_{k+1}]$. Because ω is a function of μ, μ', and ϕ [cf. Eq. (2.2)], there exist corresponding limits of the μ' and ϕ integrals of Eq. (3.32) outside of which the integrand is identically zero. In this section we will consider the specific limits of the μ' and ϕ integrals for Eq. (3.32) and the form of the integrands in each of the resulting integration subranges.

3.2.1 Restriction of the Azimuthal Integration Range

In order to evaluate the inner integral (i.e., the integral over ϕ) of Eq. (3.32), it is first necessary to determine the precise limits of ϕ for which $\sigma^k_{g'\to g}(\omega)$ is nonzero. The desired limits can be found from the iso-ω contours in the (μ', ϕ) integration plane as shown in Figs. 3.1 - 3.3. These contours are obtained by plotting ϕ as a function of μ' for fixed values of μ and ω, using Eq. (2.2). The minimum and maximum values of ϕ for which $\sigma^k_{g'\to g}(\omega)$ is nonzero depend on μ and μ' and equal, respectively, the ϕ values on the ω_{k+1} and ω_k contours (or their

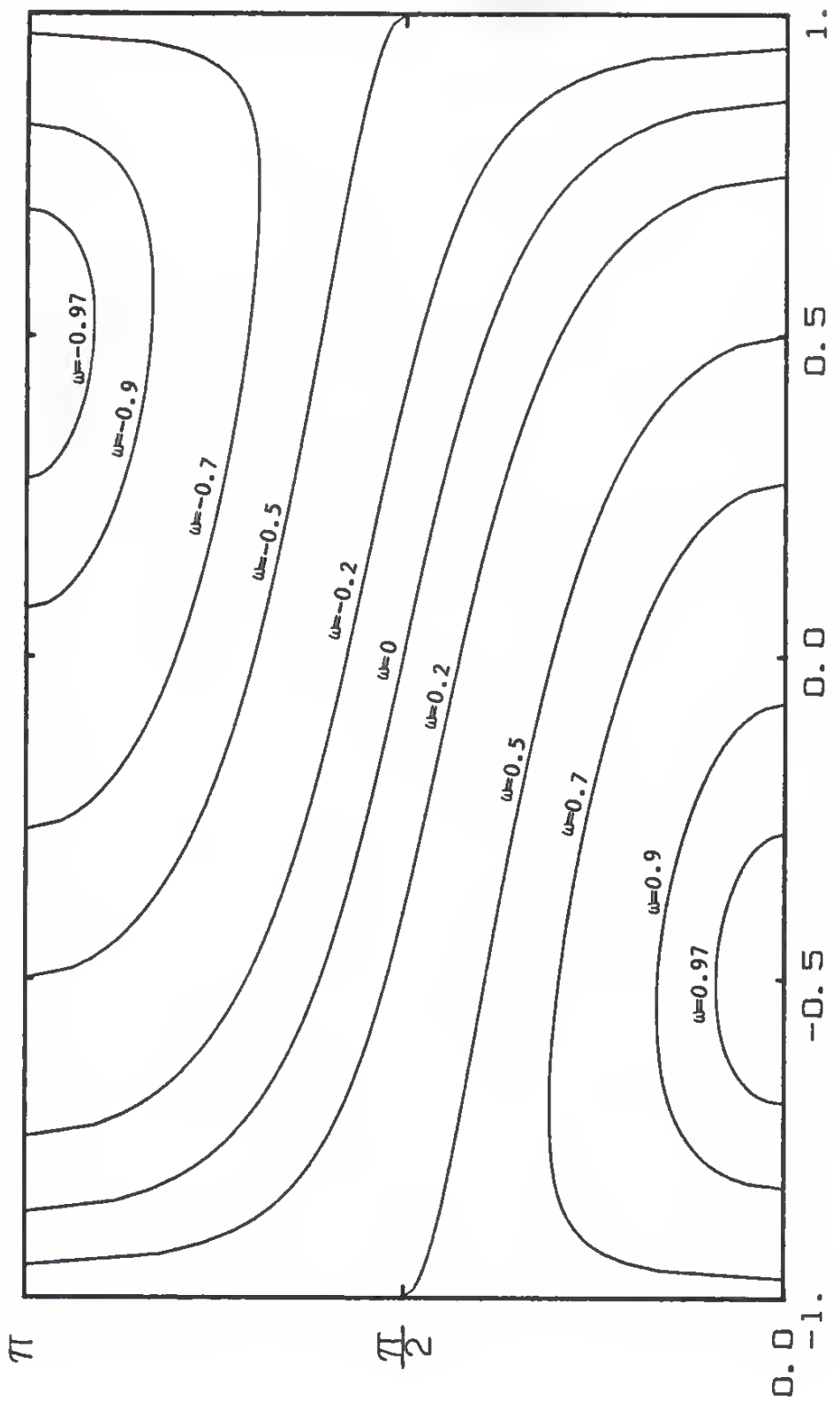

Fig. 3.1. Iso-ω contours in the μ'-φ plane for μ = -0.5.

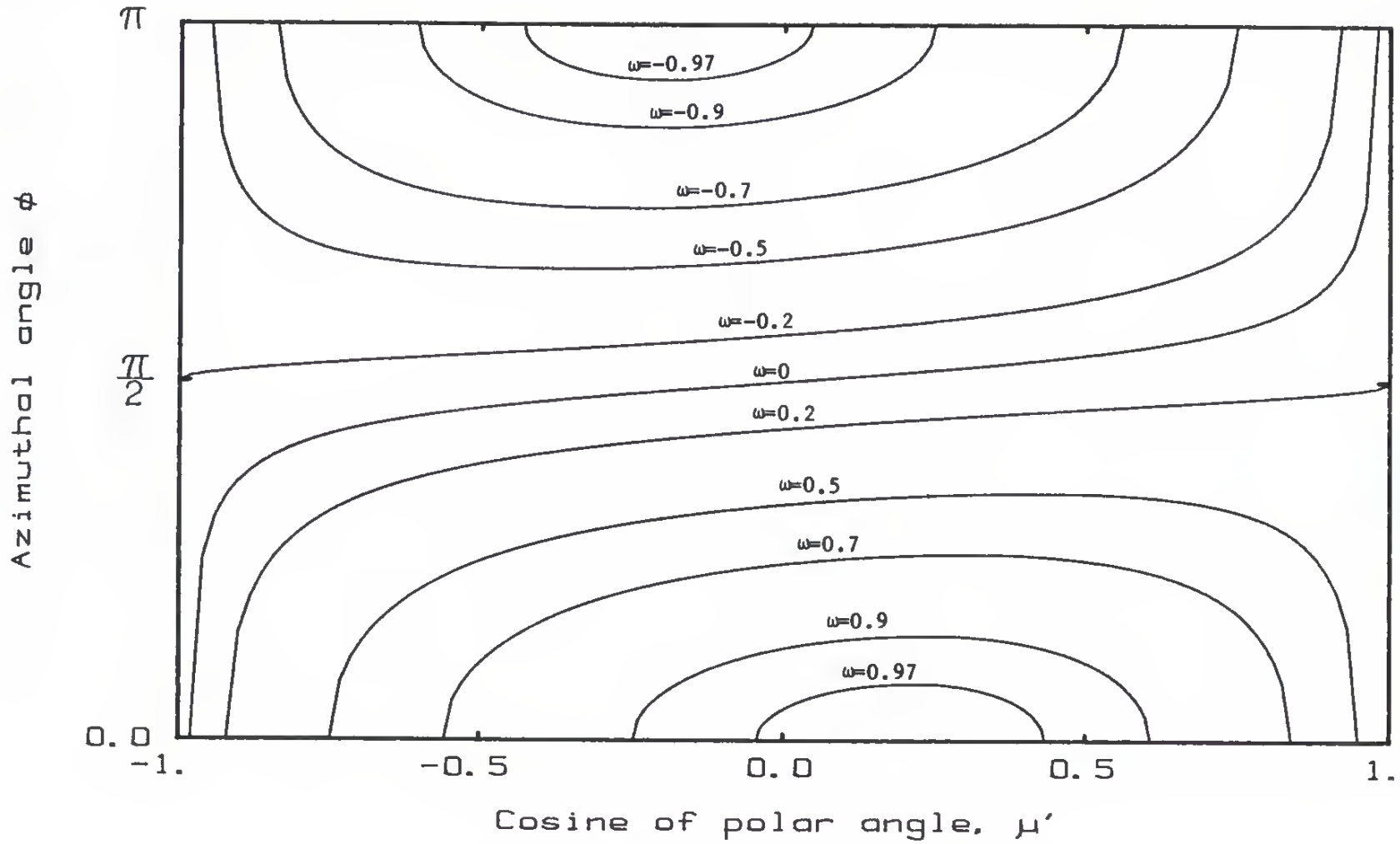

Fig. 3.2. Iso-ω contours in the μ'-ϕ plane for μ = 0.2.

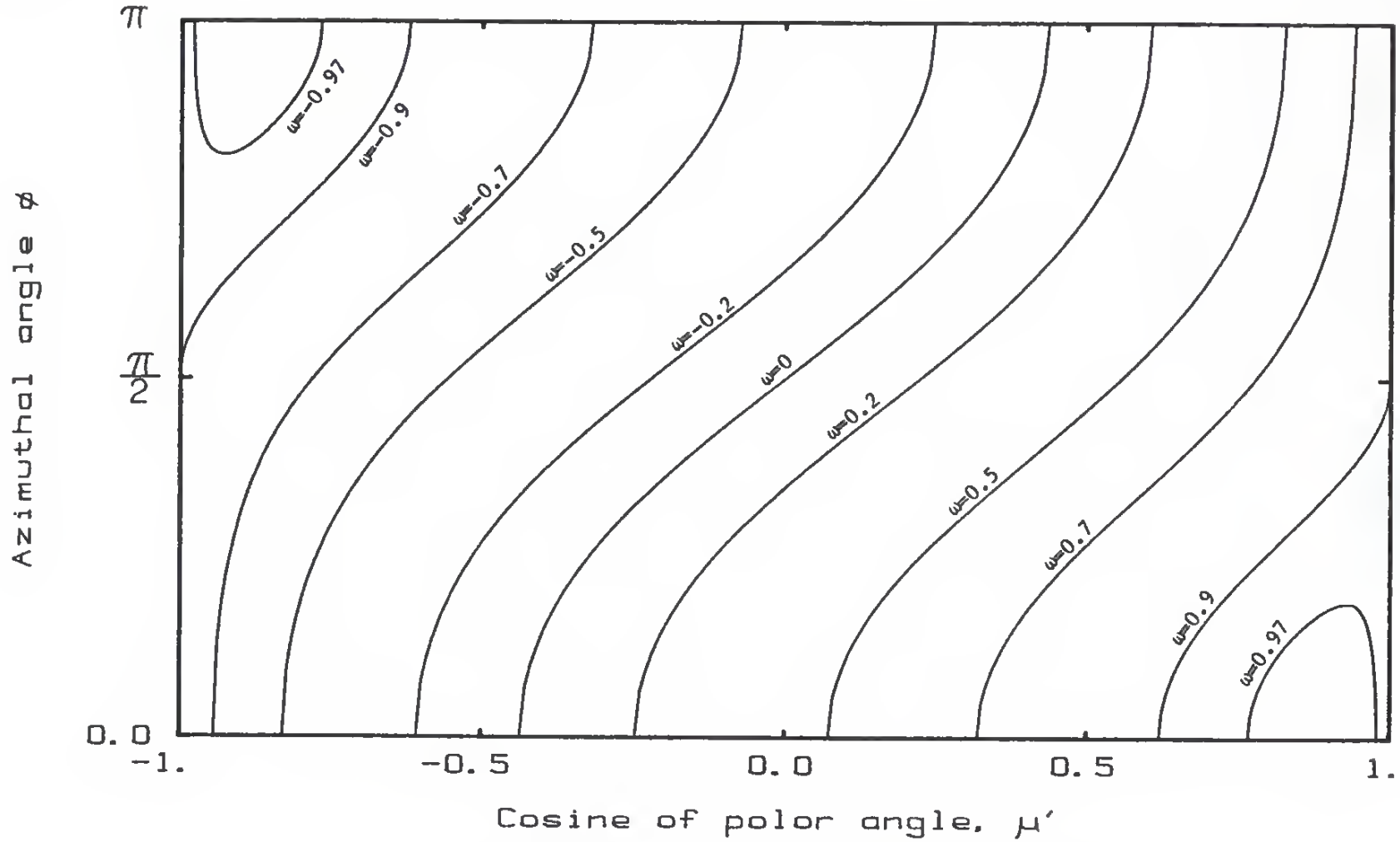

Fig. 3.3. Iso-ω contours in the μ'-φ plane for μ = 0.9.

limiting values of $\phi = 0$ and $\phi = \pi$). The ϕ integration range is thus reduced from $[0, \pi]$ to $[\phi^{k+1}(\mu,\mu'), \phi^{k}(\mu,\mu')]$, where, from Eq. (2.2),

$$\phi^{k}(\mu,\mu') \equiv \cos^{-1}\left[\left[-1, \frac{\omega_k - \mu\mu'}{(1-\mu^2)^{\frac{1}{2}}\,(1-\mu'^2)^{\frac{1}{2}}}, 1\right]\right]. \tag{3.33}$$

The inner integral of Eq. (3.32) thus becomes

$$I^{k}(\mu,\mu') \equiv \int_0^{\pi} d\phi\ \sigma^{k}_{g'\to g}(\omega) = \int_{\phi^{k+1}}^{\phi^{k}} d\phi\ (a_k\omega^2 + b_k\omega + c_k), \tag{3.34}$$

which, upon use of Eq. (2.2), can be integrated to give

$$\begin{aligned} I^{k}(\mu,\mu') &= [a_k\mu^2\mu'^2 + b_k\mu\mu' + c_k]\,(\phi^{k} - \phi^{k+1}) \\ &+ (1-\mu^2)^{\frac{1}{2}}(1-\mu'^2)^{\frac{1}{2}}[2a_k\mu\mu' + b_k](\sin\phi^{k} - \sin\phi^{k+1}) \\ &+ \frac{a_k}{2}(1-\mu^2)(1-\mu'^2)[\phi^{k} - \phi^{k+1} + \sin\phi^{k}\cos\phi^{k} - \sin\phi^{k+1}\cos\phi^{k+1}]. \end{aligned} \tag{3.35}$$

Substitution of Eq. (3.34) into Eq. (3.32) yields

$$S^{k}(\mu) = 2\int_{-1}^{1} d\mu'\ I^{k}(\mu,\mu')\ \Phi_{g'}(\mu'). \tag{3.36}$$

Before we proceed with the evaluation of the μ' integral of Eq. (3.36), it is instructive to examine the scattering source as defined by Eqs. (3.31) and (3.36), i.e.,

$$S_{g'\to g}(\mu) = \sum_{k=1}^{k_{max}} 2\int_{-1}^{1} d\mu'\ I^{k}(\mu,\mu')\ \Phi_{g'}(\mu'). \tag{3.37}$$

This expression could be evaluated by numerical quadrature to yield

$$S_{g'\to g}(\mu) = \sum_{k=1}^{k_{max}} \sum_{j=1}^{NM+1} 2\ I^{k}(\mu,\mu_j)\ w_j\ \Phi_{g'}(\mu_j). \tag{3.38}$$

Comparison of Eq. (3.38) with Eq. (2.48) shows that the exact kernel cross section defined in Section 2.5 can thus be calculated as

$$\sigma_{g'\to g}(\mu_j\to\mu_i) = 2 \sum_{k=1}^{k_{max}} I^k(\mu_i,\mu_j) \tag{3.39}$$

3.2.2 Evaluation of the Polar Integral

In order to evaluate the μ' integral of Eq. (3.36) analytically, it is first necessary to decompose the μ' integration range into several subranges, in each of which $I^k(\mu,\mu')$ and $\phi_{g'}(\mu')$ assume a single functional form. The form of $I^k(\mu,\mu')$ in each subrange is dependent on ϕ^k and ϕ^{k+1}, which take on different forms depending on μ'. From Figs. 3.1 - 3.3, it is seen that ϕ^k and ϕ^{k+1} assume a single functional form (namely, 0, π, or $\cos^{-1}\{(\omega-\mu\mu')/[(1-\mu^2)^{\frac{1}{2}}(1-\mu'^2)]\}$) in at most five subintervals of $\mu' \in [-1,1]$. Let the μ' breakpoints which define these subintervals be denoted by $\mu'_{k\ell}$, $\ell = 1,\ldots, 6$. These breakpoints, which are dependent on μ, ω_k, and ω_{k+1}, are the μ' values at which the ω_k and ω_{k+1} contours in the μ'-ϕ space of Figs. 3.1 - 3.3 intersect the lines $\phi = 0$ and $\phi = \pi$. In particular, $\mu'_{k1} = -1$, $\mu'_{k6} = 1$, and the other four values are the ordered roots of Eq. (2.2) with $\phi = 0$ or $\phi = \pi$, i.e.,

$$\{\mu'_{k2},\mu'_{k3},\mu'_{k4},\mu'_{k5}\} = \text{Ordered } [\bar{\mu}'_{k2},\bar{\mu}'_{k3},\bar{\mu}'_{k4},\bar{\mu}'_{k5}], \tag{3.40}$$

where

$$\bar{\mu}'_{k2} = \mu\omega_k + [(1-\mu^2)(1-\omega_k^2)]^{\frac{1}{2}}, \tag{3.41}$$

$$\bar{\mu}'_{k3} = \mu\omega_k - [(1-\mu^2)(1-\omega_k^2)]^{\frac{1}{2}}, \tag{3.42}$$

$$\bar{\mu}'_{k4} = \mu\omega_{k+1} + [(1-\mu^2)(1-\omega_{k+1}^2)]^{\frac{1}{2}}, \tag{3.43}$$

and

$$\bar{\mu}'_{k5} = \mu\omega_{k+1} - [(1-\mu^2)(1-\omega_{k+1}^2)]^{\frac{1}{2}} \quad . \tag{3.44}$$

Unless ω_k or ω_{k+1} is equal to $\pm\mu$, ϕ^k and ϕ^{k+1} will both equal 0 or π in the intervals $[\mu'_{k1}, \mu'_{k2}]$ and $[\mu'_{k5}, \mu'_{k6}]$. Thus $I^k(\mu,\mu')$ will vanish in these intervals, so they can be neglected when evaluating Eq. (3.36).

Further decomposition of the μ' integration range can be achieved by considering the piecewise polynomial representation of the angular flux. In each $[\bar{\mu}_j,\bar{\mu}_{j+1}]$ segment the flux is represented by Eq. (3.26), where the interpolating polynomial of Eq. (3.27) can be expressed more simply as

$$L_i(\mu) = \sum_{n=0}^{N} C_n^i \mu^n \quad , \quad \bar{\mu}_j \leq \mu \leq \bar{\mu}_{j+1} \tag{3.45}$$

Because the coefficients C_n^i are different in each of the j segments, the integrand of Eq. (3.36) assumes a different form in each segment.

There are thus 6 breakpoints $\{\mu'_{k\ell}\}$ in the μ' integration range of Eq. (3.36) imposed by the functional form of $I^k(\mu,\mu')$, and M+1 breakpoints $\{\bar{\mu}_j\}$ imposed by the flux interpolating polynomials. However, $\mu'_{k1} = \bar{\mu}_1 = -1$ and $\mu'_{k6} = \bar{\mu}_{M+1} = 1$, so the number of distinct breakpoints is at most M+5 (note that it is possible for some of the other $\mu'_{k\ell}$ and $\bar{\mu}_j$ breakpoints to be coincident). These breakpoints divide the μ' integration range into at most M+4 subranges, in each of which the integrand of Eq. (3.36) assumes a single functional form.

Let $\{\nu_\ell^k\}$ represent the ordered values of $\{\mu'_{k\ell}\}$ and $\{\bar{\mu}_j\}$. Equation (3.36) can then be rewritten as

$$S^k(\mu) = 2 \sum_{\ell=1}^{M+4} \int_{\nu_\ell^k}^{\nu_{\ell+1}^k} d\mu' \; I^k(\mu,\mu') \; \Phi_{g'}(\mu'). \tag{3.46}$$

Use of Eqs. (3.28) and (3.45) allows Eq. (3.46) to be expressed as

$$S^k(\mu) = 2 \sum_{i=1}^{NM+1} \left\{ \sum_{\ell=1}^{M+4} \sum_{n=0}^{N} F^{k\ell in}(\mu) \right\} \Phi_{g'}(\mu_i), \tag{3.47}$$

where

$$F^{k\ell in}(\mu) \equiv C_n^i \int_{\nu_\ell^k}^{\nu_{\ell+1}^k} d\mu' \; \mu'^n \; I^k(\mu,\mu'). \tag{3.48}$$

The problem of evaluating the scattering source components $S^k(\mu)$ is thus reduced to the evaluation of the integrals $F^{k\ell in}(\mu)$ as defined by Eq. (3.48). In the next section we will examine the analytical evaluation of these integrals.

3.3 Evaluation of the $F^{k\ell in}$ Integrals

In order to evaluate the integrals $F^{k\ell in}(\mu)$ of Eq. (3.48), we must consider the exact form of the integrand in each of the integration subranges $[\nu_\ell^k, \nu_{\ell+1}^k]$. Substitution of Eq. (3.35) into Eq. (3.48) yields

$$F^{k\ell in}(\mu) = C_n^i \{ G^{k\ell n}(\mu;k) - G^{k\ell n}(\mu;k+1) \}, \tag{3.49}$$

where

$$\begin{aligned} G^{k\ell n}(\mu;k') \equiv \int_{\nu_\ell^k}^{\nu_{\ell+1}^k} d\mu' \Big\{ & \mu'^n [a_k \mu^2 \mu'^2 + b_k \mu\mu' + c_k] \; \phi^{k'} \\ & + \mu'^n (1-\mu^2)^{\frac{1}{2}} (1-\mu'^2)^{\frac{1}{2}} [2a_k \mu\mu' + b_k] \sin\phi^{k'} \\ & + \frac{a_k}{2} \mu'^n \; (1-\mu^2)(1-\mu'^2)[\phi^{k'} + \sin\phi^{k'} \cos\phi^{k'}] \Big\}. \end{aligned} \tag{3.50}$$

The exact form of $G^{k\ell n}(\mu;k')$ depends on the form taken by $\phi^{k'}$. In Section 3.2 it was shown that $\phi^{k'}$ can, in general, take on three forms (cf. Eq. (3.33)), although only one in a given integration subrange. Thus $G^{k\ell n}(\mu;k')$ is given by one of three possible forms, viz.:

Case 1: $\phi^{k'} = 0;$

$$G^{k\ell n}(\mu;k') = 0 \ . \tag{3.51}$$

Case 2: $\phi^{k'} = \pi;$

$$G^{k\ell n}(\mu;k') = \pi \left\{ \left(\frac{a_k \mu^2}{n+3} - \frac{a_k(1-\mu^2)}{2(n+3)} \right) \left[(\nu^k_{\ell+1})^{n+3} - (\nu^k_\ell)^{n+3} \right] \right.$$

$$+ \frac{b_k \mu}{n+2} \left[(\nu^k_{\ell+1})^{n+2} - (\nu^k_\ell)^{n+2} \right]$$

$$\left. + \left(\frac{c_k}{n+1} + \frac{a_k(1-\mu^2)}{2(n+1)} \right) \left[(\nu^k_{\ell+1})^{n+1} - (\nu^k_\ell)^{n+1} \right] \right\} . \tag{3.52}$$

Case 3: $\phi^{k'} = \cos^{-1}\left(\frac{\omega_{k'} - \mu\mu'}{(1-\mu^2)^{\frac{1}{2}}(1-\mu'^2)^{\frac{1}{2}}} \right);$

$$\sin\phi^{k'} = \left(\frac{(1 - \mu^2 - \omega^2_{k'} + 2\omega_{k'}\mu\mu' - \mu'^2)^{\frac{1}{2}}}{(1 - \mu^2)^{\frac{1}{2}} (1 - \mu'^2)^{\frac{1}{2}}} \right);$$

$$G^{k\ell n}(\mu;k') = \left\{ \left(\frac{a_k}{2} (3\mu^2 - 1) \right) f^{n+2}(\mu') + b_k \mu \, f^{n+1}(\mu') \right.$$

$$+ \left(c_k + \frac{a_k}{2} (1 - \mu^2) \right) f^n(\mu')$$

$$\left. + \frac{3}{2} a_k \mu g^{n+1}(\mu') + \left(b_k + \frac{a_k}{2} \omega_{k'} \right) g^n(\mu') \right\} \Bigg|_{\nu^k_\ell}^{\nu^k_{\ell+1}} , \tag{3.53}$$

where the functions $f^n(\mu')$ and $g^n(\mu')$ are defined by

$$f^n(\mu') \equiv \int \mu'^n \cos^{-1}\left(\frac{a - b\mu'}{(1-\mu'^2)^{\frac{1}{2}}}\right) d\mu' \tag{3.54}$$

and

$$g^n(\mu') \equiv \int \mu'^n (c + d\mu' - \mu'^2)^{\frac{1}{2}} d\mu' , \tag{3.55}$$

with

$$a = \omega_k'/(1-\mu^2)^{\frac{1}{2}}, \tag{3.56}$$

$$b = \mu/(1-\mu^2)^{\frac{1}{2}}, \tag{3.57}$$

$$c = 1 - \mu^2 - \omega_k^2,, \tag{3.58}$$

and $$d = 2\omega_k,\mu. \tag{3.59}$$

The integrals of Eqs. (3.54) and (3.55), although somewhat complex, can be evaluated analytically. In the following two subsections we will examine the results of these integrals for n = 0, 1, and 2. These results are sufficient for using linear or quadratic interpolation for the angular flux. If a piecewise linear representation of the scattering cross section is used (i.e., $a_k = 0$), these results also permit the use of cubic interpolation for the flux.

3.3.1 Evaluation of the Functions $f^n(\mu')$

The argument of the arccosine in the integrand of Eq. (3.54) is singular at $\mu' = \pm 1$. From examination of Figs. 3.1 - 3.3, it is clear that, when $\mu' = 1$, $\phi = 0$ or π (except when ω is exactly equal to μ). Thus for $\mu' = 1$, $G^{k\ell n}(\mu;k')$ is given by case 3 only if $\omega_{k'} = \mu$. If $\omega_{k'} = \mu$, it is clear from Eqs. (3.56) and (3.57) that a = b. The singularity in the integrand of Eq. (3.54) can then be removed by factorization, i.e.

$$\left.\frac{a - b\mu'}{(1-\mu'^2)^{\frac{1}{2}}}\right|_{\mu'=1} = \left.\frac{a(1-\mu')}{(1+\mu')^{\frac{1}{2}}(1-\mu')^{\frac{1}{2}}}\right|_{\mu'=1} = 0 \ . \tag{3.60}$$

The singularity at $\mu' = -1$ can be removed in the same manner.

With the singularities removed, the functions $f^n(\mu')$ of Eq. (3.54) can be evaluated analytically using integration by parts and integral tables.[32,33] The following results are obtained for $f^n(\mu')$:

$$f^0(\mu') = \mu' h_1(\mu') + \frac{a}{r} h_2(\mu') + h_3(\mu') - h_4(\mu'), \tag{3.61}$$

$$f^1(\mu') = \frac{1}{2}\left\{\mu'^2 h_1(\mu') + \left(\frac{at - br^2}{r^3}\right) h_2(\mu') - h_3(\mu') - h_4(\mu') + a h_5(\mu')\right\}, \tag{3.62}$$

$$f^2(\mu') = \frac{1}{3}\left\{\mu'^3 h_1(\mu') + \frac{a}{2r}[p(3t^2p - 2b^2 - a^2 + 1) + 2]\, h_2(\mu') + h_3(\mu') - h_4(\mu') + \frac{1}{2}[a\mu' - 2b + 3atp]\, h_5(\mu')\right\}, \tag{3.63}$$

$$f^3(\mu') = \frac{1}{4}\left\{\mu'^4 h_1(\mu') + \frac{a^2}{2r^5}[5bt^2p - 3bs]\, h_2(\mu') - \frac{b}{2r^3}[3t^2p - 3a^2 + 2r^2 + 1]\, h_2(\mu') - h_3(\mu') - h_4(\mu') - \frac{b}{2}[\mu' + 3tp]\, h_5(\mu') + \frac{a}{6}[2\mu'^2 + 5tp\mu' - 4sp + 15t^2p^2 + 6]\, h_5(\mu')\right\}, \tag{3.64}$$

and

$$f^4(\mu') = \frac{1}{5}\left\{\mu'^5 h_1(\mu') + \frac{t}{2r^5}\left(\frac{7at}{4r^2} - b\right)[5t^2p - 3s]h_2(\mu')\right.$$

$$+ \frac{a}{2r^3}[3t^2p - 2b^2 + 2r^2 - s]\, h_2(\mu')$$

$$- \frac{3as}{8r^5}[3t^2p - s]\, h_2(\mu') + h_3(\mu') - h_4(\mu')$$

$$+ \left(\frac{7atp^2 - 4bp}{24}\right)\left(\frac{2\mu'^2}{p} + 5t\mu' - 4s + 15t^2p\right) h_5(\mu')$$

$$\left. + \left(\frac{a}{2} - \frac{3asp}{8}\right)[\mu' + 3tp]\, h_5(\mu') + \left(\frac{a\mu'^3}{4} - b\right) h_5(\mu')\right\}, \qquad (3.65)$$

where

$$h_1(\mu') \equiv \cos^{-1}\left(\frac{a - b\mu'}{(1-\mu'^2)^{\frac{1}{2}}}\right), \qquad (3.66)$$

$$h_2(\mu') \equiv \sin^{-1}\left(\frac{-(b^2+1)\mu' + ab}{(1-a^2+b^2)^{\frac{1}{2}}}\right), \qquad (3.67)$$

$$h_3(\mu') \equiv \frac{1}{2}\frac{a+b}{|a+b|}\sin^{-1}\left(\frac{(ab+b^2+1)(\mu'+1) - (a+b)^2}{|\mu'+1|\ (1-a^2+b^2)^{\frac{1}{2}}}\right), \qquad (3.68)$$

$$h_4(\mu') \equiv \frac{1}{2}\frac{a-b}{|a-b|}\sin^{-1}\left(\frac{(ab-b^2-1)(\mu'-1) - (a-b)^2}{|\mu'-1|\ (1-a^2+b^2)^{\frac{1}{2}}}\right), \qquad (3.69)$$

$$h_5(\mu') \equiv \frac{\sqrt{-(b^2+1)\mu'^2 + 2ab\mu' - (a^2-1)}}{b^2+1}, \qquad (3.70)$$

$$p \equiv (b^2+1)^{-1}, \qquad (3.71)$$

$$r \equiv (b^2+1)^{\frac{1}{2}} , \tag{3.72}$$

$$s \equiv a^2 - 1, \tag{3.73}$$

and

$$t \equiv ab . \tag{3.74}$$

3.3.2 Evaluation of the Functions $g^n(\mu')$

The functions $g^n(\mu')$ of Eq. (3.55) can be evaluated using integral tables.[32] The following results are obtained for $g^n(\mu')$:

$$g^0(\mu') = \frac{(2\mu'-d)(c+d\mu'-\mu'^2)^{\frac{1}{2}}}{4} - \frac{d^2 + 4c}{8} h_6(\mu'), \tag{3.75}$$

$$g^1(\mu') = -\frac{(c+d\mu'-\mu'^2)^{3/2}}{3} - \frac{d(d-2\mu')(c+d\mu'-\mu'^2)^{\frac{1}{2}}}{8}$$

$$- \frac{d(d^2+4c)}{16} h_6(\mu'), \tag{3.76}$$

$$g^2(\mu') = -\left(\mu' + \frac{5d}{6}\right) \frac{(c+d\mu'-\mu'^2)^{3/2}}{4} + \frac{5d^2+4c}{16} g^0(\mu'), \tag{3.77}$$

and

$$g^3(\mu') = -\frac{\mu'^2(c+d\mu'-\mu'^2)^{3/2}}{5} + \frac{7d}{10} g^2(\mu') + \frac{2c}{5} g^1(\mu'), \tag{3.78}$$

where

$$h_6(\mu') = \sin^{-1}\left(\frac{d-2\mu'}{(d^2+4c)^{\frac{1}{2}}}\right). \tag{3.79}$$

It can be shown that the function $h_6(\mu')$ defined by Eq. (3.79) is equivalent to the function $h_2(\mu')$ defined by Eq. (3.67).

3.4 Final Form of the Scattering Source Term

With the results of sections 3.1 - 3.3, the final form of the scattering source term can be written as (cf. Eqs. (3.31) and (3.47))

$$S_{g'\to g}(\mu) = \sum_{i=1}^{NM+1} F_{g'\to g}(\mu_i \to \mu)\, \Phi_{g'}(\mu_i), \tag{3.80}$$

where

$$F_{g'\to g}(\mu_i \to \mu) \equiv 2 \sum_{k=1}^{k_{max}} \sum_{\ell=1}^{M+4} \sum_{n=0}^{N} F^{k\ell in}(\mu). \tag{3.81}$$

It should be noted that the form of Eq. (3.80) is exactly the same as the form of the exact kernel scattering source term (Eq. (2.48)). Thus any discrete ordinates code based on the exact kernel method can be used with the above results.

In the next chapter, several slab albedo problems are examined. Specifically, results for these problems obtained using the approximated scattering kernel method are compared to those obtained using the exact kernel and Legendre expansion methods.

4. USE OF THE APPROXIMATED SCATTERING KERNEL METHOD IN DISCRETE-ORDINATES TRANSPORT CALCULATIONS

In the previous chapter, a new method of evaluating the scattering source term in discrete-ordinates transport calculations was examined. The purpose of deriving this method was to find a means of evaluating the scattering source term which, for highly anisotropic problems, provides better accuracy than does the Legendre expansion method and which does not suffer from the problem of angular coverage associated with the exact kernel method.

In this chapter we will apply this new method, termed the approximated scattering kernel method, to several one-speed slab albedo transport problems and compare the results obtained to those obtained using the exact kernel and Legendre expansion methods. However, before examining the results of these calculations, let us consider the general form of the slab albedo problem.

4.1 The Slab Albedo Problem

Consider a source-free, infinite, homogeneous slab of thickness τ mean-free-path lengths in a vacuum. The slab is illuminated on one face by a monodirectional beam of particles. This problem has been widely studied[1,26,34] and is known as the "slab albedo problem". Let the incident flux at $x = 0$ be in direction $\mu_s > 0$, where μ_s is one of the discrete ordinates $\{\mu_i\}$. The boundary conditions are then

$$\Phi(0,\mu) = \delta(\mu-\mu_s) \quad , \quad \mu > 0 \tag{4.1}$$

and

$$\Phi(\tau,\mu) = 0 \qquad , \ \mu < 0 \tag{4.2}$$

where $\delta(\mu-\mu_s)$ is the Dirac delta distribution.

For the simple case of isotropic scattering, the exact analytical solution for the reflected and transmitted angular fluxes can be obtained by using the X-Y functions of radiative transfer.[34] In terms of these X and Y functions, the reflected and transmitted angular fluxes are given by

$$\Phi(0,\mu) = \frac{c\mu_s}{2(\mu+\mu_s)} [X(\mu)X(\mu_s) - Y(\mu)Y(\mu_s)] \quad , \ \mu < 0 \tag{4.3}$$

and

$$\Phi(\tau,\mu) = \frac{c\mu_s}{2(\mu-\mu_s)} [Y(\mu)X(\mu_s) - X(\mu)Y(\mu_s)] \quad , \ \mu > 0 \ . \tag{4.4}$$

Values of $X(\mu)$ and $Y(\mu)$ are tabulated in Ref. 35 for various values of c and τ.

For both isotropic and anisotropic scattering, the diffusely reflected and transmitted angular fluxes obey an important reciprocity principle.[34] [The diffusely reflected and transmitted fluxes consist only of those particles which have undergone one or more scattering processes. Thus the uncollided transmitted flux in the source direction, $\Phi(0,\mu_s)\exp(-\tau/\mu_s)$, is not included in the diffusely transmitted flux $\Phi(\tau,\mu_s)$.] The reciprocity principle can be stated as follows:

$$\mu\Phi(0;\mu_s;-\mu) = \mu_s\Phi(0;\mu;-\mu_s) \tag{4.5}$$

and

$$\mu\Phi(\tau;\mu_s;\mu) = \mu_s\Phi(\tau;\mu;\mu_s) \tag{4.6}$$

where $\Phi(x;\mu_s;\mu)$ is the angular flux at position x in direction μ due to an incident flux at x = 0 in direction μ_s.

The difference between the diffusely transmitted flux and the total transmitted flux depends on the source angle of the incident flux as well as the slab thickness. In some cases, such as a normally incident flux on a thin slab, the uncollided transmitted flux may be much greater than the diffusely transmitted flux. Since we are primarily interested in the effects of scattering source calculations in this study, we will compare only the diffuse fluxes in the problems of Sections 4.2 and 4.3.

4.1.1 Incident-Flux Normalization in Discrete-Ordinates Transport Calculations

To obtain the proper angular fluxes when performing discrete-ordinates transport calculations, it is necessary to normalize the incident flux $\Phi(0,\mu_s)$ in accordance with the boundary condition given in Eq. (4.1). The presence of the delta distribution in Eq. (4.1) implies that, for $\mu > 0$

$$\Phi(0,\mu) = 0 \ , \ \mu \neq \mu_s \tag{4.7}$$

and

$$\int_0^1 d\mu \ \Phi(0,\mu) = 1 \ . \tag{4.8}$$

The specific form of the source normalization is dependent on the method used to evaluate the integral of Eq. (4.8). When numerical quadrature is used (as in the exact kernel or Legendre expansion methods), Eq. (4.8) is evaluated as

$$\sum_{i=1}^{NM+1} w_i \Phi(0,\mu_i) = 1 \tag{4.9}$$

where NM+1 is the number of discrete ordinates. Because the incident flux is zero in all directions other than μ_s, the effective source strength or normalization required to satisfy Eqs. (4.7) and (4.8) is thus (for $\mu_i > 0$)

$$\Phi(0,\mu_i) = \begin{cases} 0 & , \quad \mu_i \neq \mu_s \\ \dfrac{1}{w_s} & , \quad \mu_i = \mu_s \end{cases} \tag{4.10}$$

When the approximated scattering kernel method is used, the source normalization is somewhat more complex. Substitution of Eqs. (3.28) and (3.29) into Eq. (4.8) yields

$$1 = \int_0^1 \sum_{i=1}^{NM+1} \sum_{j=1}^{M} \left\{ \prod_{\substack{k=jN-N+1 \\ k\neq i}}^{jN+1} \frac{\mu-\mu_k}{\mu_i-\mu_k} \right\} H([\mu_i-\bar{\mu}_j][\bar{\mu}_{j+1}-\mu_i])\ \Phi(0,\mu_i)\ d\mu \ . \tag{4.11}$$

Since the incident flux is zero in all directions except μ_s, Eq. (4.11) can be simplified to

$$1 = \Phi(0,\mu_s) \int_0^1 \sum_{j=1}^{M} \left\{ \prod_{\substack{k=jN-N+1 \\ k\neq s}}^{jN+1} \frac{\mu-\mu_k}{\mu_s-\mu_k} \right\} H([\mu_s-\bar{\mu}_j][\bar{\mu}_{j+1}-\mu_s])\ d\mu \ . \tag{4.12}$$

Because the integrand of Eq. (4.12) is zero outside the interval $[\bar{\mu}_j,\bar{\mu}_{j+1}]$ for each j, we can rewrite Eq. (4.12) as

$$1 = \Phi(0,\mu_s) \sum_{j=1}^{M} H([\mu_s-\bar{\mu}_j][\bar{\mu}_{j+1}-\mu_s]) \int_{\bar{\mu}_j}^{\bar{\mu}_{j+1}} \prod_{\substack{k=jN-N+1 \\ k\neq s}}^{jN+1} \frac{\mu-\mu_k}{\mu_s-\mu_k}\, d\mu \ , \qquad (4.13)$$

so that the source normalization becomes

$$\Phi(0,\mu_s) = \left\{ \sum_{j=1}^{M} H([\mu_s-\bar{\mu}_j][\bar{\mu}_{j+1}-\mu_s] \int_{\bar{\mu}_j}^{\bar{\mu}_{j+1}} \prod_{\substack{k=jN-N+1 \\ k\neq s}}^{jN+1} \frac{\mu-\mu_k}{\mu_s-\mu_k}\, d\mu \right\}^{-1} . \qquad (4.14)$$

4.1.2 Treatment of the Discontinuity in the Angular Flux at μ=0

It may be recalled from Sec. 2.3.1 that the angular flux is discontinuous at μ = 0 at any interfaces in a slab. For a homogeneous slab, the only interfaces are the slab surfaces. The angular flux is therefore continuous throughout the interior of the slab and discontinuous at x = 0 and x = τ. Because the angular flux is treated as a piecewise continuous function in the approximated scattering kernel method, this discontinuity can be expected to produce some error in the calculation of the reflected and transmitted angular fluxes.

One means by which this error can be minimized is to place the ordinates immediately on each side of μ = 0 as close to 0 as is practical. However, it must be remembered that the number of spatial nodes required to ensure positivity of the calculated angular fluxes increases as the absolute value of the ordinate closest to μ = 0 decreases [cf. Eq. 2.38)]. This restriction places a practical limitation on how close to zero the discrete ordinates can be located.

An approach to eliminate the effects of the discontinuity at μ = 0 is to let the point μ = 0 be one of the discrete ordinates. More

specifically, by letting $\mu = 0$ be one of the boundaries $\bar{\mu}_j$ in the piecewise polynomial expansion of the angular flux, the scattering source term will not be integrated across $\mu = 0$. This approach is similar to that utilized in the DP_N method, in that the scattering source term is evaluated in the two half-ranges [-1,0] and [0,1] rather than the full range [-1,1].

While this approach would eliminate integration across the flux discontinuity, it introduces another problem, namely, the evaluation of the angular flux at $\mu = 0$. The standard discrete-ordinates equations [Eqs. (2.36) and (2.37)] cannot be used for $\mu = 0$. Hence an alternative method of evaluating the angular fluxes would have to be utilized to calculate $\Phi(x,0)$.

If the flux around $\mu = 0$ were smooth, one could interpolate the flux at 0 with a reasonable degree of accuracy. When the flux is discontinuous, however, interpolation could produce very poor results. Essentially, then, interpolation of the flux at $\mu = 0$ offers no advantage over integrating across $\mu = 0$. As an alternative approach one could evaluate the flux at $\mu = 0+\varepsilon$ and $\mu = 0-\varepsilon$, where ε is a very small number, by extrapolating the flux from the positive and negative directions. Under certain conditions, this approach could work very well. Consider, for example, the transmitted flux emerging from a slab at $x = \tau$. The angular flux in this case is zero for $\mu < 0$, and non-zero for $\mu > 0$. Extrapolation of the flux at $0-\varepsilon$ would produce the correct value (i.e., $\Phi(\tau,0-\varepsilon) = 0$). The accuracy of the extrapolation of $\Phi(\tau,0+\varepsilon)$, however, would depend on the behavior of the flux near $\mu = 0$, as well as on the location of the discrete ordinates used to extrapolate

the flux. If the flux were smooth near $\mu = 0$, the extrapolation could be very accurate. However, if the flux varied rapidly near $\mu = 0$, extrapolation could yield a very poor estimate of $\Phi(\tau,0+\varepsilon)$.

In the transport calculations performed in this work, it was found that the best results were usually obtained by using the full-range expansion of the scattering source term (and thus ignoring the discontinuity at the slab surfaces). In some problems, the use of flux extrapolation produced results which were slightly more accurate than those obtained without extrapolation. However, in most cases the use of flux extrapolation produced no improvement, and, in fact, often led to significant errors. It was therefore decided that the use of flux extrapolation should be avoided because it is not a reliable method of improving the accuracy of transport calculations.

4.2 Results for Isotropic Scattering

The first problem considered is the slab albedo problem with isotropic scattering. The transport medium is a one mean-free-path slab with $c = 1$. Figure 4.1 shows the diffusely reflected and transmitted angular fluxes resulting from unit incident fluxes in directions $\mu_s = 1.0$, $\mu_s = 0.566331$, and $\mu_s = 0.66838$, as calculated using the X-Y functions.

The reflected and transmitted fluxes for the normally incident case were first calculated using each of the scattering source treatments (exact kernel, Legendre expansion, and approximated scattering kernel) with a Lobatto-12 discrete-ordinates set. The approximated scattering kernel calculations used an additional ordinate which was needed to obtain an integral number of flux intervals for piecewise quadratic and

cubic flux expansions. This additional ordinate was placed at $\mu = 0.04$ in an attempt to minimize the error produced by the discontinuity at $\mu = 0$. The results of all the calculations were within about 1% of the fluxes calculated using the X-Y functions. The fluxes calculated using the approximated scattering kernel method with linear, quadratic, and cubic flux expansions were actually somewhat more accurate than the fluxes calculated using the exact kernel and Legendre expansion methods. This difference may be due at least in part to the extra ordinate used in the approximated scattering kernel calculations.

An obvious means of reducing the error in the calculated fluxes is to increase the number of discrete ordinates. To illustrate this effect, the transport calculations were next carried out for the normally incident case with a Lobatto-24 discrete-ordinates set. The approximated scattering kernel calculations again utilized an additional ordinate at $\mu = 0.04$. For each of the scattering source treatments used, nearly all the angular fluxes were within 0.25% of the X-Y results.

Finally, calculations were performed with the Lobatto-24 set for source angles of 0.566331 and 0.066838. For the source angle of 0.566331, the angular fluxes calculated using each of the scattering source treatments were again nearly all within 0.25% of the X-Y fluxes. For the source angle of 0.066838, the error was slightly greater, with all the fluxes within about 0.5% of the X-Y results.

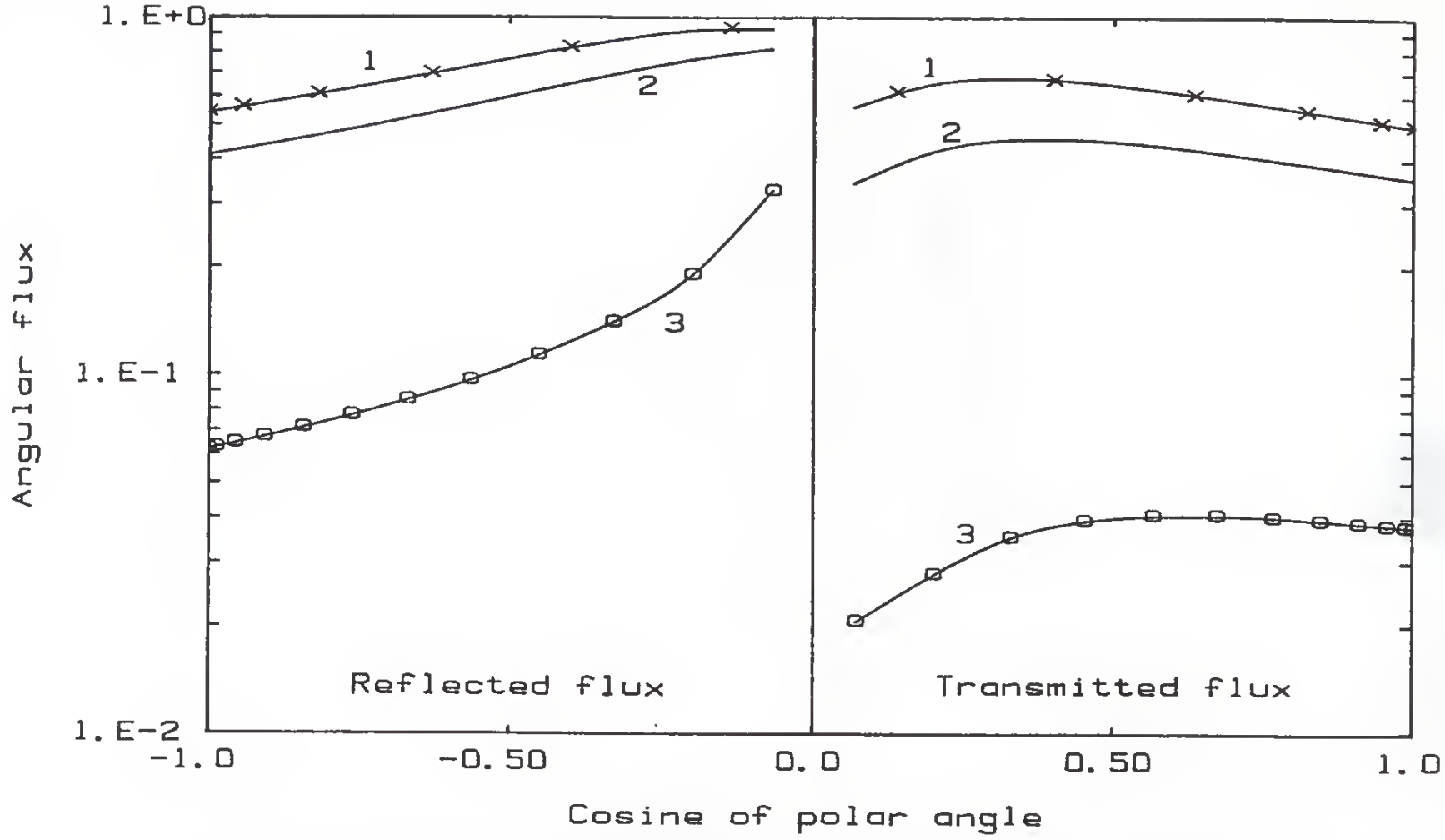

Fig. 4.1. The diffusely reflected and transmitted angular fluxes for a one mean-free-path slab with isotropic scattering and c=1, as calculated using the X-Y functions of radiative transfer. The incident flux directions are: 1) μ_s = 1.0, 2) μ_s = 0.566331, 3) μ_s = 0.066838. The x's on curve 1 indicate the location of the Lobatto-12 ordinates; the o's on curve 3 indicate the location of the Lobatto-24 ordinates.

4.3 Results for Anisotropic Scattering

We next consider three problems which exhibit increasing degrees of scattering anisotropy. The transport medium in each problem is again a one mean-free-path slab with c = 1.

Problem 4.3.1

The first anisotropic scattering problem considered has a scattering cross section whose range of angular support is $\omega \in [0, 1]$. This cross section, which is shown in Fig. 4.2, is representative of the scattering of neutrons by hydrogen.[36]

The reflected and transmitted angular fluxes resulting from a unit incident flux were calculated for source angles of 1.0, 0.566331, and 0.066838 using each of the methods discussed for the evaluation of the scattering source term. A Lobatto-24 discrete-ordinates set was used in all the calculations. The approximated scattering kernel calculations with the quadratic and cubic flux expansions contained an additional ordinate which was needed to obtain an integral number of flux intervals. This additional ordinate was placed at $\mu = 0.04$ in an attempt to minimize the error incurred by interpolating across $\mu = 0$.

The results of the exact kernel calculations, which were judged to be the most accurate on the basis of reciprocity, are shown in Fig. 4.3. The percent deviations in the angular fluxes as calculated by the Legendre expansion method and the approximated scattering kernel method with linear, quadratic, and cubic flux expansions are plotted in Figs. 4.4 - 4.6.

It can be seen from Figs. 4.4 - 4.6 that the fluxes calculated by the approximated scattering kernel method with a linear flux expansion

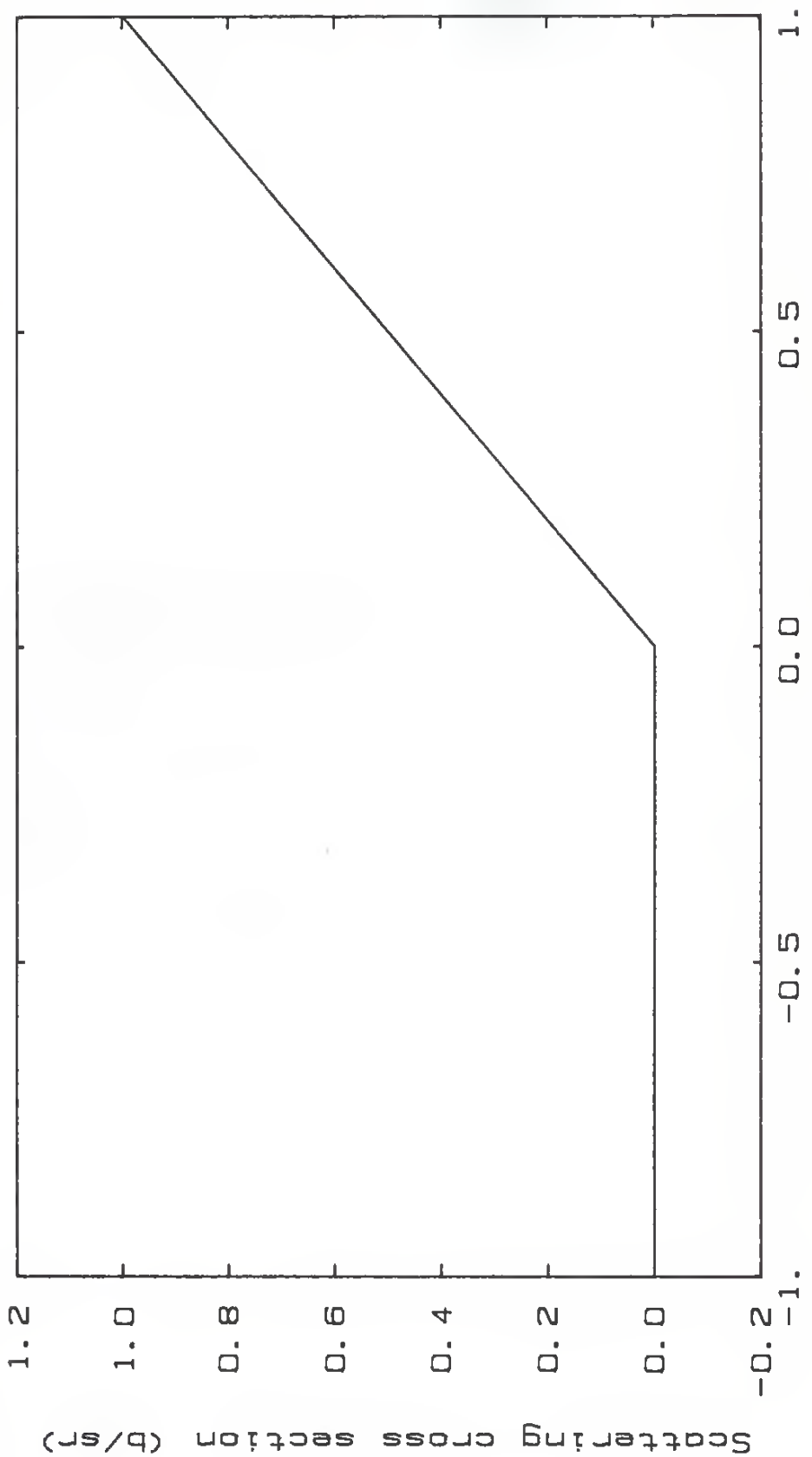

Fig. 4.2. The scattering cross section for Problem 4.3.1.

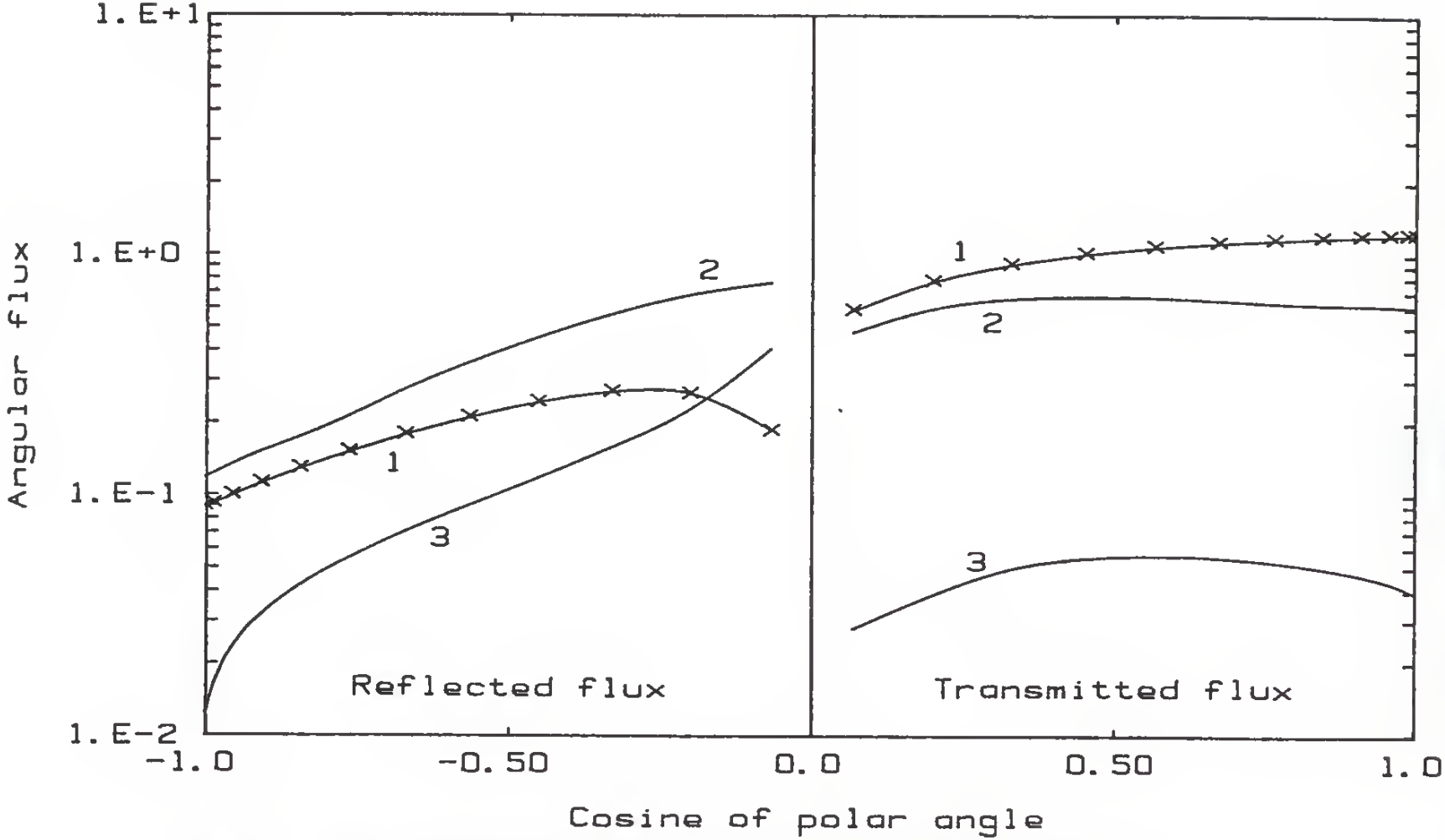

Fig. 4.3. The diffusely reflected and transmitted angular fluxes for a one mean-free-path slab with the scattering cross section of Fig. 4.2 and c=1, as calculated using the exact kernel method. The incident flux directions are: 1) $\mu_s = 1.0$, 2) $\mu_s = 0.566331$, 3) $\mu_s = 0.066838$. The x's on curve 1 indicate the location of the Lobatto-24 ordinates.

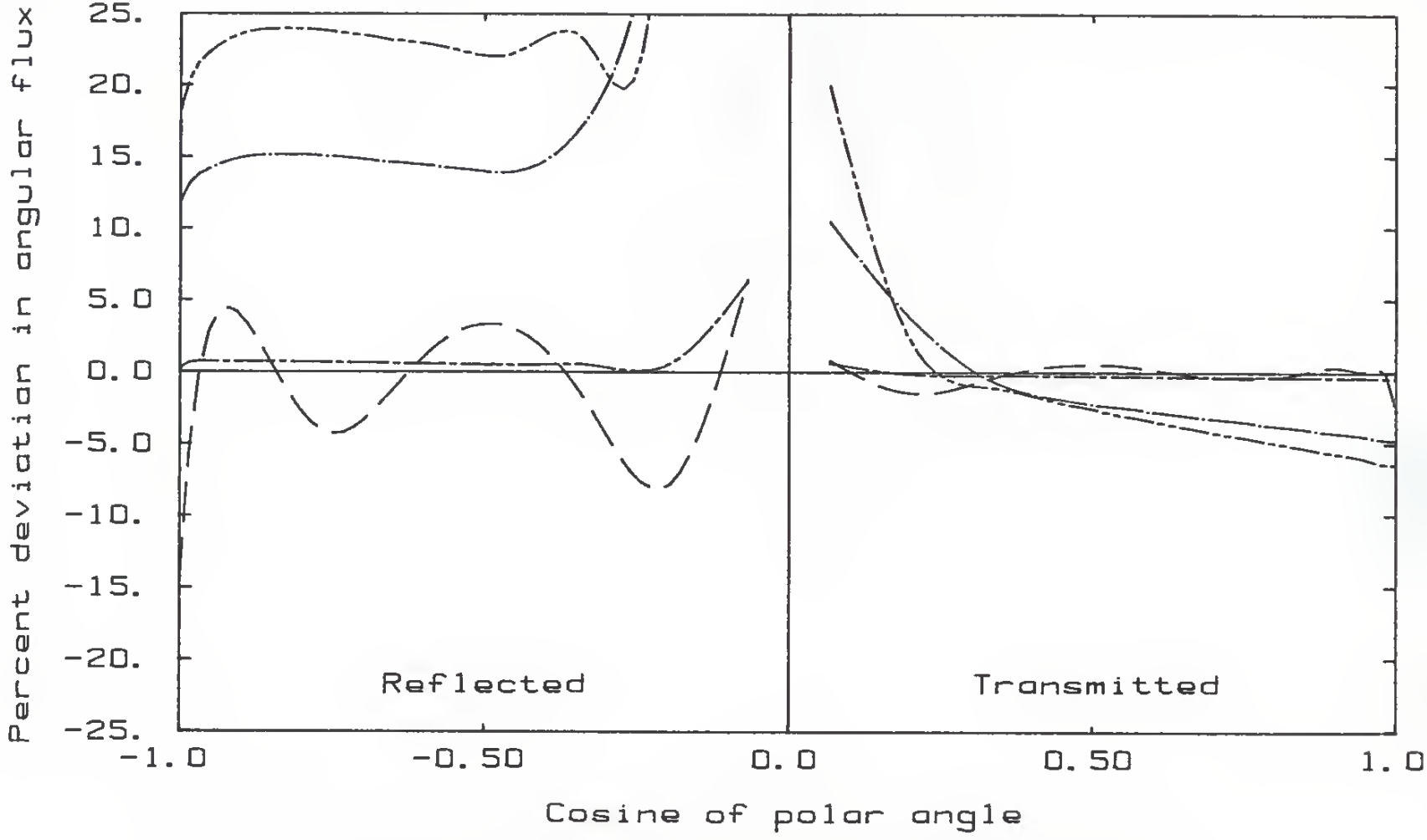

Fig. 4.4. The percentage deviation in the angular fluxes calculated using the Legendre expansion and approximated scattering kernel (A.S.K.) methods as compared to the exact kernel fluxes shown in Fig. 4.3, for the incident flux in direction $\mu_s = 1.0$. The curves represent the following methods: (——) Legendre expansion; (— — —) A.S.K. with linear flux expansion; (— — — —) A.S.K. with quadratic flux expansion; (— · —) A.S.K. with cubic flux expansion.

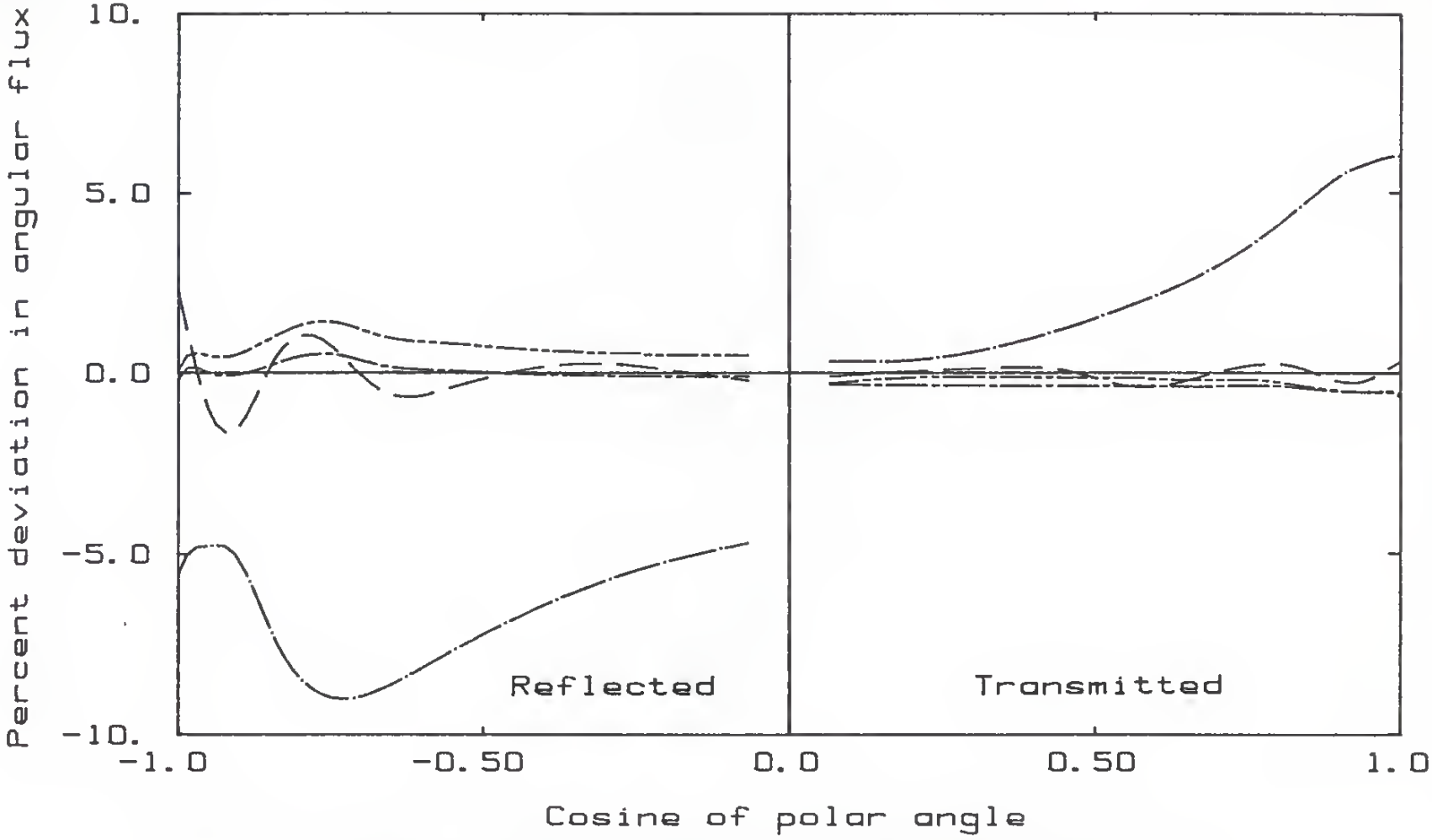

Fig. 4.5. The percentage deviation in the angular fluxes calculated using the Legendre expansion and approximated scattering kernel (A.S.K.) methods as compared to the exact kernel fluxes shown in Fig. 4.3, for the incident flux in direction $\mu_s = 0.566331$. The curves represent the following methods: (——) Legendre expansion; (— - —) A.S.K. with linear flux expansion; (— — —) A.S.K. with quadratic flux expansion; (— · —) A.S.K. with cubic flux expansion.

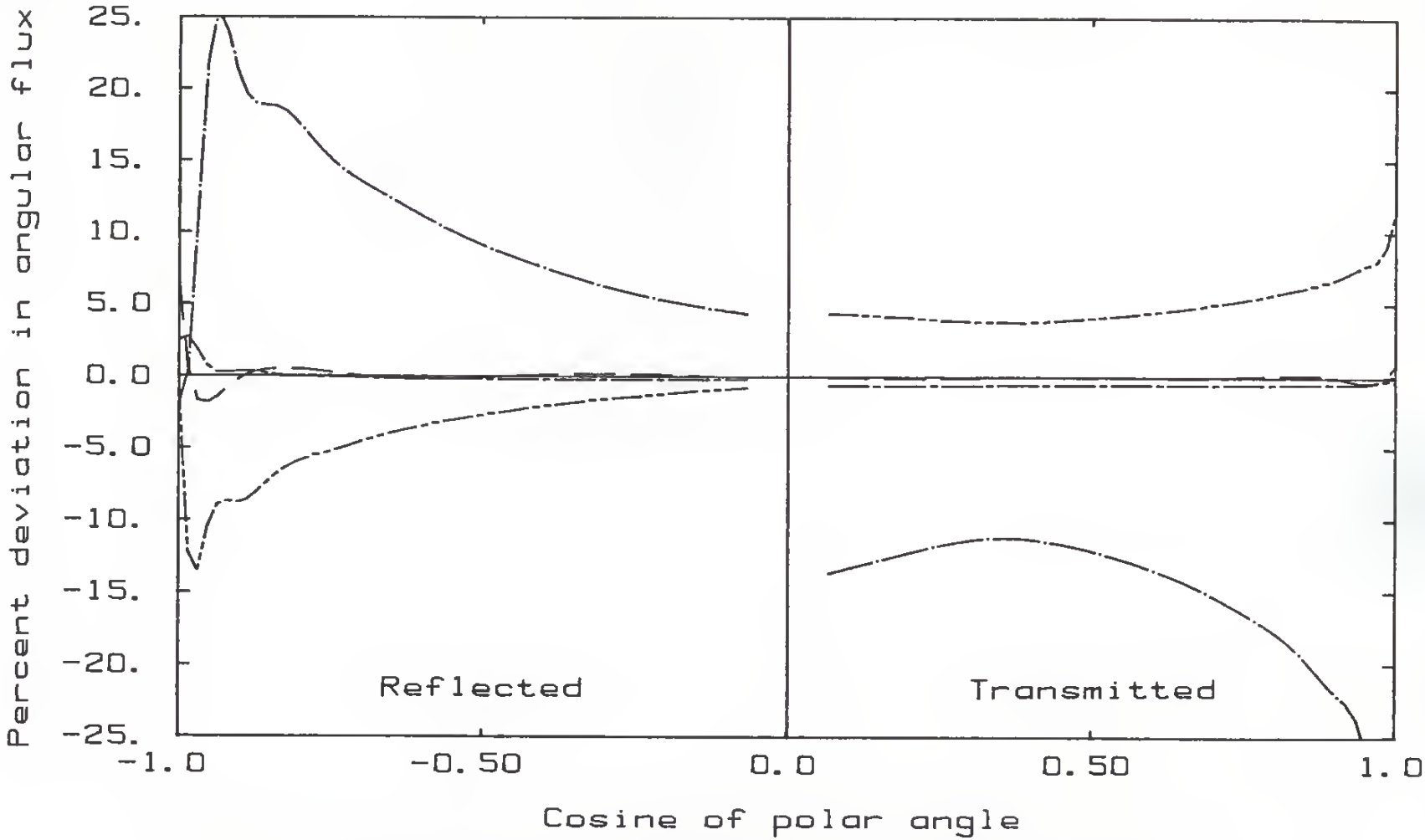

Fig. 4.6. The percentage deviation in the angular fluxes calculated using the Legendre expansion and approximated scattering kernel (A.S.K.) methods as compared to the exact kernel fluxes shown in Fig. 4.3, for the incident flux in direction $\mu_s = 0.066838$. The curves represent the following methods: (— — —) ^{S}Legendre expansion; (— - —) A.S.K. with linear flux expansion; (— - - —) A.S.K. with quadratic flux expansion; (— · —) A.S.K. with cubic flux expansion.

give consistently good results. Nearly all of the fluxes calculated by this method are within 1% of the exact kernel fluxes.

Use of quadratic and cubic flux expansion flux expansions in the approximated scattering kernel method led to rather erratic results. These methods often led to fluxes which were badly over- or underestimated. The reason for this behavior is discussed in Section 4.5.

The fluxes calculated using an eighth-order Legendre expansion of the scattering cross section exhibited oscillatory behavior, particularly for the reflected fluxes. These oscillations were worst for the normally incident case.

Problem 4.3.2

The second anisotropic scattering problem considered has a scattering cross section whose range of angular support is $\omega \in [0.8, 1]$. This fictitious piecewise linear cross section, which is representative of an in-group scattering cross section for a multigroup energy structure, is shown in Fig. 4.7.

The reflected and transmitted angular fluxes resulting from a unit incident flux were calculated for source angles of 1.0, 0.566331, and 0.066838 using the same discrete-ordinates set as in Problem 4.3.1. The results of these calculations are shown in Figs. 4.8 - 4.10. Many of the fluxes calculated using the Legendre expansion and approximated scattering kernel methods show significant deviations from the exact kernel fluxes.

The fluxes calculated using the Legendre expansion method generally exhibit oscillatory behavior. The oscillations are most severe for the

normally incident flux, in which case most of the reflected fluxes were actually calculated to be negative. For the other two source angles, the oscillations were again most pronounced for the reflected fluxes. Note that these results are qualitatively similar to those obtained in Problem 4.3.1 (cf. Figs. 4.4 - 4.6).

The fluxes calculated using the approximated scattering kernel method also exhibit the same type of behavior shown in the results of Problem 4.3.1. Calculations using a linear expansion of the flux generally yielded the closest agreement with the exact kernel fluxes. The deviation between the two, however, was much more significant than in Problem 4.3.1. For the normally incident case, the reflected fluxes calculated using a linear flux expansion were up to 40% higher than the exact kernel fluxes. The transmitted fluxes were up to 20% higher than those calculated using the exact kernel method. For the other two source angles, the reflected fluxes calculated using a linear flux expansion were generally within 10% of the exact kernel fluxes, and the transmitted fluxes within 5%.

The fluxes calculated using quadratic and cubic flux expansions again yielded rather erratic results. It can be seen from Fig. 4.8 that the quadratic and cubic flux expansions produced unrealistic transmitted flux distributions in the normally incident case. The oscillatory behavior of these fluxes is most likely due to the inability of piecewise quadratic and cubic expansions to model the angular flux distributions realistically. This phenomenon is discussed more thoroughly in Sec. 4.5.

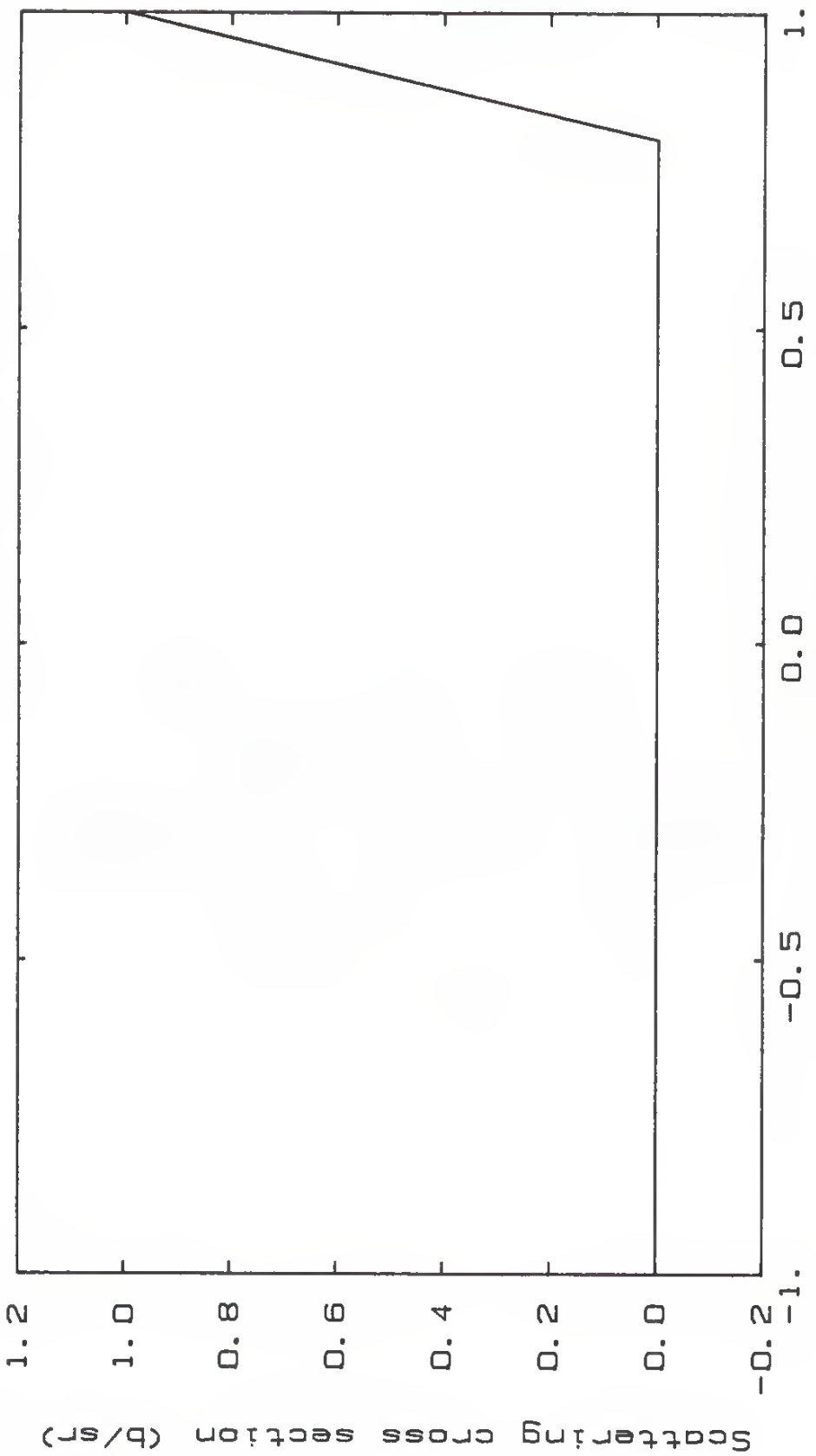

Fig. 4.7. The scattering cross section for Problem 4.3.2.

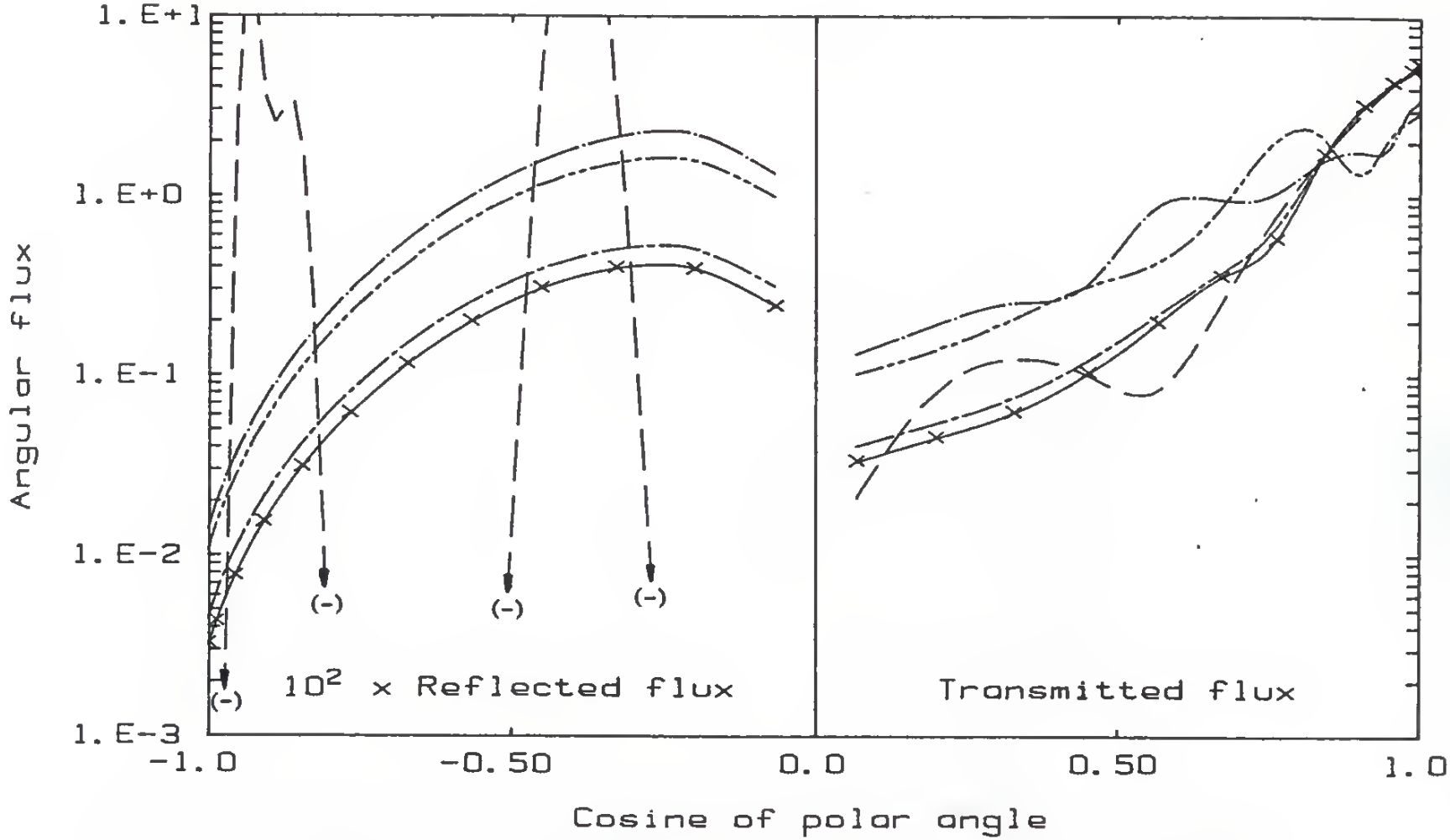

Fig. 4.8. The diffusely reflected and transmitted angular fluxes for a one mean-free-path slab with the scattering cross section of Fig. 4.7 and c=1, as calculated using the following methods: (———) exact kernel; (— —) Legendre expansion; (— - —) approximated scattering kernel (A.S.K.) with linear flux expansion; (— - - —) A.S.K. with quadratic flux expansion; (— · —) A.S.K. with cubic flux expansion. The incident flux is in direction μ_s = 1.0. The x's on the exact kernel curve indicate the location of the Lobatto-24 ordinates.

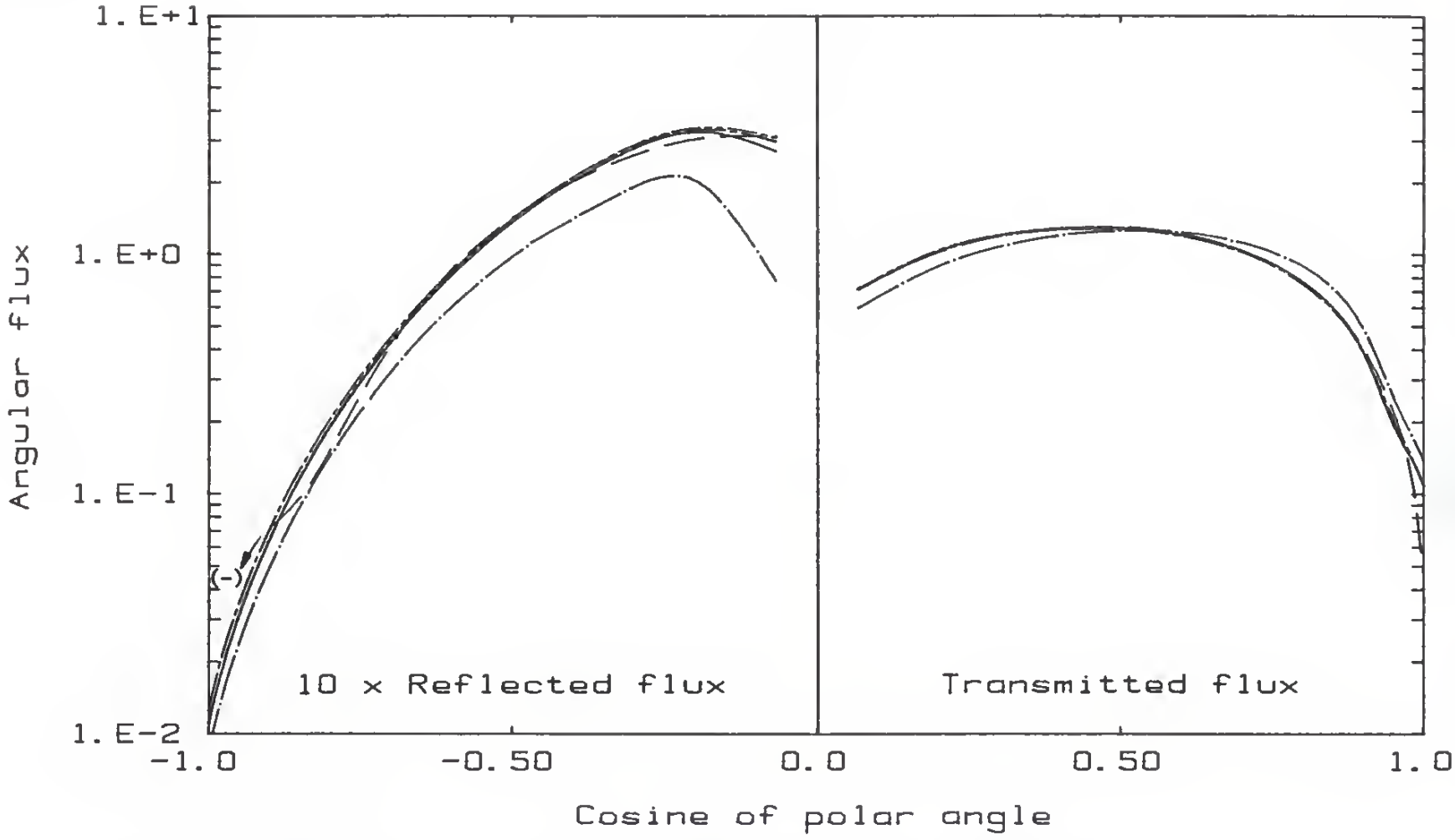

Fig. 4.9. The diffusely reflected and transmitted angular fluxes for a one mean-free-path slab with the scattering cross section of Fig. 4.7 and c=1, as calculated using the following methods: (———) exact kernel; (— —) Legendre expansion; (— - —) approximated scattering kernel (A.S.K.) with linear flux expansion; (— - - —) A.S.K. with quadratic flux expansion; (— · —) A.S.K. with cubic flux expansion. The incident flux is in direction $\mu_s = 0.566331$.

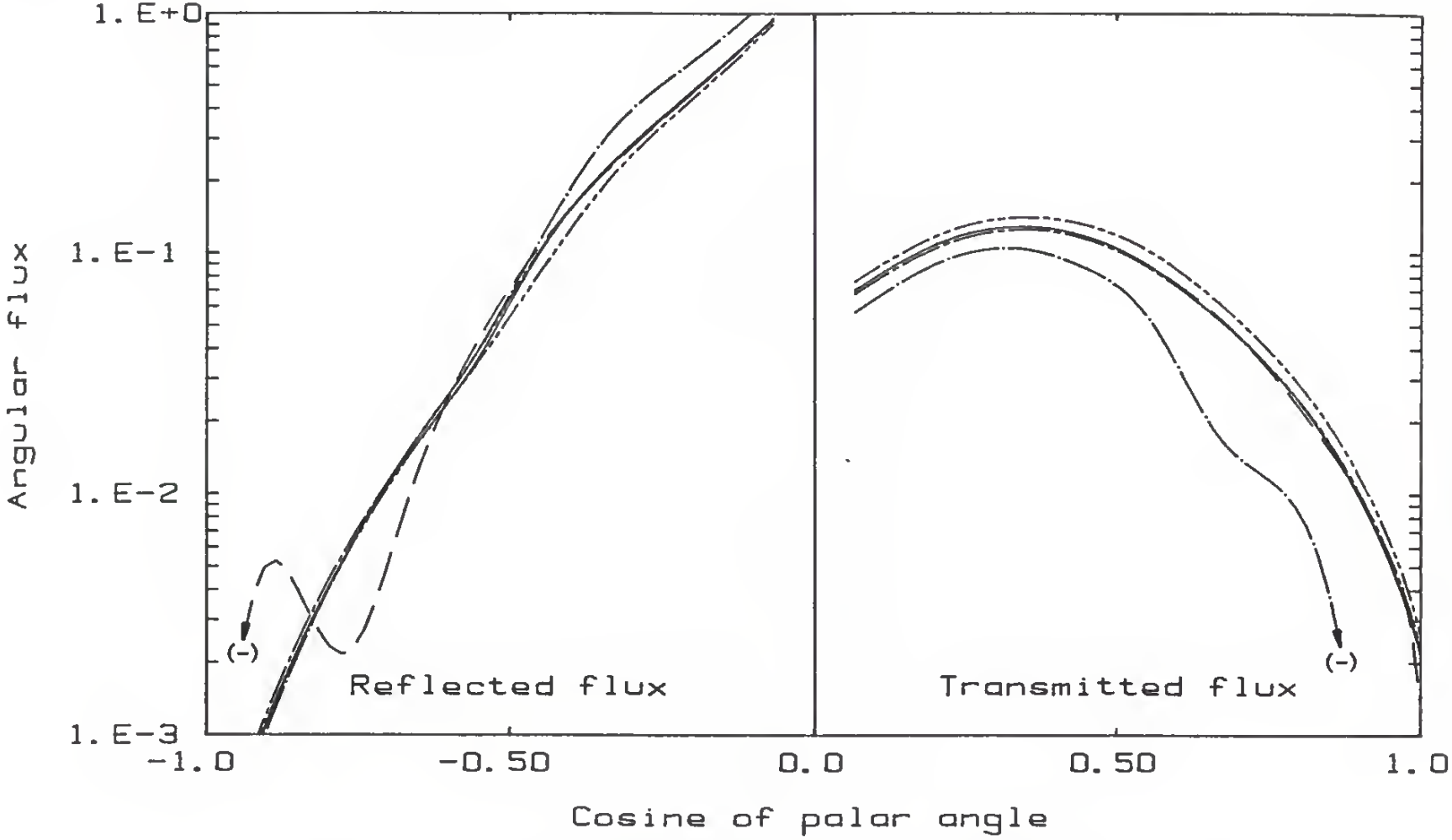

Fig. 4.10. The diffusely reflected and transmitted angular fluxes for a one mean-free-path slab with the scattering cross section of Fig. 4.7 and c=1, as calculated using the following methods: (————) exact kernel; (— —) Legendre expansion; (— - —) approximated scattering kernel (A.S.K.) with linear flux expansion; (— - - —) A.S.K. with quadratic flux expansion; (— · —) A.S.K. with cubic flux expansion. The incident flux is in direction $\mu_s = 0.066838$.

For the incident flux at 0.566331, the quadratic expansion results were in better agreement with the exact kernel fluxes than were those obtained using any of the other methods tested. The cubic flux expansion yielded the poorest results for this case. Finally, the fluxes calculated using quadratic and cubic flux expansions gave rather poor results for the source angle of 0.066838. Calculations using the cubic flux expansion actually predicted negative angular fluxes near $\mu = 1$.

Problem 4.3.3

The final problem considered has scattering that is even more anisotropic than the previous problem, with a scattering cross section whose range of angular support is $\omega \in [0.95, 1]$. This fictitious piecewise linear scattering cross section, which is shown in Fig. 4.11, is typical of in-group neutron scattering from light elements or with a fine-energy-group structure (cf. Fig. 2.3).

The reflected and transmitted angular fluxes resulting from a unit incident flux were calculated for source angles of 1.0, 0.544182, and 0.044247. A Lobatto-36 discrete-ordinates set was used in all the calculations. The approximated scattering kernel calculations with quadratic and cubic flux expansions again contained an additional ordinate at $\mu = 0.04$.

Figure 4.12 shows the reflected and transmitted angular fluxes for the normally incident case as calculated using the exact kernel method and the approximated scattering kernel method with a linear flux expansion. Calculations using the Legendre expansion method and the

approximated scattering kernel method with quadratic and cubic flux expansions yielded oscillatory and negative flux values for both the reflected and transmitted fluxes.

Note that the fluxes calculated using the linear flux expansion significantly overpredict the exact kernel fluxes over the entire reflected range and much of the transmitted range. This behavior is qualitatively similar to that shown in the results of Problem 4.3.2 (cf. Fig. 4.8). It is of interest to note that Odom[20] found that small inaccuracies in scattering source calculations can produce relatively large inaccuracies in the angular flux, particularly in reflected fluxes.

The reflected and transmitted angular fluxes as calculated by the exact kernel method and the approximated scattering kernel method with linear, quadratic, and cubic flux expansions are shown in Fig. 4.13 for the incident flux in direction 0.544182. The results obtained using linear and quadratic expansions of the flux are in good agreement with the exact kernel fluences, particularly for the transmitted fluxes. The fluxes calculated using a cubic expansion show poor behavior in the transmitted directions. Calculations using the Legendre expansion method again produced oscillatory and negative angular fluxes.

The reflected and transmitted angular fluxes as calculated by the exact kernel method and the approximated scattering kernel method with linear and quadratic flux expansions are shown in Fig. 4.14 for the incident flux in direction 0.044247. Both of the approximated scattering kernel flux profiles are in good agreement with the exact kernel fluxes. Calculations using the Legendre expansion method and the

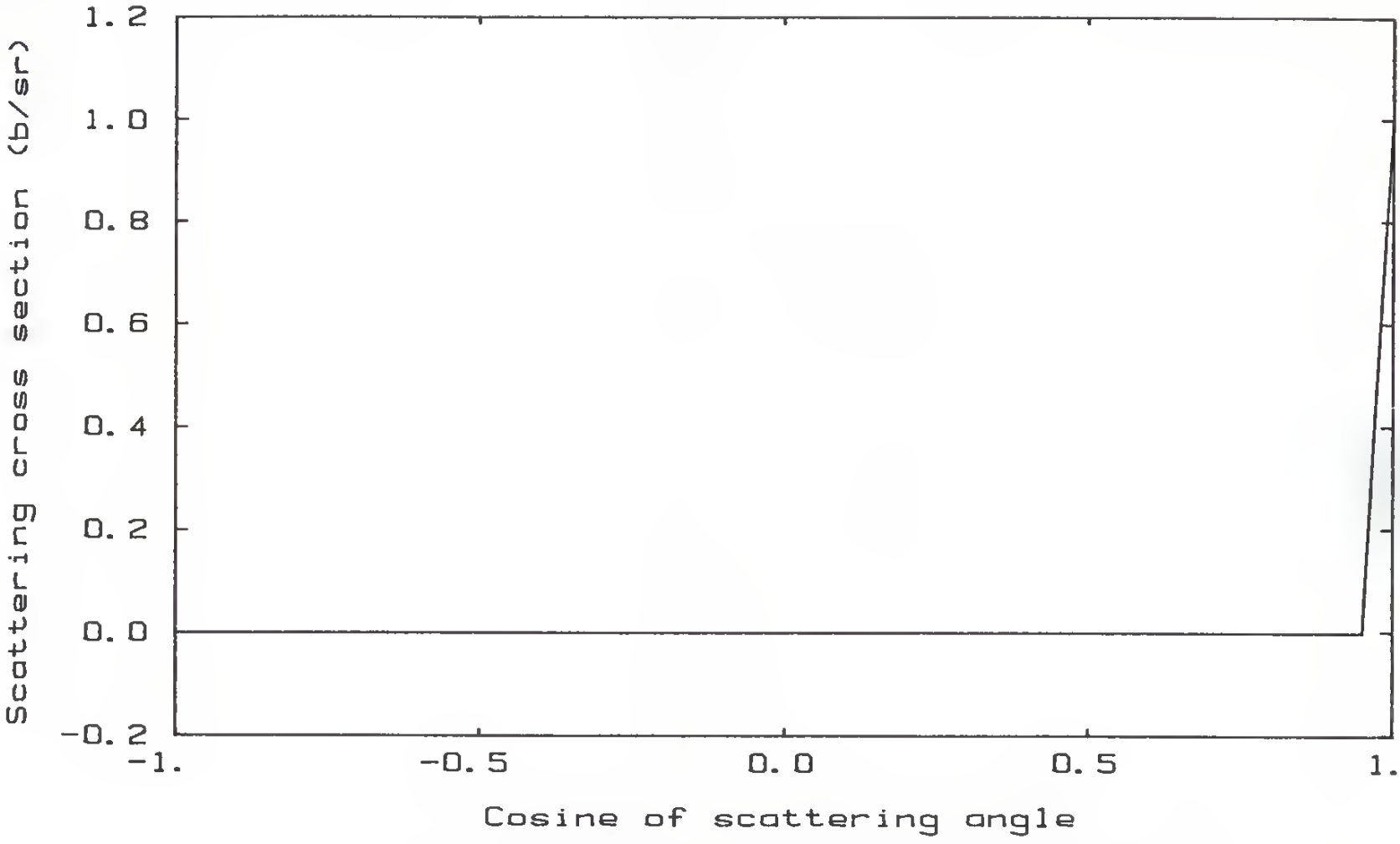

Fig. 4.11. The scattering cross section for Problem 4.3.3.

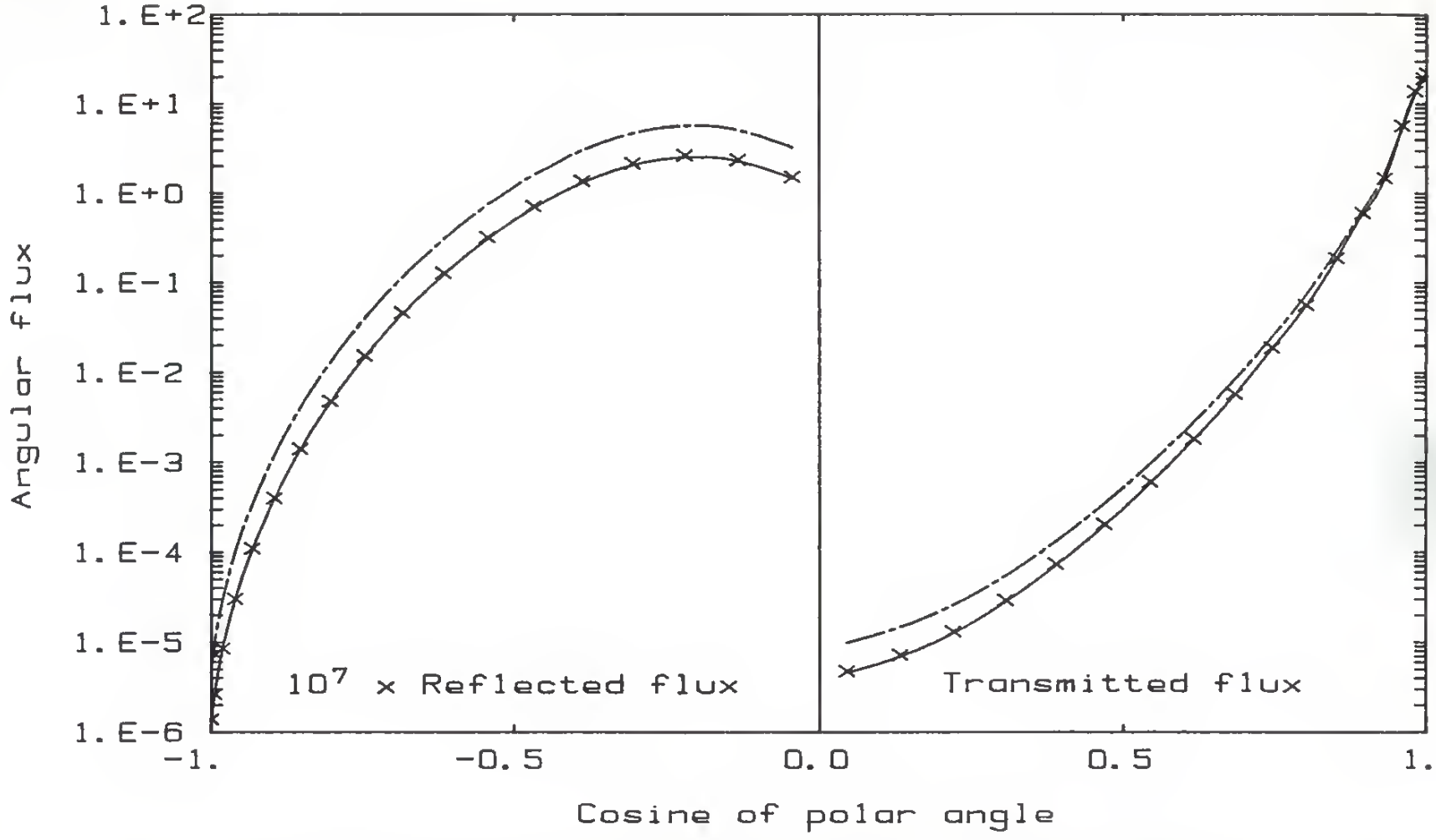

Fig. 4.12. The diffusely reflected and transmitted angular fluxes for a one mean-free-path slab with the scattering cross section of Fig. 4.11 and c = 1, as calculated using the following methods; (———) exact kernel; (— — —) approximated scattering kernel with linear flux expansion. The incident flux direction is $\mu_s = 1.0$. The x's on the exact kernel curve indicate the location of the Lobatto-36 ordinates.

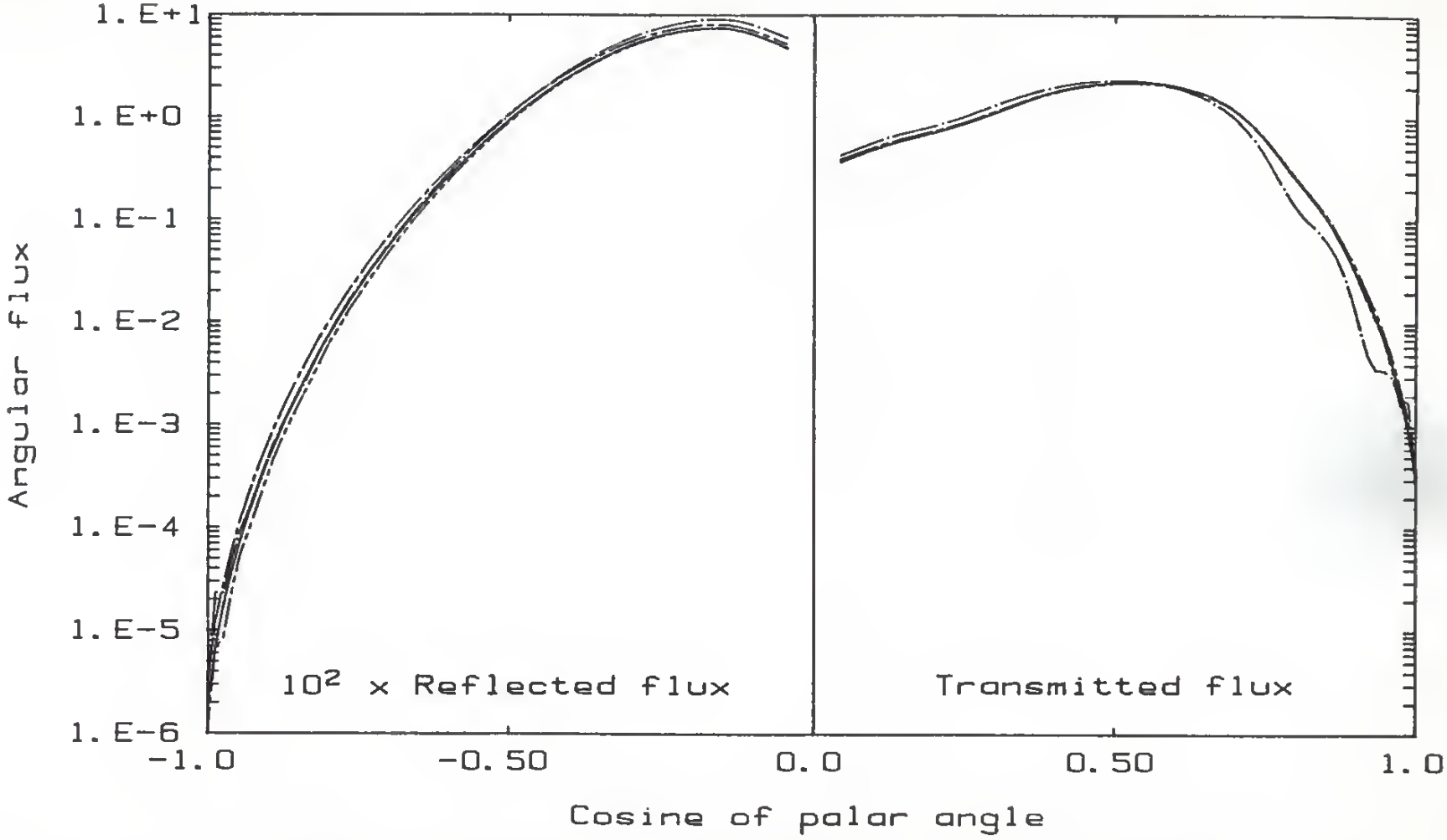

Fig. 4.13. The diffusely reflected and transmitted angular fluxes for a one mean-free-path slab with the scattering cross section of Fig. 4.11 and c = 1, as calculated using the following methods: (———) exact kernel; (– – –) approximated scattering kernel (A.S.K.) with linear flux expansion; (– – – –) A.S.K. with quadratic flux expansion; (—·—) A.S.K. with cubic flux expansion. The incident flux direction is $\mu_s = 0.544182$.

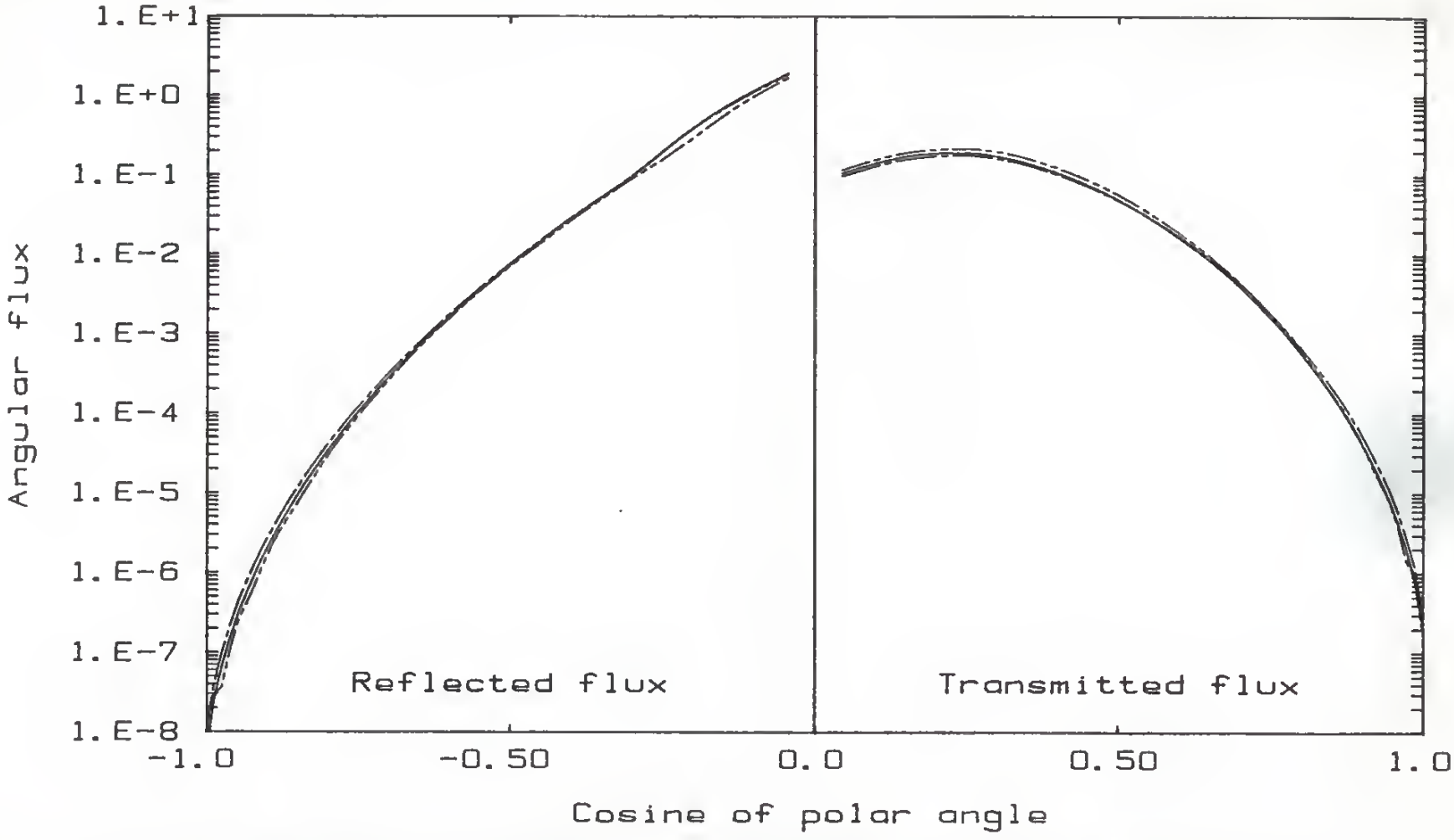

Fig. 4.14. The diffusely reflected and transmitted angular fluxes for a one mean-free-path slab with the scattering cross section of Fig. 4.11 and c = 1, as calculated using the following methods: (———) exact kernel; (– – –) approximated scattering kernel (A.S.K.) with linear flux expansion; (– – – –) A.S.K. with quadratic flux expansion. The incident flux direction is $\mu_s = 0.044247$.

approximated scattering kernel method with a cubic flux expansion yielded oscillatory and negative flux values.

4.4 Angular Redistribution in the Approximated Scattering Kernel Method

It can be seen from the results of the problems in Sec. 4.3 that the approximated scattering kernel method provides better accuracy than the conventional Legendre expansion method for highly anisotropic problems. This increased accuracy was the first objective in developing the approximated scattering kernel method. In this section we will examine the second objective, namely, the elimination of the angular coverage problem which limits the exact kernel method for low-order quadrature.

The failure of the exact kernel method to produce angular redistribution of scattered particles for coarse quadrature sets is due to the discretization of the angular variable μ. The approximated scattering kernel method, on the other hand, treats the incident particle direction μ' as a continuous variable [cf. Eqs. (3.47) and (3.48)]. Thus, instead of only those particles in some discrete direction μ_j contributing to the scattering source term in some other direction μ_i, all those particles with incident direction μ' in some specified range are considered. This specified range is determined by the breakpoints described in Sec. 3.2.2.

The ability of the approximated scattering kernel method to allow angular redistribution for problems in which the exact kernel method fails to can be illustrated by the following example. Consider a unit flux normally incident on the slab described in Problem 4.3.3. Let the

discrete ordinates be given by a Lobatto-10 quadrature set. It can be shown by use of Eqs. (2.51) - (2.53) that the Lobatto-10 quadrature set has "zero order of angular coverage" and hence is unsuitable for exact kernel transport calculations. The normally incident particles fail to scatter into any other discrete directions and hence the fluxes in all other directions are calculated to be zero (see Table 4.1). Use of the approximated scattering kernel method, on the other hand, allows angular redistribution from the source direction to all other directions (see Table 4.1).

Although use of the approximated scattering kernel method will allow angular redistribution with any discrete-ordinates set, the accuracy obtained may be poor. For example, the fluxes calculated using the approximated scattering kernel method in the example above show significant difference from those calculated using the exact kernel method with a Lobatto-36 quadrature set. The reasons for this discrepancy are discussed in the next section.

4.5 Analysis of the Approximated Scattering Kernel Results

It can be seen from the problems examined in Sections 4.2 - 4.4 that the use of the approximated scattering kernel method in discrete-ordinates transport calculations sometimes leads to very accurate results, and yet at other times results in very poor estimates of angular fluxes. In this section, we will examine the factors which affect the accuracy of the approximated scattering kernel method.

The first, and probably most important, factor to consider is the degree of anisotropy in the angular flux. Examination of the results of

Table 4.1. The reflected and transmitted angular fluxes resulting from a unit flux normally incident on a one mean-free-path slab with c = 1 and the scattering cross section of Fig. 4.11. The discrete ordinates are given by a Lobatto-10 quadrature set.

Cosine of Polar Angle (μ)	Exact Kernel Flux	Approximated Scattering Kernel Flux	Reference Flux[a]
-1.0	0.000	5.923(-8)[b]	1.333(-13)
-0.919534	0.000	1.184(-6)	1.602(-11)
-0.738774	0.000	2.107(-5)	1.657(-9)
-0.477925	0.000	1.916(-4)	6.166(-8)
-0.165279	0.000	4.813(-4)	2.433(-7)
0.165279	0.000	7.899(-3)	8.550(-6)
0.477925	0.000	4.062(-2)	2.315(-4)
0.738774	0.000	3.809(-1)	1.518(-2)
0.919534	0.000	3.570	9.714(-1)
1.0	2.371(1)	1.144(1)	2.108(1)

[a]The reference flux values were calculated by performing cubic spline interpolation on the exact kernel fluxes calculated with a Lobatto-36 quadrature set (cf. Fig. 4.12).

[b]Read as 5.923×10^{-8}

the problems in Sections 4.2 and 4.3 reveals that, as the degree of anisotropy in the angular flux increases, the difference between the approximated scattering kernel results and the exact kernel results becomes greater. This increased error is due to the inability of piecewise polynomial interpolation to accurately model highly anisotropic angular fluxes. This can be shown more precisely by considering the error associated with polynomial interpolation, which is given by[37]

$$E(\mu) = \frac{f^{(n+1)}(\xi)}{(n+1)!} \prod_{i=j}^{j+n} (\mu-\mu_i) , \qquad (4.15)$$

where $E(\mu)$ is the error in interpolating the function at μ, $f(\mu)$ is the continuous function which is approximated by the interpolating polynomial, the μ_i are the n+1 values of μ at which the function is known, and ξ is a function of μ and is within the range of the μ_i, but is otherwise unknown.

Equation (4.15) does not allow us to calculate the interpolation error, for we do not know the function $f(\mu)$ which describes the angular flux, nor do we know the value of ξ. However, Eq. (4.15) does indicate that the interpolation error is proportional to the (n+1)'th derivative of $f(\mu)$. This derivative would be expected to increase as the angular flux becomes more anisotropic.

Another factor which affects the accuracy obtained in discrete-ordinates calculations which utilizes the approximated scattering kernel method is the order of flux expansion used. Use of a piecewise linear flux expansion yields results which are often very accurate, and are

always at least physically realistic. Use of quadratic and cubic flux expansions, on the other hand, can lead to erratic results. In some cases these expansions perform very well, while at other times they lead to estimates of oscillatory and even negative angular fluxes. This behavior should not be surprising, as one of the difficulties associated with polynomial interpolation is the oscillatory behavior which it is possible for high order interpolating polynomials to assume.[37]

For example, consider the following transmitted fluxes for the normally incident case in Problem 4.3.3 as calculated by the exact kernel method:

μ_i	$\Phi(\mu_i)$
0.851155	0.17756
0.894266	0.56950
0.930378	1.4096
0.959209	5.4667
0.980532	13.299
0.994179	18.654
1.0	252.84

These points are plotted in Fig. 4.15, along with the piecewise linear, quadratic, and cubic polynomials that pass through the exact kernel results. (The flux in direction $\mu_i = 1.0$ consists of a diffusely transmitted component of magnitude 21.08 and an uncollided component of magnitude 231.76. Only the diffusely transmitted flux is plotted in Fig. 4.12.)

Between $\mu_i = 0.851155$ and $\mu_i = 0.959209$, the flux exhibits very smooth behavior and all the piecewise fits produce essentially the same results. Between $\mu_i = 0.959209$ and $\mu_i = 1.0$, the results are much

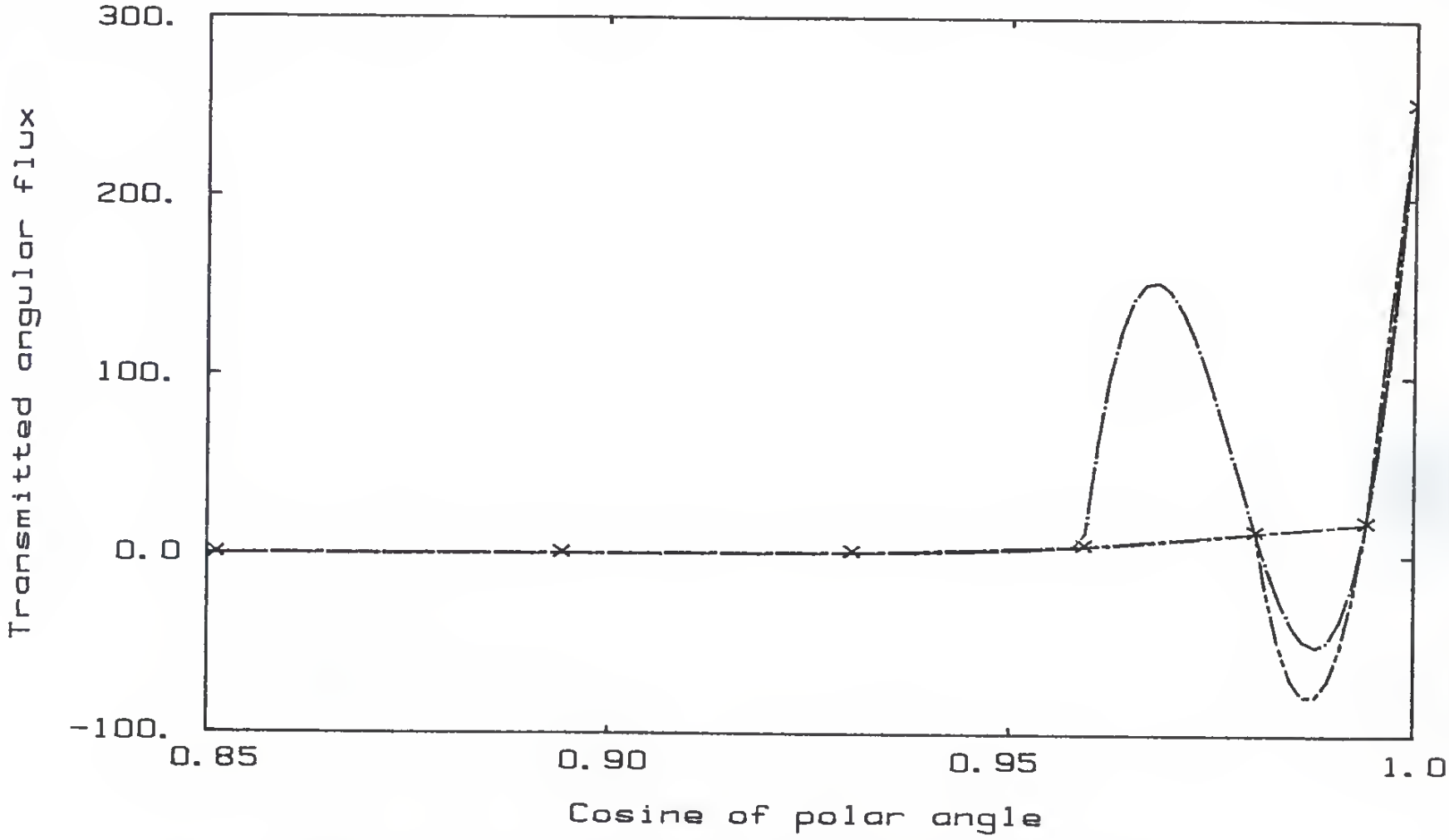

Fig. 4.15. The total (diffuse plus uncollided) transmitted angular flux near $\mu = 1.0$ for Problem 4.3.3 with $\mu_g = 1.0$. The x's are the flux values calculated using the exact kernel method. The curves are the following piecewise polynomial fits to the exact kernel data: (——) piecewise linear; (– – –), piecewise quadratic; (—·—) piecewise cubic.

different. The "jump" in the angular flux at $\mu_i = 1.0$ produces serious oscillations in the quadratic and cubic expansions for the segments which contain $\mu_i = 1.0$. The piecewise linear expansion appears to be a much more realistic fit in this region.

Although there is no way to determine *a priori* when quadratic and cubic flux expansions will fail to produce accurate flux profiles, it is obvious from the results of Problems 4.3.1 - 4.3.3 (as well as the above example) that quadratic and cubic expansions are very sensitive to the degree of anisotropy in the flux. Thus one should be very cautious about using quadratic or cubic flux expansions when dealing with problems that are likely to yield highly anisotropic angular fluxes. The results of Problems 4.3.2 and 4.3.3 show that cubic flux expansions are particularly prone to error.

Another factor which affects the accuracy which can be obtained when the approximated scattering kernel method is used is the number of discrete ordinates which are used. In Sec. 4.2, increasing the number of discrete ordinates resulted in a decrease in error no matter which method was used to evaluate the scattering source. Similar comparisons (which are not presented here) for the anisotropic scattering problems of Section 4.3 revealed the same behavior. On the other hand, decreasing the number of discrete ordinates in Problem 4.3.3 led to a significant increase in error (cf. Sec. 4.4). It is of interest to note that Atkinson[38] states that, when using piecewise polynomial interpolation, it is often more advantageous to increase the number of interpolation nodes then to increase the degree of the interpolating polynomial, due to the tendency of higher order polynomials to cause

large oscillations between the nodes. Such appears to be the best procedure for increasing the accuracy of the approximated scattering kernel results.

An obvious means of avoiding the spurious oscillations in the interpolated flux profiles would be to utilize a "smoother" interplation technique, such as cubic spline interpolation. However, the use of a technique such as cubic spline interpolation would require a significant modification of the approximated scattering kernel method.

When Lagrange interpolation is used, the angular flux in the segment $[\bar{\mu}_j, \bar{\mu}_{j+1}]$ is expanded as [cf. Eqs. (3.26) and (3.45)]

$$\Phi_g(\mu) = \sum_{i=jN-N+1}^{jN+1} \left\{ \sum_{n=0}^{N} C_n^i \mu^n \right\} \Phi_g(\mu_i) \quad , \quad \bar{\mu}_j \leq \mu \leq \bar{\mu}_{j+1} \, . \tag{4.16}$$

Cubic spline interpolation, on the other hand, leads to an expansion of the form

$$\Phi_g(\mu) = \sum_{n=0}^{3} A_n^j \mu^n \quad , \quad \bar{\mu}_j \leq \mu \leq \bar{\mu}_{j+1} \, . \tag{4.17}$$

Comparison of Eqs. (4.16) and (4.17) reveals why cubic spline interpolation cannot be used in the approximated scattering kernel method as derived in Chapter 3. In Eq. (4.16), the quantities which change with each "inner iteration" of the discrete-ordinates solution algorithm are the angular flux values $\Phi_g(\mu_i)$. The expansion coefficients C_n^i are dependent only on the discrete-ordinates set and hence are independent of the iterative process. Thus the approximated scattering kernel transfer matrix needs to be calculated only once for a particular transport medium and discrete-ordinates set.

On the other hand, if cubic spline interpolation were used [i.e., Eq. (4.17)], the quantities which change with each flux iteration would be the expansion coefficients A_n^j. These coefficients are dependent on the discrete ordinates used as well as on the angular flux values. Hence the approximated scattering kernel transfer matrix would have to be recalculated with each inner iteration. While such an approach is possible, it would add considerably to the computational effort of the transport calculations, and has not been pursued in this study.

5. CONCLUSIONS

In this work a new method of evaluating the scattering source term in discrete-ordinates transport calculations has been studied. This method, termed the approximated scattering kernel method, was developed especially for use in highly anisotropic problems (i.e., those problems which are characterized by highly anisotropic angular fluxes as well as by highly anisotropic scattering). The objectives in developing the approximated scattering kernel method were twofold -- to achieve better accuracy than that afforded by the conventional Legendre expansion method, and to eliminate the problem of angular redistribution that limits the exact kernel method for low quadrature orders.

The first objective, achieving better accuracy than the Legendre expansion method, was easily met when the piecewise linear flux expansion model was utilized. For the problems considered in Chapter 4, use of the approximated scattering kernel method with a piecewise linear flux expansion consistently yielded angular fluxes which were as accurate as, or more accurate than, the Legendre expansion results. For highly anisotropic slab albedo problems, the approximated scattering kernel results were far superior to the Legendre expansion results, which exhibited oscillatory and even negative angular fluxes.

The second objective of the approximated scattering kernel method, the elimination of angular coverage problems, was also met. In the final example problem in Chapter 4, use of the approximated scattering kernel method with a piecewise linear flux expansion produced nonzero fluxes while the exact kernel method failed to achieve any angular redistribution at all. The ability of the approximated scattering

kernel method to achieve angular redistribution with any number of discrete ordinates is due to the piecewise polynomial expansion of the angular flux. In this sense, the approximated scattering kernel method can be considered a combination modal and nodal method, in that it uses a modal approach (expansion of the angular flux and the scattering cross section) to generated nodal quantities (the elements of the approximated scattering kernel transfer matrix).

As is the case with both the Legendre expansion method and the exact kernel method, the approximated scattering kernel method is not without its limitations. Like the exact kernel method, it is somewhat more cumbersome to use than the Legendre expansion method, due to the necessity of generating and storing a complete transfer matrix rather than just a few expansion coefficients. Furthermore, it yields results which are generally not as accurate as the exact kernel method for the same discrete-ordinates set. In addition, the use of piecewise quadratic and piecewise cubic flux expansions in the approximated scattering kernel method leads to inconsistent results. Although these methods sometimes work well, they produce oscillatory and even negative angular fluxes in other instances. The reason for these erratic results is the oscillatory behavior which the piecewise quadratic and cubic interpolating polynomials can assume. It was found that this oscillatory behavior is very sensitive to the degree of anisotropy in the angular flux.

In general, it can be concluded that the adequacy of the approximated scattering kernel method is entirely dependent on the degree to which the angular flux exhibits low-order, piecewise

polynomial behavior. If the angular flux can be well modeled by a piecewise polynomial expansion, the approximated scattering kernel method can be expected to work well. If the angular flux exhibits "non-polynomial" behavior (e.g., a highly anisotropic profile), the approximated scattering kernel method may produce very poor results. Thus, any factors which affect the anisotropy of the angular flux can significantly affect the accuracy of discrete-ordinates transport calculations which utilize the approximated scattering kernel method. For example, use of the approximated scattering kernel method with a linear flux expansion in Problem 4.3.3 yielded accurate fluxes for a grazing angle of incidence ($\mu_s = 0.044247$), yet greatly overestimated many of the angular fluxes for the same problem when the slab was normally illuminated ($\mu_s = 1.0$).

In spite of its shortcomings, however, the approximated scattering kernel method is a practical method for scattering source term calculations in discrete-ordinates transport calculations. Provided a piecewise linear flux expansion is utilized, the approximated scattering kernel method yields positive (and apparently physically realistic) angular fluxes for problems in which the Legendre expansion method fails. Unlike the exact kernel method, it produces angular redistribution of scattered particles with any number of discrete ordinates. Furthermore, by obviating the need for numerical quadrature in the scattering source term calculation, it allows one to choose a discrete-ordinates set without the usual constraints involved in that process.

Further studies in this area could deal with ways of minimizing the error associated with interpolation of the angular flux. One possibility would be to attempt to optimize the location of the discrete ordinates. This problem has been widely studied for global polynomial interpolation, in which case choosing the N discrete ordinates as the zeroes of the N'th order Chebyshev polynomial tends to (but does not always) minimize the maximum value of the interpolation error.[37] However, this procedure does not apply to piecewise polynomial interpolation.

If one knew *a priori* approximately what the angular flux profile for a particular problem was, one could minimize the interpolation error by locating many discrete ordinates where the angular flux varies rapidly. However, while it may be possible to choose such an optimal discrete-ordinates set for a particular problem (e.g., a flux incident at some angle μ_s on a slab of a certain thickness with a certain scattering cross section), a change in any one of the problem parameters (such as the source angle) could result in a flux profile substantially different from the original one, so that the discrete ordinates would no longer be optimally located. It should be obvious that it would be extremely inconvenient as well as inefficient to use a different discrete-ordinates set (and hence have to generate a new approximated scattering kernel transfer matrix) for every transport problem one wished to solve.

Perhaps a more feasible means of improving the accuracy of the approximated scattering kernel method would be to investigate other functional representations for the angular flux. Such representations

might employ exponential or logarithmic terms, or even rational functions. Use of such non-polynomial representations would require significant changes in the approximated scattering kernel method as derived in Chapter 3.

Finally, the approximated scattering kernel method could be applied to multigroup problems in plane or spherical geometry. This would require no change in the calculation of the approximated scattering kernel transfer matrices, and only minor changes in the transport code utilized in this work.

6. ACKNOWLEDGEMENTS

The author wishes to express his appreciation to D. J. K. Shultis for his steadfast support and advice throughout the course of this work. He would also like to thank Dr. R. E. Faw and Dr. O. L. Weaver for serving on his advisory committee.

The financial support provided by the Kansas State University Department of Nuclear Engineering is gratefully acknowledged.

A special thanks goes to Mrs. Connie Schmidt for her skill (and patience) in typing the manuscript.

The author's deepest gratitude goes to his wife, Barbara. Her continued love, support, and encouragement made the completion of this work possible. Finally, the author would like to acknowledge and thank God for the help and grace He provides.

7. REFERENCES

1. J.J. Duderstadt and W.R. Martin, *Transport Theory*, (John Wiley & Sons, New York, 1979).

2. G.I. Bell and S. Glasstone, *Nuclear Reactor Theory*, (Van Nostrand Reinhold, New York, 1970).

3. K.D. Lathrop, Reactor Technol., 15, 107 (1972).

4. R.E. Lapp and H.L. Andrews, *Nuclear Radiation Physics*, 4th ed. (Prentice-Hall, Englewood Cliffs, N.J., 1972).

5. J.A. Weinman, Icarus 9, 67 (1968).

6. G.E. Hunt, J. Quant. Spectrosc. Radiat. Transfer 10, 857 (1970).

7. W.J. Mikols and J.K. Shultis, Nucl. Sci. Eng. 62, 738 (1977).

8. J.E. Morel, Nucl. Sci. Eng. 71, 64 (1979).

9. H. Brockmann, Nucl. Sci. Eng. 77, 377 (1981).

10. J.P. Odom and J.K. Shultis, Nucl. Sci. Eng. 59, 278 (1976).

11. B. Davison, *Neutron Transport Theory*, (Oxford University Press, London, 1958).

12. K.D. Lathrop, Nucl. Sci. Eng. 21, 498 (1965).

13. A. Razani, J. Quant. Spectrosc. Radiat. Transfer 14, 339 (1974).

14. G.I. Bell, G.E. Hansen, and H.A. Sandmeier, Nucl. Sci. Eng. 28, 376 (1967).

15. E.A. Attia and A.A. Harms, Nucl. Sci. Eng. 59, 319 (1976).

16. S. Pearlstein, Nucl. Sci. Eng. 49, 162 (1972).

17. L.L. Carter and C.A. Forest, Nucl. Sci. Eng. 59, 27 (1976).

18. K. Takeuchi, J. Nucl. Sci. Technol. 8 (3), 141 (1971).

19. B.G. Carlson and K.D. Lathrop, in *Computing Methods in Reactor Physics*, edited by H. Greenspan, C.N. Kelber, and K. Okrent (Grodon and Breach, New York, 1968).

20. J.P. Odom, Ph.D. Dissertation, Kansas State University, 1975.

21. W.J. Mikols, M.S. Thesis, Kansas State University, 1976.

22. J.C. Ryman, Ph.D. Dissertation, Kansas State University, 1979.

23. K.J. Hong, Ph.D. Dissertation, Kansas State University, 1980.

24. F. Beranek and R.W. Conn, Nucl. Sci. Eng. 71, 100 (1979).

25. A.B. Chilton, J.K. Shultis, and R.E. Faw, *Principles of Radiation Shielding*, (Prentice-Hall, Englewood Cliffs, N.J., 1984).

26. K.M. Case and P.F. Zweifel, *Linear Transport Theory*, (Addison-Wesley, Reading, Mass., 1967).

27. W.J. Mikols and J.K. Shultis, Nucl. Sci. Eng. 63, 91 (1977).

28. R.J. Cerbone and K.D. Lathrop, Nucl. Sci. Eng. 35, 139 (1969).

29. M. Abramowitz and I.A. Stegun (eds.), *Handbook of Mathematical Functions*, (Dover, New York, 1965).

30. H. Khalil, Nucl. Sci. Eng. 90, 263 (1985).

31. E.E. Lewis and W.F. Miller, *Computational Methods of Neutron Transport* (John Wiley & Sons, New York, 1984).

32. I.S. Gradshteyn and I.M. Ryzhik, *Table of Integrals, Series, and Products*, (Academic Press, New York, 1965).

33. W. Grobner and N. Hofreiter, *Integraltafel*, (Springer-Verlag, Vienna, 1961).

34. S. Chandrasekhar, *Radiative Transfer*, (Dover, New York, 1960).

35. J.L. Carlstedt and T.M. Mullikin, Astrophys. J., Suppl. Ser. 12 (113), 449 (1966).

36. J.R. Lamarsh, *Introduction to Nuclear Reactor Theory*, (Addison-Wesley, Reading, Mass., 1966).

37. R.W. Hornbeck, *Numerical Methods*, (Quantum Publishers, New York, 1975).

38. K.E. Atkinson, *An Introduction to Numerical Analysis*, (John Wiley & Sons, New York, 1978).

8. APPENDIX

Computer Codes

The three main computer programs which were utilized in this work are listed in this appendix. A brief description of each code is given here. The code listings are supplied with comment cards to facilitate the understanding and use of the programs. All the programs are written in FORTRAN-77. They were run on the Kansas State University Computing Center's NAS 6630, which is functionally equivalent to an IBM 4831.

The first code listed is EXKERNEL, which is used to generate exact kernel transfer matrices. EXKERNEL uses a piecewise linear or piecewise quadratic approximation of the scattering cross section. This method allows the exact kernel cross sections to be evaluated without recourse to numerical quadrature. The only input data required are the breakpoints in the scattering cross section, the values of the cross section at the breakpoints (plus the cross section values at an additional point in each subdomain if a piecewise quadratic cross section approximation is used), and a set of polar quadrature ordinates (i.e., the discrete ordinates $\{\mu_i\}$).

The second code listed is ASKERNEL, which is used to generate approximated scattering kernel transfer matrices. For transfer between any two directions of a discrete-ordinates set, ASKERNEL calculates the various breakpoints in the integration range of the scattering source, determines the form of the integrand in each subrange, performs the required integrations, and sums the various components to obtain the approximated scattering kernel. The input requirements are basically

the same as those for EXKERNEL. In addition, the user must specify what order of piecewise flux expansion he wishes to use (N) as well as the number of flux intervals (M). The sum NM+1 must equal the number of discrete ordinates which are used.

The final code listed is TRANS, which performs one-dimensional, azimuthally symmetric plane geometry discrete-ordinates transport calculations. The version of TRANS listed here uses the approximated scattering kernel technique for the evaluation of the scattering source term. Modified versions of TRANS were used to perform transport calculations with the Legendre expansion and exact kernel methods. The input requirements, which vary slightly according to the version used, are described in the program listing.

```
C
C                  ***  PROGRAM NAME:  EXKERNEL  ***
C
C     PROGRAM TO INTEGRATE SCATTERING CROSS SECTIONS OVER THE
C     AZIMUTHAL ANGLE TO GENERATE AZIMUTHALLY INDEPENDENT EXACT
C     KERNEL CROSS SECTIONS.  A PIECEWISE LINEAR OR PIECEWISE
C     QUADRATIC CROSS SECTION EXPANSION IS USED SO THAT THE EXACT
C     KERNEL CROSS SECTIONS CAN BE INTEGRATED ANALYTICALLY.  THIS
C     ALLOWS A MUCH MORE RAPID COMPUTATION THAN DOES THE USE OF
C     NUMERICAL QUADRATURE.
C
C     MAJOR VARIABLES ARE AS FOLLOWS:
C     'NR'          = NUMBER OF REFLECTED POLAR QUADRATURE DIRECTIONS
C     'NT'          = NUMBER OF TRANSMITTED POLAR QUADRATURE DIRECTIONS
C     'KMAX'        = NUMBER OF DISTINCT BREAKPOINTS IN THE
C                     DIFFERENTIAL SCATTERING CROSS SECTION (I.E., DO
C                     NOT COUNT DUPLICATE BREAKPOINT VALUES MORE THAN
C                     ONCE)
C     'W(I)'        = BREAKPOINTS IN THE ANGULAR CROSS SECTION (PLUS
C                     THE MIDPOINTS OF EACH CROSS SECTION SUBRANGE IF
C                     A QUADRATIC CROSS SECTION EXPANSION IS USED)
C     'SIG(I)'      = CROSS SECTION VALUES AT THE W(I) VALUES
C     'NORD'        = ORDER OF CROSS SECTION FIT. INPUT '1' FOR A
C                     LINEAR CROSS SECTION FIT AND '2' FOR A
C                     QUADRATIC CROSS SECTION FIT.
C     'U(N)'        = POLAR QUADRATURE ORDINATES
C
      IMPLICIT REAL*8(A-H,O-Z)
      DIMENSION A(64,64)
      COMMON/BLOCK1/ AA(3),BB(3),CC(3),W(7),SIG(7)
      COMMON/BLOCK2/ WB(4),SIGB(4),U(64)
C
      READ(5,800) KMAX,NORD
  800 FORMAT(2(I5))
      KMAX=KMAX-1
      KMAX1=KMAX*NORD+1
C
C     READ IN ANGULAR BREAKPOINTS AND THEIR CORRESPONDING SCATTERING
C     CROSS SECTIONS
      READ(5,801) (W(I),I=1,KMAX1)
      READ(5,801) (SIG(I),I=1,KMAX1)
  801 FORMAT(4(D18.8))
C
      KMAX2=KMAX+1
      DO 1 I=1,KMAX2
      WB(I)=W((I-1)*NORD+1)
      SIGB(I)=SIG((I-1)*NORD+1)
    1 CONTINUE
C
C     READ QUADRATURE ORDINATES
      READ(5,802) NTOT
  802 FORMAT(I5)
      READ(5,803) (U(I),I=1,NTOT)
  803 FORMAT(3(D24.15))
```

```
C
C     CHECK FOR SYMMETRY OF ANGULAR MESH.  IF IT IS SYMMETRIC, ONLY
C     ONE-HALF THE EXACT KERNEL CROSS SECTIONS NEED BE CALCULATED.
      IFLAG=1
      DO 2 I=1,NTOT
      IF(U(I).NE.-U(NTOT+1-I)) THEN
        IFLAG=0
        GO TO 3
      END IF
    2 CONTINUE
    3 CONTINUE
C
      IF(IFLAG.EQ.1) THEN
        NTOT1=IFIX((NTOT+1)/2.)
      ELSE
        NTOT1=NTOT
      END IF
C
C     CALL SUBROUTINE TO EVALUATE EXPANSION COEFFICIENTS FOR CROSS
C     SECTION EVALUATION.
C
      CALL COEFF(KMAX,NORD)
C
      DO 5 I=1,NTOT1
      DO 5 J=1,NTOT
      OMEGA1=U(I)*U(J)+DSQRT((1.-U(I)**2)*(1.-U(J)**2))
      OMEGA2=U(I)*U(J)-DSQRT((1.-U(I)**2)*(1.-U(J)**2))
C
C     IF SCATTERING RANGES IMPOSED BY KINEMATICS AND BY QUADRATURE
C     SET DO NOT OVERLAP, CROSS-SECTION IS ZERO
C
      IF(OMEGA1.LT.W(1).OR.OMEGA2.GT.W(KMAX2)) THEN
        A(I,J)=0.
        GO TO 4
      ELSE
        A(I,J)=FNSIGG(I,J,KMAX)
      END IF
C
    4 CONTINUE
      IF(IFLAG.EQ.1) A(NTOT+1-I,NTOT+1-J)=A(I,J)
C
    5 CONTINUE
      WRITE(6,900) ((A(I,J),J=1,NTOT),I=1,NTOT)
  900 FORMAT(4(D18.8))
      STOP
      END
C
C
C
C
C     SUBROUTINE TO EVALUATE EXPANSION COEFFICIENTS FOR LINEAR OR
C     QUADRATIC CROSS SECTION FIT.
      SUBROUTINE COEFF(KMAX,NORD)
      IMPLICIT REAL*8 (A-H,O-Z)
```

```
      COMMON/BLOCK1/ AA(3),BB(3),CC(3),W(7),SIG(7)
C
C     EVALUATE COEFFICIENTS FOR LINEAR FIT
      IF(NORD.EQ.1) THEN
      DO 100 K=1,KMAX
      K1=K
      K2=K+1
C
      AA(K)=0.
      BB(K)=(SIG(K1)-SIG(K2))/(W(K1)-W(K2))
      CC(K)=(W(K1)*SIG(K2)-W(K2)*SIG(K1))/(W(K1)-W(K2))
  100 CONTINUE
C
C     EVALUATE COEFFICIENTS FOR QUADRATIC FIT
      ELSE
      DO 200 K=1,KMAX
      K1=(K-1)*2+1
      K2=K1+1
      K3=K1+2
C        .
      D=W(K1)**2*(W(K2)-W(K3))-W(K2)**2*(W(K1)-W(K3))+W(K3)**2*(W(K1)-W(
     @K2))
      D1=SIG(K1)*(W(K2)-W(K3))-SIG(K2)*(W(K1)-W(K3))+SIG(K3)*(W(K1)-W(K2
     @))
      D2=W(K1)**2*(SIG(K2)-SIG(K3))-W(K2)**2*(SIG(K1)-SIG(K3))+W(K3)**2*
     @(SIG(K1)-SIG(K2))
      D3=W(K1)**2*(W(K2)*SIG(K3)-W(K3)*SIG(K2))-W(K2)**2*(W(K1)*SIG(K3)-
     @W(K3)*SIG(K1))+W(K3)**2*(W(K1)*SIG(K2)-W(K2)*SIG(K1))
C
      AA(K)=D1/D
      BB(K)=D2/D
      CC(K)=D3/D
  200 CONTINUE
C
      END IF
C
  500 RETURN
      END
C
C
C
C
C     FUNCTION SUBROUTINE TO EVALUATE THE EXACT KERNEL CROSS SECTION
C     BY ANALYTICAL INTEGRATION OF THE PIECEWISE CROSS SECTION
C     EXPANSION
      DOUBLE PRECISION FUNCTION FNSIGG(I,J,KMAX)
      IMPLICIT REAL*8(A-H,O-Z)
      DIMENSION PHI(4)
      COMMON/BLOCK1/ AA(3),BB(3),CC(3),W(7),SIG(7)
      COMMON/BLOCK2/ WB(4),SIGB(4),U(64)
      KMAX2=KMAX+1
      PI=4.*DATAN(1.DO)
      SIGMA=0.
C
```

```
      Y=U(I)*U(J)
      Z=DSQRT((1.-U(I)**2)*(1.-U(J)**2))
C
      DO 15 K=1,KMAX
      IF(U(I).EQ.-1..OR.U(I).EQ.1..OR.U(J).EQ.-1..OR.U(J).EQ.1.) THEN
        DO 5 L=1,KMAX2
        IF(Y.EQ.WB(L)) THEN
          SIGMA=PI*SIGB(L)
          GO TO 20
        END IF
    5   CONTINUE
        K1=K+1
        DO 10 L=K,K1
        IF(WB(L).GT.Y) THEN
          PHI(L)=0.
        ELSE
          PHI(L)=PI
        END IF
   10   CONTINUE
      ELSE
        ARG1=DMIN1((WB(K)-Y)/Z,1.D0)
        ARG1=DMAX1(-1.D0,ARG1)
        PHI(K)=DACOS(ARG1)
        ARG2=DMIN1((WB(K+1)-Y)/Z,1.D0)
        ARG2=DMAX1(-1.D0,ARG2)
        PHI(K+1)=DACOS(ARG2)
      END IF
C
      SIGMA=SIGMA+((AA(K)/4.)*Z**2)*(DSIN(2.*PHI(K))-DSIN(2.*PHI(K+1)))+
     @(2.*AA(K)*Y*Z+BB(K)*Z)*(DSIN(PHI(K))-DSIN(PHI(K+1)))+((AA(K)/2.)*Z
     @**2+AA(K)*Y**2+BB(K)*Y+CC(K))*(PHI(K)-PHI(K+1))
   15 CONTINUE
C
   20 FNSIGG=2.*SIGMA
      RETURN
      END
```

```
C
C                    ***  PROGRAM NAME:  ASKERNEL  ***
C
C     PROGRAM TO GENERATE THE APPROXIMATED SCATTERING KERNEL
C     TRANSFER MATRIX FOR A GIVEN DIFFERENTIAL SCATTERING
C     CROSS SECTION, DISCRETE-ORDINATES SET, AND ORDER OF
C     ANGULAR FLUX EXPANSION.  THE SCATTERING CROSS SECTION
C     CAN BE REPRESENTED BY EITHER A PIECEWISE LINEAR OR
C     PIECEWISE QUADRATIC EXPANSION BETWEEN THE BREAKPOINTS
C     IN THE SCATTERING CROSS SECTION.  THE ANGULAR FLUX CAN BE
C     APPROXIMATED BY A PIECEWISE LINEAR OR PIECEWISE QUADRATIC
C     EXPANSION.  IN ADDITION, IF A PIECEWISE LINEAR EXPANSION OF
C     THE SCATTERING CROSS SECTION IS USED, THE ANGULAR FLUX CAN
C     BE REPRESENTED BY A PIECEWISE CUBIC EXPANSION.
C
C     INPUT VARIABLES ARE AS FOLLOWS:
C     'NMAX'      = ORDER OF FLUX EXPANSION
C     'M'         = TOTAL NUMBER OF FLUX INTERVALS
C     'NP'        = TOTAL NUMBER OF FLUX DIRECTIONS (NUMBER OF
C                   DISCRETE ORDINATES)
C     'NBREAK'    = NUMBER OF DISTINCT BREAKPOINTS IN THE
C                   DIFFERENTIAL SCATTERING CROSS SECTION
C     'NORD'      = ORDER OF CROSS SECTION EXPANSION
C     'WB(I)'     = BREAKPOINTS IN THE SCATTERING CROSS SECTION
C                   (PLUS THE MIDPOINTS OF EACH CROSS SECTION
C                   SUBRANGE IF A QUADRATIC CROSS SECTION
C                   EXPANSION IS USED)
C     'SIG(I)'    = CROSS SECTION VALUES AT THE WB(I) VALUES
C     'U(J)'      = DISCRETE ORDINATES
C
      IMPLICIT REAL*8 (A-H,O-Z)
      DIMENSION A(50,50),SIG(7),WB(7),SIGT(50)
      COMMON/BLOCK1/ U(50),W(4),AA(3),BB(3),CC(3)
      COMMON/BLOCK2/ NMAX,KMAX,M,NP,NORD
C
C     READ INPUT DATA
C
      READ(5,800) NMAX,M,NP
  800 FORMAT(3(I5))
      READ(5,802) NBREAK,NORD
  802 FORMAT(2(I5))
C
      KMAX=NBREAK-1
      KMAX1=KMAX*NORD+1
      NMAX1=NMAX+1
      LMAX=M+4
C
      READ(5,803) (WB(I),I=1,KMAX1)
      READ(5,803) (SIG(I),I=1,KMAX1)
  803 FORMAT(4(D18.8))
      READ(5,804) (U(J),J=1,NP)
  804 FORMAT(3(D24.15))
C
C     CALL SUBROUTINE TO EVALUATE ANGULAR CROSS SECTION EXPANSION
```

```
C     COEFFICIENTS
C
      CALL XSEC(KMAX,NORD,SIG,WB)
C
      DO 5 I=1,NBREAK
      W(I)=WB((I-1)*NORD+1)
    5 CONTINUE
C
C     CHECK FOR SYMMETRY OF THE ANGULAR MESH.  IF THE MESH
C     IS SYMMETRIC, ONLY ONE-HALF OF THE APPROXIMATED
C     SCATTERING KERNEL VALUES A(I,J) NEED TO BE CALCULATED.
C     THE OTHERS MAY BE DETERMINED FROM SYMMETRY CONDITIONS.
C
      IFLAG=1
      DO 10 I=1,NP
      IF(U(I).NE.-U(NP+1-I)) THEN
        IFLAG=0
        GO TO 15
      END IF
   10 CONTINUE
   15 CONTINUE
C
      IF(IFLAG.EQ.1) THEN
        NP1=IFIX((NP+1)/2.)
      ELSE
        NP1=NP
      END IF
C
      NP2=NP+1
C
C     BEGIN LOOP TO CALCULATE SCATTERING KERNEL MATRIX ELEMENTS A(I,J)
C
      DO 20 I=1,NP1
      DO 20 J=1,NP
C
      A(I,J)=0.DO
C
C     CALL SUBROUTINE TO DETERMINE WHETHER A PARTICULAR A(I,J)
C     SCATTERING KERNEL IS NONZERO.
C
      CALL COVER(I,J,IFLAG2)
C
      IF(IFLAG2.EQ.1) THEN
        WRITE(9,920) I,J
  920   FORMAT(5X,I2,',',I2)
        DO 25 N=1,NMAX1
        DO 25 L=1,LMAX
        DO 25 K=1,KMAX
        A(I,J)=A(I,J)+F(K,L,I,N,J)
   25   CONTINUE
      END IF
C
      A(I,J)=2.DO*A(I,J)
      IF(IFLAG.EQ.1) A(NP2-I,NP2-J)=A(I,J)
```

```
   20 CONTINUE
C
C     CHECK ACCURACY OF A(I,J) VALUES BY SUMMING UP THE SCATTERING
C     SOURCE TERM FOR EACH U(I), ASSUMING A UNIFORM FLUX.  IF THE
C     A(I,J) VALUES ARE CORRECT, THE RESULTING SOURCE TERM FOR
C     EACH U(I) SHOULD EQUAL THE GROUP SCATTERING CROSS SECTION.
C
      DO 50 I=1,NP
      SIGT(I)=0.
      DO 50 J=1,NP
      SIGT(I)=SIGT(I)+A(J,I)
   50 CONTINUE
C
      DO 60 I=1,NP
      WRITE(6,900) U(I),SIGT(I)
   60 CONTINUE
  900 FORMAT(5X,'SIGMA(',F9.6,') = ',D13.6)
C
      WRITE(6,901)
  901 FORMAT(/////)
C
      WRITE(6,902) ((A(I,J),J=1,NP),I=1,NP)
  902 FORMAT(4(D18.8))
      STOP
      END
C
C
C
C  **********************************************************************
C  **********************   SUBROUTINE XSEC   ***************************
C  **********************************************************************
C
C     SUBROUTINE TO EVALUATE EXPANSION COEFFICIENTS FOR LINEAR OR
C     QUADRATIC CROSS SECTION FIT.
      SUBROUTINE XSEC(KMAX,NORD,SIG,WB)
      IMPLICIT REAL*8 (A-H,O-Z)
      DIMENSION SIG(7),WB(7)
      COMMON/BLOCK1/ U(50),W(4),AA(3),BB(3),CC(3)
C
C     EVALUATE COEFFICIENTS FOR LINEAR FIT
      IF(NORD.EQ.1) THEN
        DO 100 K=1,KMAX
        K1=K
        K2=K+1
C
        AA(K)=0.
        BB(K)=(SIG(K1)-SIG(K2))/(WB(K1)-WB(K2))
        CC(K)=(WB(K1)*SIG(K2)-WB(K2)*SIG(K1))/(WB(K1)-WB(K2))
  100   CONTINUE
C
C       EVALUATE COEFFICIENTS FOR QUADRATIC FIT
      ELSE
        DO 200 K=1,KMAX
        K1=(K-1)*2+1
```

```
          K2=K1+1
          K3=K1+2
C
          D=WB(K1)**2*(WB(K2)-WB(K3))-WB(K2)**2*(WB(K1)-WB(K3))+WB(K3)**2*
     @   (WB(K1)-WB(K2))
          D1=SIG(K1)*(WB(K2)-WB(K3))-SIG(K2)*(WB(K1)-WB(K3))+SIG(K3)*(WB(K
     @   1)-WB(K2))
          D2=WB(K1)**2*(SIG(K2)-SIG(K3))-WB(K2)**2*(SIG(K1)-SIG(K3))+WB(K3
     @   )**2*(SIG(K1)-SIG(K2))
          D3=WB(K1)**2*(WB(K2)*SIG(K3)-WB(K3)*SIG(K2))-WB(K2)**2*(WB(K1)*S
     @   IG(K3)-WB(K3)*SIG(K1))+WB(K3)**2*(WB(K1)*SIG(K2)-WB(K2)*SIG(K1))
C
          AA(K)=D1/D
          BB(K)=D2/D
          CC(K)=D3/D
  200     CONTINUE
C
        END IF
C
  500 RETURN
        END
C
C
C
C  ***********************************************************************
C  **********************   SUBROUTINE COVER   ***************************
C  ***********************************************************************
C
C     SUBROUTINE TO DETERMINE WHETHER A PARTICULAR SCATTERING KERNEL
C     A(I,J) IS NONZERO.
      SUBROUTINE COVER(I,J,IFLAG2)
      IMPLICIT REAL*8(A-H,O-Z)
      DIMENSION THETA(50),UBAR(50)
      COMMON/BLOCK1/ U(50),W(4),AA(3),BB(3),CC(3)
      COMMON/BLOCK2/ NMAX,KMAX,M,NP,NORD
C
      PI=4.*DATAN(1.DO)
      THEMAX=DACOS(W(1))
      THEMIN=DACOS(W(KMAX+1))
C
      DO 10 II=1,NP
      THETA(II)=DACOS(U(II))
   10 CONTINUE
C
      M1=M+1
      DO 20 JK=1,M1
      UBAR(JK)=U((JK-1)*NMAX+1)
   20 CONTINUE
C
      IF(I.EQ.1) THEN
        IL=1
        IU=NMAX+1
      ELSE IF(I.EQ.NP) THEN
        IL=NP-NMAX
```

```
          IU=NP
        ELSE
          DO 30 JK=1,M1
          IF(U(I).EQ.UBAR(JK)) THEN
            IL=I-NMAX
            IU=I+NMAX
            GO TO 40
          ELSE IF(U(I).GT.UBAR(JK).AND.U(I).LT.UBAR(JK+1)) THEN
            IL=(JK-1)*NMAX+1
            IU=IL+NMAX
            GO TO 40
          END IF
   30     CONTINUE
        END IF
C
C       DETERMINE POLAR BOUNDS FOR SCATTERING
C
   40   CONTINUE
        DO 50 II=IL,IU
        IF(THETA(II)+THEMAX.LE.PI) THEN
          BETMAX=THETA(II)+THEMAX
        ELSE IF(THETA(II)+THEMIN.GE.PI) THEN
          BETMAX=2.*PI-THETA(II)-THEMIN
        ELSE
          BETMAX=PI
        END IF
C
        IF(THEMAX.LT.THETA(II)) THEN
          BETMIN=THETA(II)-THEMAX
        ELSE IF(THETA(II).LT.THEMIN) THEN
          BETMIN=THEMIN-THETA(II)
        ELSE
          BETMIN=0.
        END IF
C
        IF(THETA(J).GE.BETMIN.AND.THETA(J).LE.BETMAX) THEN
          IFLAG2=1
          GO TO 500
        ELSE
          IFLAG2=0
        END IF
C
   50   CONTINUE
C
  500   RETURN
        END
C
C
C
C  ***********************************************************************
C  ***************************   FUNCTION F   ****************************
C  ***********************************************************************
C
C       SUBROUTINE TO EVALUATE THE FUNCTION F(K,L,I,N,J)
```

```
      DOUBLE PRECISION FUNCTION F(K,L,I,N,J)
      IMPLICIT REAL*8 (A-H,O-Z)
      COMMON/BLOCK1/ U(50),W(4),AA(3),BB(3),CC(3)
      COMMON/BLOCK2/ NMAX,KMAX,M,NP,NORD
      COMMON/BLOCK3/ V(54)
C
C     CALL SUBROUTINE TO EVALUATE MU-PRIME BREAKPOINTS AND ORDER THE
C     LIMITS OF INTEGRATION.
C
      CALL LIMITS(K,J)
C
C     CALCULATE F(K,L,I,N,J)
      K1=K+1
      COEF=COEFF(L,N,I)
      IF(COEF.NE.0.D0) THEN
        IF(NORD.EQ.1) THEN
C
C       IF A LINEAR CROSS SECTION EXPANSION IS USED, THE 'SHORT'
C       VERSION OF THE FUNCTION G(K,L,N,U,KK) IS UTILIZED.
          F=COEF*(FNGA(K,L,N,U(J),K)-FNGA(K,L,N,U(J),K1))
        ELSE
C       IF A QUADRATIC CROSS SECTION EXPANSION IS USED, THE 'LONG'
C       VERSION OF THE FUNCTION G(K,L,N,U,KK) IS UTILIZED.
          F=COEF*(FNGB(K,L,N,U(J),K)-FNGB(K,L,N,U(J),K1))
        END IF
      ELSE
        F=0.D0
      END IF
C
      RETURN
      END
C
C
C
C ***********************************************************************
C ***********************  SUBROUTINE LIMITS  ***************************
C ***********************************************************************
C
C     SUBROUTINE TO EVALUATE THE MU-PRIME BREAKPOINTS AND ORDER THE
C     INTEGRATION LIMITS
      SUBROUTINE LIMITS(K,J)
      IMPLICIT REAL*8 (A-H,O-Z)
      DIMENSION UPR(4),UBAR(50)
      COMMON/BLOCK1/ U(50),W(4),AA(3),BB(3),CC(3)
      COMMON/BLOCK2/ NMAX,KMAX,M,NP,NORD
      COMMON/BLOCK3/ V(54)
      EQUIVALENCE (V(1),UPR(1)),(V(5),UBAR(1))
C
      M1=M+1
      M5=M+5
C
      DO 10 JJ=1,M1
      UBAR(JJ)=U((JJ-1)*NMAX+1)
   10 CONTINUE
```

```
C
      WW=W(K)
      WW1=W(K+1)
      UU=U(J)
      UPR(1)=UU*WW+DSQRT((1.-UU**2)*(1.-WW**2))
      UPR(2)=UU*WW-DSQRT((1.-UU**2)*(1.-WW**2))
      UPR(3)=UU*WW1+DSQRT((1.-UU**2)*(1.-WW1**2))
      UPR(4)=UU*WW1-DSQRT((1.-UU**2)*(1.-WW1**2))
C
      CALL SORT(V,M5)
C
      RETURN
      END
C
C
C
C  ***********************************************************************
C  **************************   SUBROUTINE SORT   ************************
C  ***********************************************************************
C
      SUBROUTINE SORT(A,N)
      IMPLICIT REAL*8 (A-H,O-Z)
      DIMENSION A(54)
      JUMP=N
   10 JUMP=JUMP/2
      IF(JUMP.EQ.0) GO TO 500
      J2=N-JUMP
      DO 25 J=1,J2
   15 I=J
   20 J3=I+JUMP
      IF(A(I).LE.A(J3)) GO TO 25
      HOLD=A(I)
      A(I)=A(J3)
      A(J3)=HOLD
      I=I-JUMP
      IF(I.GT.0) GO TO 20
   25 CONTINUE
      GO TO 10
  500 RETURN
      END
C
C
C
C  ***********************************************************************
C  **************************   FUNCTION COEFF   *************************
C  ***********************************************************************
C
C     SUBROUTINE TO EVALUATE THE COEFFICIENTS OF THE ANGULAR
C     FLUX EXPANSION.
      DOUBLE PRECISION FUNCTION COEFF(L,N,I)
      IMPLICIT REAL*8 (A-H,O-Z)
      DIMENSION H(3),UBAR(50),UN(4)
      COMMON/BLOCK1/ U(50),W(4),AA(3),BB(3),CC(3)
      COMMON/BLOCK2/ NMAX,KMAX,M,NP,NORD
```

```
      COMMON/BLOCK3/ V(54)
C
      M1=M+1
      DO 100 JJ=1,M1
      UBAR(JJ)=U((JJ-1)*NMAX+1)
  100 CONTINUE
C
      DO 150 J=1,M
      H(1)=(U(I)-UBAR(J))*(UBAR(J+1)-U(I))
      H(2)=(V(L)-UBAR(J))*(UBAR(J+1)-V(L))
      H(3)=(V(L+1)-UBAR(J))*(UBAR(J+1)-V(L+1))
C
      HH=1.D0
C
      DO 200 II=1,3
      IF(H(II).GE.0.D0) THEN
        H(II)=1.D0
        ELSE
        H(II)=0.D0
      END IF
C
      HH=HH*H(II)
  200 CONTINUE
C
      COEFF=0.D0
C
      IF(HH.EQ.0.D0) GO TO 150
C
      JL=J*NMAX-NMAX+1
      JU=JL+NMAX
C
      IF(NMAX.EQ.2) GO TO 300
      IF(NMAX.EQ.3) GO TO 400
C
C     EVALUATE EXPANSION COEFFICIENTS FOR FIRST ORDER FIT
C
      DO 250 K=JL,JU
      IF(U(K).NE.U(I)) THEN
        IF(N.EQ.1) THEN
          COEFF=(-U(K)/(U(I)-U(K)))
        ELSE
          COEFF=(1/(U(I)-U(K)))
        END IF
      END IF
  250 CONTINUE
      IF(COEFF.NE.0.D0) GO TO 500
      GO TO 150
C
  300 CONTINUE
C
C     EVALUATE EXPANSION COEFFICIENTS FOR SECOND ORDER FIT
C
      DENOM=1.D0
      DNUM1=0.D0
```

```
      DNUM2=1.DO
      DO 350 K=JL,JU
      IF(K.NE.I) THEN
        DENOM=DENOM*(U(I)-U(K))
        DNUM1=DNUM1-U(K)
        DNUM2=DNUM2*U(K)
      END IF
  350 CONTINUE
C
      IF(N.EQ.1) THEN
        COEFF=(DNUM2/DENOM)
      ELSE IF(N.EQ.2) THEN
        COEFF=(DNUM1/DENOM)
      ELSE
        COEFF=(1.DO/DENOM)
      END IF
C
      IF(COEFF.NE.0.DO) GO TO 500
      GO TO 150
C
  400 CONTINUE
C
C     EVALUATE EXPANSION COEFFICIENTS FOR THIRD ORDER FIT
C
      DENOM=1.DO
      DNUM1=0.DO
      DNUM2=0.DO
      DNUM3=1.DO
      JJ=0
      DO 450 K=JL,JU
      IF(K.NE.I) THEN
        JJ=JJ+1
        DENOM=DENOM*(U(I)-U(K))
        DNUM1=DNUM1-U(K)
        DNUM3=DNUM3*U(K)
        UN(JJ)=U(K)
      END IF
  450 CONTINUE
C
      DNUM2=UN(1)*UN(2)+UN(1)*UN(3)+UN(2)*UN(3)
C
      IF(N.EQ.1) THEN
        COEFF=-DNUM3/DENOM
      ELSE IF (N.EQ.2) THEN
        COEFF=DNUM2/DENOM
      ELSE IF(N.EQ.3) THEN
        COEFF=DNUM1/DENOM
      ELSE
        COEFF=1.DO/DENOM
      END IF
C
      IF(COEFF.NE.0.DO) GO TO 500
C
  150 CONTINUE
```

```
C
  500 RETURN
      END
C
C
C
C  ***********************************************************************
C  ************************   FUNCTION FNGA   ************************
C  ***********************************************************************
C
C     SUBROUTINE TO EVALUATE THE FUNCTION FNG(K,L,N,U,KK)
C     WHEN A PIECEWISE LINEAR CROSS SECTION EXPANSION IS USED
      DOUBLE PRECISION FUNCTION FNGA(K,L,N,UU,KK)
      IMPLICIT REAL*8 (A-H,O-Z)
      COMMON/BLOCK1/ U(50),W(4),AA(3),BB(3),CC(3)
      COMMON/BLOCK3/ V(54)
C
      PI=4.DO*DATAN(1.DO)
      WW=W(KK)
      V1=V(L)
      V2=V(L+1)
      VV=5.D-01*(V1+V2)
C
      IF(WW.EQ.1.) THEN
        FNGA=0.
        GO TO 500
      END IF
C
      IF(V1.EQ.V2) THEN
        FNGA=0.
        GO TO 500
      END IF
C
      DNUM=WW-UU*VV
      DENOM=DSQRT((1.-UU**2)*(1.-VV**2))
C
      IF(DENOM.EQ.0..OR.V1.EQ.-1..OR.V2.EQ.1.) THEN
        IF(DNUM.GT.0.) THEN
          FNGA=0.
          GO TO 500
        ELSE IF(DNUM.LT.0.) THEN
          ARG=-1.
          GO TO 50
        ELSE IF(DNUM.EQ.0.) THEN
          IF(V1.EQ.-1.) THEN
            V1=-0.99999
          END IF
          IF(V2.EQ.1.)THEN
            V2=0.99999
          END IF
        GO TO 100
        END IF
      END IF
C
```

```
   40 CONTINUE
      ARG=DNUM/DENOM
C
      IF(ARG.LT.1.DO.AND.ARG.GT.-1.DO) GO TO 100
C
   50 CONTINUE
C
      IF(ARG.GE.1.DO) THEN
        FNGA=0.DO
C
      ELSE IF(ARG.LE.-1.DO) THEN
        A1=(BB(K)*UU/(N+1))*(V2**(N+1)-V1**(N+1))
        A2=(CC(K)/N)*(V2**N-V1**N)
        FNGA=PI*(A1+A2)
C
      END IF
      GO TO 500
C
  100 IF(N.EQ.1) THEN
        FNGA=BB(K)*UU*(FNF1(V2,WW,UU)-FNF1(V1,WW,UU))+CC(K)*(FNFO(V2,WW,
     @  UU)-FNFO(V1,WW,UU))+BB(K)*(FNGO(V2,WW,UU)-FNGO(V1,WW,UU))
C
      ELSE IF(N.EQ.2) THEN
        FNGA=BB(K)*UU*(FNF2(V2,WW,UU)-FNF2(V1,WW,UU))+CC(K)*(FNF1(V2,WW,
     @  UU)-FNF1(V1,WW,UU))+BB(K)*(FNG1(V2,WW,UU)-FNG1(V1,WW,UU))
C
      ELSE IF(N.EQ.3) THEN
        FNGA=BB(K)*UU*(FNF3(V2,WW,UU)-FNF3(V1,WW,UU))+CC(K)*(FNF2(V2,WW,
     @  UU)-FNF2(V1,WW,UU))+BB(K)*(FNG2(V2,WW,UU)-FNG2(V1,WW,UU))
C
      ELSE IF(N.EQ.4) THEN
        FNGA=BB(K)*UU*(FNF4(V2,WW,UU)-FNF4(V1,WW,UU))+CC(K)*(FNF3(V2,WW,
     @  UU)-FNF3(V1,WW,UU))+BB(K)*(FNG3(V2,WW,UU)-FNG3(V1,WW,UU))
C
      END IF
C
  500 RETURN
      END
C
C
C
C ***********************************************************************
C ************************  FUNCTION FNGB  ******************************
C ***********************************************************************
C
C     SUBROUTINE TO EVALUATE THE FUNCTION FNG(K,L,N,U,KK)
C     WHEN A PIECEWISE QUADRATIC CROSS SECTION EXPANSION IS USED
      DOUBLE PRECISION FUNCTION FNGB(K,L,N,UU,KK)
      IMPLICIT REAL*8 (A-H,O-Z)
      COMMON/BLOCK1/ U(50),W(4),AA(3),BB(3),CC(3)
      COMMON/BLOCK3/ V(54)
C
      PI=4.DO*DATAN(1.DO)
      WW=W(KK)
```

```
      V1=V(L)
      V2=V(L+1)
      VV=5.D-01*(V1+V2)
C
      IF(WW.EQ.1.) THEN
        FNGB=0.
        GO TO 500
      END IF
C
      IF(V1.EQ.V2) THEN
        FNGB=0.
        GO TO 500
      END IF
C
      DNUM=WW-UU*VV
      DENOM=DSQRT((1.-UU**2)*(1.-VV**2))
C
      IF(DENOM.EQ.0..OR.V1.EQ.-1..OR.V2.EQ.1.) THEN
        IF(DNUM.GT.0.) THEN
          FNGB=0.
          GO TO 500
        ELSE IF(DNUM.LT.0.) THEN
          ARG=-1.
          GO TO 50
        ELSE IF(DNUM.EQ.0.) THEN
          IF(V1.EQ.-1.) THEN
            V1=-0.99999
          END IF
          IF(V2.EQ.1.) THEN
            V2=0.99999
          END IF
        END IF
      END IF
C
   40 CONTINUE
      ARG=DNUM/DENOM
C
      IF(ARG.LT.1.D0.AND.ARG.GT.-1.D0) GO TO 100
C
   50 CONTINUE
C
      IF(ARG.GE.1.D0) THEN
        FNGB=0.D0
C
      ELSE IF(ARG.LE.-1.D0) THEN
        A1=(AA(K)*UU**2/(N+2)-AA(K)*(1.-UU**2)/(2.*(N+2)))*(V2**(N+2)-V1
     @  **(N+2))
        A2=(BB(K)*UU/(N+1))*(V2**(N+1)-V1**(N+1))
        A3=(CC(K)/N+AA(K)*(1.-UU**2)/(2.*N))*(V2**N-V1**N)
        FNGB=PI*(A1+A2+A3)
C
      END IF
      GO TO 500
C
```

```
  100 IF(N.EQ.1) THEN
        FNGB=AA(K)/2.*(3.*UU**2-1.)*(FNF2(V2,WW,UU)-FNF2(V1,WW,UU))+BB(K
     @  )*UU*(FNF1(V2,WW,UU)-FNF1(V1,WW,UU))+(CC(K)+AA(K)*(1.-UU**2)/2.)
     @  *(FNFO(V2,WW,UU)-FNFO(V1,WW,UU))+3./2.*AA(K)*UU*(FNG1(V2,WW,UU)-
     @  FNG1(V1,WW,UU))+(BB(K)+AA(K)*WW/2.)*(FNGO(V2,WW,UU)-FNGO(V1,WW,U
     @  U))
C
      ELSE IF(N.EQ.2) THEN
        FNGB=AA(K)/2.*(3.*UU**2-1.)*(FNF3(V2,WW,UU)-FNF3(V1,WW,UU))+BB(K
     @  )*UU*(FNF2(V2,WW,UU)-FNF2(V1,WW,UU))+(CC(K)+AA(K)*(1.-UU**2)/2.)
     @  *(FNF1(V2,WW,UU)-FNF1(V1,WW,UU))+3./2.*AA(K)*UU*(FNG2(V2,WW,UU)-
     @  FNG2(V1,WW,UU))+(BB(K)+AA(K)*WW/2.)*(FNG1(V2,WW,UU)-FNG1(V1,WW,U
     @  U))
C
      ELSE IF(N.EQ.3) THEN
        FNGB=AA(K)/2.*(3.*UU**2-1.)*(FNF4(V2,WW,UU)-FNF4(V1,WW,UU))+BB(K
     @  )*UU*(FNF3(V2,WW,UU)-FNF3(V1,WW,UU))+(CC(K)+AA(K)*(1.-UU**2)/2.)
     @  *(FNF2(V2,WW,UU)-FNF2(V1,WW,UU))+3./2.*AA(K)*UU*(FNG3(V2,WW,UU)-
     @  FNG3(V1,WW,UU))+(BB(K)+AA(K)*WW/2.)*(FNG2(V2,WW,UU)-FNG2(V1,WW,U
     @  U))
      END IF
C
  500 RETURN
      END
C
C
C
C
C  **********************************************************************
C  **********************   FUNCTION SUBROUTINES   **********************
C  **********************************************************************
C
C     SUBROUTINE TO EVALUATE THE FUNCTION FO(X,W,U)
      DOUBLE PRECISION FUNCTION FNFO(X,W,U)
      IMPLICIT REAL*8 (A-H,O-Z)
      A=W/DSQRT(1.-U**2)
      B=U/DSQRT(1.-U**2)
      A1=A/DSQRT(B**2+1.)
      FNFO=X*FNH1(X,A,B)+A1*FNH2(X,A,B)+FNH3(X,A,B)-FNH4(X,A,B)
      RETURN
      END
C
C
C
C
C     SUBROUTINE TO EVALUATE THE FUNCTION F1(X,W,U)
      DOUBLE PRECISION FUNCTION FNF1(X,W,U)
      IMPLICIT REAL*8 (A-H,O-Z)
      A=W/DSQRT(1.-U**2)
      B=U/DSQRT(1.-U**2)
      A1=(A**2*B-B*(B**2+1.))/((DSQRT(B**2+1.))**3)
      FNF1=(X**2*FNH1(X,A,B)+A1*FNH2(X,A,B)-FNH3(X,A,B)-FNH4(X,A,B)+A*FN
     @H5(X,A,B))/2.
      RETURN
```

```
      END
C
C
C
C
C     SUBROUTINE TO EVALUATE THE FUNCTION F2(X,W,U)
      DOUBLE PRECISION FUNCTION FNF2(X,W,U)
      IMPLICIT REAL*8 (A-H,O-Z)
      A=W/DSQRT(1.-U**2)
      B=U/DSQRT(1.-U**2)
      A1=3.*A**2*B**2/((B**2+1.)**2)
      A2=A1+2.-(2.*B**2+A**2-1.)/(B**2+1.)
      A3=A*A2/(2.*DSQRT(B**2+1.))
      A4=(A*X-2.*B+(3.*A**2*B/(B**2+1.)))/2.
      FNF2=(X**3*FNH1(X,A,B)+A3*FNH2(X,A,B)+FNH3(X,A,B)-FNH4(X,A,B)+A4*F
     @NH5(X,A,B))/3.
      RETURN
      END
C
C
C
C
C     FUNCTION SUBROUTINE TO EVALUATE F3(X,W,U)
      DOUBLE PRECISION FUNCTION FNF3(X,W,U)
      IMPLICIT REAL*8(A-H,O-Z)
      A=W/DSQRT(1.-U**2)
      B=U/DSQRT(1.-U**2)
      P=1./(B**2+1.)
      R=DSQRT(B**2+1.)
      A1=(5.*A**2*B**3*P-3.*B*(A**2-1.))*A**2/(2.*R**5)
      A2=(3.*A**2*B**2*P-3.*A**2+1.+2.*R**2)*B/(2.*R**3)
      A3=(X+3.*A*B*P)*B/2.
      A4=(X**2/3.+5.*A*B*P*X/6.-2.*(A**2-1.)*P/3.+1.)
      A5=A*(A4+5.*A**2*B**2*P**2/2.)
      FNF3=(X**4*FNH1(X,A,B)+(A1-A2)*FNH2(X,A,B)-FNH3(X,A,B)-FNH4(X,A,B)
     @+(A5-A3)*FNH5(X,A,B))/4.
      RETURN
      END
C
C
C
C
C     SUBROUTINE TO EVALUATE THE FUNCTION F4(X,W,U)
      DOUBLE PRECISION FUNCTION FNF4(X,W,U)
      IMPLICIT REAL*8 (A-H,O-Z)
      A=W/DSQRT(1.-U**2)
      B=U/DSQRT(1.-U**2)
      P=1./(B**2+1.)
      R=DSQRT(B**2+1.)
      S=A**2-1.
      T=A*B
      A1=(7.*A*T/(4.*R**2)-B)*(5.*T**2*P-3.*S)*T/(2.*R**5)
      A2=(3.*A*T**2*P/2.-A*S/2.-B*T+A*R**2)/(R**3)
      A3=(3.*A*S/(8.*R**5))*(3.*T**2*P-S)
```

```
      A2=A1+A2-A3
      A5=(X**2/(3.*P)+5.*T*X/6.-2.*S/3.+5.*T**2*P/2.)*7.*A*T*P**2/4.
      A6=(X+3.*T*P+(X**3)/2.)*A/2.-(X+3.*T*P)*3.*A*S*P/8.
      A7=(X**2/3.+5.*T*P*X/6.-2.*S*P/3.+5.*T**2*P**2/2.+1.)*B
      A5=A5+A6-A7
      FNF4=(X**5*FNH1(X,A,B)+A2*FNH2(X,A,B)+FNH3(X,A,B)-FNH4(X,A,B)+A5*F
     @NH5(X,A,B))/5.
      RETURN
      END
C
C
C
C     SUBROUTINE TO EVALUATE THE FUNCTION GO(X,W,U)
      DOUBLE PRECISION FUNCTION FNGO(X,W,U)
      IMPLICIT REAL*8 (A-H,O-Z)
      C=1.-U**2-W**2
      D=2.*W*U
      ARG1=C+D*X-X**2
      IF(ARG1.LT.0.DO.AND.ARG1.GT.-1.D-05) ARG1=0.DO
      A1=(2.*X-D)*DSQRT(ARG1)/4.
      A2=(D**2+4.*C)/8.
      FNGO=A1-A2*FNH6(X,C,D)
      RETURN
      END
C
C
C
C
C     SUBROUTINE TO EVALUATE THE FUNCTION G1(X,W,U)
      DOUBLE PRECISION FUNCTION FNG1(X,W,U)
      IMPLICIT REAL*8 (A-H,O-Z)
      C=1.-U**2-W**2
      D=2.*W*U
      ARG1=C+D*X-X**2
      IF(ARG1.LT.0.DO.AND.ARG1.GT.-1.D-05) ARG1=0.DO
      A1=((DSQRT(ARG1))**3)/3.
      A2=DSQRT(ARG1)*D*(D-2.*X)/8.
      A3=D*(D**2+4.*C)/16.
      FNG1=-A1-A2-A3*FNH6(X,C,D)
      RETURN
      END
C
C
C
C
C     SUBROUTINE TO EVALUATE THE FUNCTION G2(X,W,U)
      DOUBLE PRECISION FUNCTION FNG2(X,W,U)
      IMPLICIT REAL*8 (A-H,O-Z)
      C=1.-U**2-W**2
      D=2.*W*U
      ARG1=C+D*X-X**2
      IF(ARG1.LT.0.DO.AND.ARG1.GT.-1.D-05) ARG1=0.DO
      A1=((DSQRT(ARG1))**3)/4.
      A2=A1*(X+5.*D/6.)
```

```
      A3=(5.*D**2+4.*C)/16.
      FNG2=-A2+A3*FNG0(X,W,U)
      RETURN
      END
C
C
C
C
C     SUBROUTINE TO EVALUATE THE FUNCTION G3(X,W,U)
      DOUBLE PRECISION FUNCTION FNG3(X,W,U)
      IMPLICIT REAL*8 (A-H,O-Z)
      C=1.-U**2-W**2
      D=2.*W*U
      ARG1=C+D*X-X**2
      IF(ARG1.LT.0.DO.AND.ARG1.GT.-1.D-05) ARG1=0.DO
      A1=((DSQRT(ARG1))**3)*X**2/5.
      A2=7.*D/10.
      A3=2.*C/5.
      FNG3=-A1+A2*FNG2(X,W,U)+A3*FNG1(X,W,U)
      RETURN
      END
C
C
C
C
C     FUNCTION SUBROUTINE FOR H1(X,A,B)
      DOUBLE PRECISION FUNCTION FNH1(X,A,B)
      IMPLICIT REAL*8 (A-H,O-Z)
      ARG1=(A-B*X)/DSQRT(1.-X**2)
      IF(ARG1.GT.1.DO.AND.DABS(ARG1-1.DO).LT.1.D-05) ARG1=1.DO
      IF(ARG1.LT.-1.DO.AND.DABS(ARG1+1.DO).LT.1.D-05) ARG1=-1.DO
      FNH1=DARCOS(ARG1)
      RETURN
      END
C
C
C
C
C     FUNCTION SUBROUTINE FOR H2(X,A,B)
      DOUBLE PRECISION FUNCTION FNH2(X,A,B)
      IMPLICIT REAL*8 (A-H,O-Z)
      A1=-1.DO*(B**2+1.DO)*X+A*B
      A2=DSQRT(1.DO-A**2+B**2)
      ARG1=A1/A2
      IF(ARG1.GT.1.DO.AND.DABS(ARG1-1.DO).LT.1.D-05) ARG1=1.DO
      IF(ARG1.LT.-1.DO.AND.DABS(ARG1+1.DO).LT.1.D-05) ARG1=-1.DO
      FNH2=DARSIN(ARG1)
      RETURN
      END
C
C
C
C
C     FUNCTION SUBROUTINE TO EVALUATE H3(X,A,B)
```

```
      DOUBLE PRECISION FUNCTION FNH3(X,A,B)
      IMPLICIT REAL*8 (A-H,O-Z)
      IF(A.EQ.-B) THEN
        FNH3=0.
        GO TO 500
      END IF
      A1=(A*B+B**2+1.DO)*(X+1.DO)-((A+B)**2)
      A2=DABS(X+1)*DSQRT(1.DO-A**2+B**2)
      A3=5.D-01*(A+B)/DABS(A+B)
      ARG1=A1/A2
      IF(ARG1.GT.1.DO.AND.DABS(ARG1-1.DO).LT.1.D-05) ARG1=1.DO
      IF(ARG1.LT.-1.DO.AND.DABS(ARG1+1.DO).LT.1.D-05) ARG1=-1.DO
      FNH3=A3*DARSIN(ARG1)
  500 RETURN
      END
C
C
C
C
C     FUNCTION SUBROUTINE TO EVALUATE THE FUNCTION H4(X,A,B)
      DOUBLE PRECISION FUNCTION FNH4(X,A,B)
      IMPLICIT REAL*8 (A-H,O-Z)
      IF(A.EQ.B) THEN
        FNH4=0.
        GO TO 500
      END IF
      A1=(A*B-B**2-1.DO)*(X-1.DO)-((A-B)**2)
      A2=DABS(X-1.DO)*DSQRT(1.DO-A**2+B**2)
      A3=5.D-01*(A-B)/DABS(A-B)
      ARG1=A1/A2
      IF(ARG1.GT.1.DO.AND.DABS(ARG1-1.DO).LT.1.D-05) ARG1=1.DO
      IF(ARG1.LT.-1.DO.AND.DABS(ARG1+1.DO).LT.1.D-05) ARG1=-1.DO
      FNH4=A3*DARSIN(ARG1)
  500 RETURN
      END
C
C
C
C
C     FUNCTION SUBROUTINE TO EVALUATE THE FUNCTION H5(X,A,B)
      DOUBLE PRECISION FUNCTION FNH5(X,A,B)
      IMPLICIT REAL*8 (A-H,O-Z)
      ARG1=(2.DO*A*B*X-(B**2+1.DO)*X**2-(A**2-1.DO))
      IF(ARG1.LT.0.DO.AND.ARG1.GT.-1.D-05) ARG1=0.DO
      A1=DSQRT(ARG1)
      A2=B**2+1.DO
      FNH5=A1/A2
      RETURN
      END
C
C
C
C
C     SUBROUTINE TO EVALUATE THE FUNCTION H6(X,C,D)
```

```
DOUBLE PRECISION FUNCTION FNH6(X,C,D)
IMPLICIT REAL*8 (A-H,O-Z)
ARG1=(D-2.*X)/DSQRT(D**2+4.*C)
IF(ARG1.GT.1.DO.AND.DABS(ARG1-1.DO).LT.1.D-05) ARG1=1.DO
IF(ARG1.LT.-1.DO.AND.DABS(ARG1+1.DO).LT.1.D-05) ARG1=-1.DO
FNH6=DARSIN(ARG1)
RETURN
END
```

```
C
C                    ***  PROGRAM NAME:  TRANS  ***
C
C     PROGRAM TO SOLVE THE ONE-DIMENSIONAL, AZIMUTHALLY SYMMETRIC
C     PLANE GEOMETRY DISCRETE ORDINATES EQUATIONS.  SCATTERING
C     CAN BE ISOTROPIC OR ANISOTROPIC.  ANISOTROPIC GROUP-TO-GROUP
C     APPROXIMATED SCATTERING KERNELS ARE GENERATED BY THE CODE
C     'ASKERNEL' AND THE RESULTING APPROXIMATED SCATTERING KERNEL
C     TRANSFER MATRIX IS INPUT INTO THIS CODE.  BECAUSE THIS CODE
C     USES THE APPROXIMATED SCATTERING KERNEL TECHNIQUE FOR
C     EVALUATION OF THE SCATTERING SOURCE TERM, THE DISCRETE
C     ORDINATES CAN BE ARBITRARILY CHOSEN (I.E., THEY DO NOT HAVE
C     TO BE A STANDARD NUMERICAL QUADRATURE SET).
C
C
C     MAJOR VARIABLES ARE AS FOLLOWS:
C     'NR'       = NUMBER OF REFLECTED DISCRETE DIRECTIONS
C     'NT'       = NUMBER OF TRANSMITTED DISCRETE DIRECTIONS
C     'NTOT'     = TOTAL NUMBER OF DISCRETE ORDINATES
C     'M'        = NUMBER OF SPATIAL NODES.  THE NODES ARE DEFINED
C                  TO BE AT THE EDGES OF THE MESH CELLS.
C     'WIDTH'    = WIDTH OF SLAB
C     'DEL'      = WIDTH OF EACH SPATIAL MESH CELL
C     'IFLAG1'   = BOUNDARY CONDITION FLAG.  SET IFLAG1=0 FOR A UNIT
C                  FLUX BOUNDARY CONDITION.  SET IFLAG1=1 FOR A UNIT
C                  CURRENT BOUNDARY CONDITION.
C     'IFLAG2'   = UNITS FLAG.  SET IFLAG2=0 FOR UNITS OF CENTIMETERS.
C                  SET IFLAG2=1 FOR UNITS OF MEAN FREE PATHS.
C     'NEXP'     = ORDER OF FLUX EXPANSION
C     'NINT'     = NUMBER OF FLUX INTERVALS
C     'EPS'      = CONVERGENCE CRITERIA FOR THE ANGULAR FLUXES
C     'IS'       = SOURCE ANGLE (DISCRETE DIRECTION NUMBER)
C     'SIGT'     = TOTAL GROUP CROSS SECTION
C     'CAP'      = CONVERGENCE ACCELERATION PARAMETER
C     'NMAX'     = MAXIMUM NUMBER OF ITERATIONS TO BE PERFORMED
C     'NUMB'     = NUMBER DENSITY OF SCATTERING MATERIAL
C     'SIGGT'    = TOTAL GROUP SCATTERING CROSS SECTION (NOT TO BE
C                  CONFUSED WITH THE TOTAL GROUP CROSS SECTION)
C
C     NOTE: THE ORDER OF THE FLUX EXPANSION ('NEXP') CAN BE
C           1 (PIECEWISE LINEAR), 2 (PIECEWISE QUADRATIC), OR
C           3 (PIECEWISE CUBIC). THE TOTAL NUMBER OF DISCRETE
C           ORDINATES USED MUST EQUAL (NEXP*NINT)+1.  THE VALUES
C           OF THESE VARIABLES MUST BE THE SAME AS THE VALUES
C           USED IN THE CODE 'ASKERNEL' TO GENERATE THE
C           APPROXIMATED SCATTERING KERNEL TRANSFER MATRIX.
C
C     NOTE: THE INPUT VALUES OF 'SIGT', 'NUMB', AND 'SIGGT' DEPEND ON
C           WHETHER UNITS OF CENTIMETERS OR MEAN FREE PATHS ARE USED.
C           THESE VALUES SHOULD BE INPUT AS FOLLOWS:
C
C           CASE (1): IF UNITS OF CENTIMETERS ARE USED (IFLAG2=0),
C                     INPUT THE TOTAL GROUP MICROSCOPIC CROSS SECTION
C                     (IN BARNS) FOR 'SIGT' (THIS INCLUDES SCATTERING
```

```
C                     AND ALL OTHER INTERACTIONS).  INPUT THE NUMBER
C                     DENSITY (1/CM**3) OF THE SCATTERING MATERIAL FOR
C                     'NUMB', AND INPUT THE TOTAL GROUP MICROSCOPIC
C                     CROSS SECTION (IN BARNS) FOR 'SIGGT'.
C
C           CASE (2): IF UNITS OF MEAN FREE PATHS ARE USED (IFLAG2=1),
C                     INPUT A VALUE OF '1' FOR 'SIGT' AND THE VALUE OF
C                     C (THE MEAN NUMBER OF SECONDARIES PER COLLISION)
C                     FOR 'NUMB'.  INPUT THE TOTAL GROUP SCATTERING
C                     CROSS SECTION (IN BARNS) FOR 'SIGGT'.
C
C     THE FOLLOWING ARRAYS ARE UTILIZED:
C     F(M,N)    = NEUTRON FLUX AT CELL EDGE
C     G(M,N)    = NEUTRON FLUX AT CELL MIDPOINT
C     Q(M,N)    = INSCATTER SOURCE
C     A(I,J)    = APPROXIMATED SCATTERING KERNEL TRANSFER MATRIX
C     U(N)      = ANGULAR MESH POINTS (THE DISCRETE ORDINATES)
C
C
      IMPLICIT REAL*8(A-H,O-Z)
      REAL*8 NORM,NUMB
      COMMON/B1/ F(200,50),G(200,50),Q(200,50),U(50),A(50,50)
      COMMON/B2/ M,NR,NT,IS,WIDTH,ERR1,ERR2,ERR3
C
C     READ INPUT PARAMETERS (DEFINED ABOVE)
C
      READ(5,800) M,WIDTH,IFLAG1,IFLAG2
  800 FORMAT(I5,D20.4,5X,2(I5))
      READ(5,803) NEXP,NINT
      READ(5,801) EPS
  801 FORMAT(5X,D20.4)
      READ(5,802) IS,NMAX,SIGT,CAP
  802 FORMAT(2(I5),D17.6,D18.4)
      READ(5,803) NR,NT
  803 FORMAT(2(I5))
C
      MM=M-1
      XMM=DFLOAT(MM)
      DEL=WIDTH/XMM
      NTOT=NR+NT
C
      READ(5,804) (U(I),I=1,NTOT)
  804 FORMAT(3(D24.10))
C
      READ(5,805) NUMB,SIGGT
  805 FORMAT(2(D24.10))
C
      IF(IFLAG2.EQ.0) THEN
        CC=SIGGT/SIGT
        SIGT=SIGT*NUMB
        SIGGT2=1.
        ELSE
        CC=NUMB
        SIGGT2=SIGGT
```

```
      END IF
C
C     READ IN APPROXIMATED SCATTERING KERNEL TRANSFER MATRIX
      READ(5,806) ((A(I,J),J=1,NTOT),I=1,NTOT)
  806 FORMAT(4(D18.8))
C
      DO 10 I=1,NTOT
      DO 10 J=1,NTOT
      A(I,J)=A(I,J)*NUMB/SIGGT2
   10 CONTINUE
C
C     INITIALIZE FLUX AND SOURCE ARRAYS AT ZERO
C
      DO 40 I=1,M
      DO 45 J=1,NTOT
      F(I,J)=0.D0
      Q(I,J)=0.D0
   45 CONTINUE
   40 CONTINUE
C
C     SET INCIDENT FLUX USING BOUNDARY CONDITION
C
      CALL NORMAL(U,IS,IFLAG1,NORM,NEXP,NINT)
C
      F(1,IS)=1./NORM
C
C     CALL SUBROUTINE TO SOLVE D.O. EQUATIONS
C
      CALL DO(DEL,EPS,SIGT,CAP,NMAX,ITER)
C
C
C     CALL SUBROUTINE TO PRINT OUT RESULTS
C
      CALL OUTPUT(IFLAG1,IFLAG2,ITER,NMAX,EPS,SIGT,CC,NEXP,NINT)
C
C
      STOP
      END
C
C
C
C     SUBROUTINE TO CALCULATE SOURCE NORMALIZATION
      SUBROUTINE NORMAL(U,II,IFLAG1,NORM,NEXP,NINT)
      IMPLICIT REAL*8 (A-H,O-Z)
      REAL*8 NORM
      DIMENSION U(50)
      NORM=0.
      DO 50 J=1,NINT
      NORM=NORM+SORCE(J,II,U,IFLAG1,NEXP,NINT)
   50 CONTINUE
      RETURN
      END
C
C
```

```
      DOUBLE PRECISION FUNCTION SORCE(J,II,U,IFLAG1,NEXP,NINT)
      IMPLICIT REAL*8 (A-H,O-Z)
      DIMENSION U(50),UBAR(50),UN(3)
      NINT1=NINT+1
      DO 10 JJ=1,NINT1
      UBAR(JJ)=U((JJ-1)*NEXP+1)
   10 CONTINUE
      H=(U(II)-UBAR(J))*(UBAR(J+1)-U(II))
      SORCE=0.
      IF(H.LT.0.) GO TO 500
C
      JL=J*NEXP-NEXP+1
      JU=JL+NEXP
      UJ1=UBAR(J+1)
      UJ=UBAR(J)
      IF(NEXP.EQ.2) GO TO 450
      IF(NEXP.EQ.3) GO TO 480
C
C     EVALUATE NORMALIZATION FOR LINEAR FLUX EXPANSION
     . DO 400 K=JL,JU
      IF(K.NE.II) THEN
        IF(IFLAG1.EQ.0) THEN
          SORCE=((UJ1**2-UJ**2)/2.-(UJ1-UJ)*U(K))/(U(II)-U(K))
        ELSE IF(IFLAG1.EQ.1) THEN
          SORCE=((UJ1**3-UJ**3)/3.-(UJ1**2-UJ**2)*U(K)/2.)/(U(II)-U(K))
        END IF
        GO TO 500
      END IF
  400 CONTINUE
C
  450 CONTINUE
C     EVALUATE NORMALIZATION FOR QUADRATIC FLUX EXPANSION
      DENOM=1.DO
      DN1=0.DO
      DN2=1.DO
      DO 475 K=JL,JU
      IF(K.NE.II) THEN
        DENOM=DENOM*(U(II)-U(K))
        DN1=DN1+U(K)
        DN2=DN2*U(K)
      END IF
  475 CONTINUE
      IF(IFLAG1.EQ.0) THEN
        SORCE=((UJ1**3-UJ**3)/3.-(UJ1**2-UJ**2)*DN1/2.+(UJ1-UJ)*DN2)/DEN
     @  OM
      ELSE IF(IFLAG1.EQ.1) THEN
        SORCE=((UJ1**4-UJ**4)/4.-(UJ1**3-UJ**3)*DN1/3.+(UJ1**2-UJ**2)*DN
     @  2/2.)/DENOM
      END IF
      GO TO 500
C
  480 CONTINUE
C     EVALUATE NORMALIZATION FOR CUBIC FLUX EXPANSION
      DENOM=1.DO
```

```
      DN1=0.DO
      DN2=0.DO
      DN3=1.DO
      JJ=0
      DO 485 K=JL,JU
      IF(K.NE.II) THEN
        JJ=JJ+1
        DENOM=DENOM*(U(II)-U(K))
        DN1=DN1+U(K)
        DN3=DN3*U(K)
        UN(JJ)=U(K)
      END IF
  485 CONTINUE
      DN2=UN(1)*UN(2)+UN(1)*UN(3)+UN(2)*UN(3)
      IF(IFLAG1.EQ.0) THEN
        SORCE=((UJ1**4-UJ**4)/4.-(UJ1**3-UJ**3)*DN1/3.+(UJ1**2-UJ**2)*DN
     @  2/2.-(UJ1-UJ)*DN3)/DENOM
      ELSE IF(IFLAG1.EQ.1) THEN
        SORCE=((UJ1**5-UJ**5)/5.-(UJ1**4-UJ**4)*DN1/4.+(UJ1**3-UJ**3)*DN
     @  2/3.-(UJ1**2-UJ**2)*DN3/2.)/DENOM
      END IF
C
  500 RETURN
      END
C
C
C
C
C     SUBROUTINE TO SOLVE THE DISCRETE ORDINATES EQUATIONS.
C
      SUBROUTINE DO(DEL,EPS,SIGT,CAP,NMAX,ITER)
      IMPLICIT REAL*8(A-H,O-Z)
      DIMENSION FP(200,50),F1(200,50),F2(200,50),X(50),Z1(50),Z2(50)
      COMMON/B1/ F(200,50),G(200,50),Q(200,50),U(50),A(50,50)
      COMMON/B2/ M,NR,NT,IS,WIDTH,ERR1,ERR2,ERR3
      MM=M-1
      NTOT=NR+NT
      NR1=NR+1
C
      XX=DEL*SIGT/2.DO
      SIGT2=SIGT/2.DO
C
      DO 1 I=1,NTOT
      X(I)=(1.DO-XX/U(I))/(1.DO+XX/U(I))
      Z1(I)=SIGT2+U(I)/DEL
      Z2(I)=SIGT2-U(I)/DEL
    1 CONTINUE
C
      ITER=0
  100 ITER=ITER+1
      DO 2 I=1,NTOT
      DO 2 K=1,M
      FP(K,I)=F(K,I)
    2 CONTINUE
```

```
C
C     SWEEP FOR FORWARD DIRECTIONS
      DO 4 I=NR1,NTOT
      DO 5 K=1,MM
      KK=K+1
      F(KK,I)=X(I)*F(K,I)+Q(KK,I)/Z1(I)
    5 CONTINUE
    4 CONTINUE
C
C     SWEEP FOR BACKWARD DIRECTIONS
      DO 6 I=1,NR
      DO 7 L=1,MM
      K=M-L+1
      KK=K-1
      F(KK,I)=F(K,I)/X(I)+Q(K,I)/Z2(I)
    7 CONTINUE
    6 CONTINUE
C
C     CALCULATE CELL-CENTER FLUXES USING DIAMOND-DIFFERENCE SCHEME
      DO 8 I=1,NTOT
      DO 9 K=2,M
      G(K,I)=(F(K-1,I)+F(K,I))/2.DO
    9 CONTINUE
    8 CONTINUE
C
C     CALCULATE THE SCATTERING SOURCE TERM
      CAPP=1.DO+CAP
      DO 10 I=1,NTOT
      DO 11 K=2,M
      QS=0.DO
      DO 12 J=1,NTOT
      QS=QS+G(K,J)*A(J,I)
   12 CONTINUE
      Q(K,I)=Q(K,I)+CAPP*(QS-Q(K,I))
   11 CONTINUE
   10 CONTINUE
C
C     CHECK FOR CONVERGENCE
C
      CALL CONVRG(F,FP,M,NR,NT,ITER,EPS,ERR1,ERR2,ERR3)
C
      WRITE(9,910) ITER,ERR1,ERR2,ERR3
  910 FORMAT(5X,I2,5X,3(D20.6))
C
C     IF CONVERGENCE REQUIREMENTS ARE SATISFIED, RETURN TO MAIN
C     PROGRAM.  IF NOT, CONTINUE WITH ITERATIONS.
C
      IF(ERR1.LE.EPS.AND.ERR2.LE.EPS.AND.ERR3.LE.EPS) GO TO 200
C
C     ADJUST CONVERGENCE ACCELERATION PARAMETER
  150 IF(CAP.GE.2.D-1) GO TO 160
      CAP=CAP*1.1
  160 CONTINUE
C
```

```
C     IF MAXIMUM NUMBER OF ITERATIONS HAVE FAILED TO PRODUCE
C     CONVERGENCE, CEASE CALCULATIONS AND EXIT TO MAIN PROGRAM.
C
      IF(ITER.GE.NMAX) GO TO 200
      GO TO 100
  200 RETURN
      END
C
C
C     SUBROUTINE TO CHECK CONVERGENCE OF ANGULAR FLUXES
      SUBROUTINE CONVRG(F,FP,M,NR,NT,ITER,EPS,ERR1,ERR2,ERR3)
      IMPLICIT REAL*8 (A-H,O-Z)
      DIMENSION F(200,50),FP(200,50)
C
      IF(ITER.EQ.1) THEN
        ERR1=1.
        ERR2=1.
        ERR3=1.
        GO TO 500
      END IF
C
C     CHECK REFLECTED FLUXES FOR CONVERGENCE
      ERR1=0.
      DO 10 I=1,NR
      IF(F(1,I).NE.0.) ERR1=DMAX1(ERR1,DABS((F(1,I)-FP(1,I))/F(1,I)))
   10 CONTINUE
C
C     CHECK TRANSMITTED FLUXES FOR CONVERGENCE
      ERR2=0.
      NR1=NR+1
      NTOT=NR+NT
      DO 20 I=NR1,NTOT
      IF(F(M,I).NE.0.) ERR2=DMAX1(ERR2,DABS((F(M,I)-FP(M,I))/F(M,I)))
   20 CONTINUE
C
      IF(ERR1.GE.EPS.OR.ERR2.GE.EPS) THEN
        ERR3=1.
        GO TO 500
      END IF
C
C     IF REFLECTED AND TRANSMITTED FLUXES HAVE CONVERGED, CHECK ALL
C     FLUXES FOR CONVERGENCE
      ERR3=0.
      DO 30 I=1,NTOT
      DO 30 K=1,M
      IF(F(K,I).NE.0.) ERR3=DMAX1(ERR3,DABS((F(K,I)-FP(K,I))/F(K,I)))
   30 CONTINUE
C
C
  500 RETURN
      END
C
C
C     SUBROUTINE TO PRINT OUT PROBLEM PARAMETERS AND RESULTS
```

```
      SUBROUTINE OUTPUT(IFLAG1,IFLAG2,ITER,NMAX,EPS,SIGT,CC,NEXP,NINT)
      IMPLICIT REAL*8(A-H,O-Z)
      REAL*8 JR,JT,JTU,JTOT
      COMMON/B1/ F(200,50),G(200,50),Q(200,50),U(50),A(50,50)
      COMMON/B2/ M,NR,NT,IS,WIDTH,ERR1,ERR2,ERR3
      NTOT=NR+NT
C
C
C     WRITE OUT PROBLEM PARAMETERS
      WRITE(6,900)
      IF(IFLAG2.EQ.0) THEN
        WRITE(6,901) WIDTH
      ELSE
        WRITE(6,902) WIDTH
      END IF
      WRITE(6,903) M
      WRITE(6,920) CC
      WRITE(6,904) NR
      WRITE(6,905) NT
      IF(IFLAG1.EQ.0) THEN
        WRITE(6,906) U(IS)
      ELSE
        WRITE(6,907) U(IS)
      END IF
      WRITE(6,908) EPS
      WRITE(6,909) ERR3
      WRITE(6,910) ITER
C
C     CHECK TO SEE IF CONVERGENCE WAS REACHED
      IF(ERR3.LE.EPS) GO TO 50
C     IF THE REQUIRED CONVERGENCE WAS NOT REACHED, WRITE OUT
C     THE NUMBER OF ITERATIONS.
   30 WRITE(6,911) NMAX
      WRITE(9,911) NMAX
      GO TO 100
C
C     WRITE OUT PROBLEM RESULTS
   50 CONTINUE
C
C     CALL SUBROUTINE TO CALCULATE THE REFLECTED AND TRANSMITTED
C     CURRENTS.
      CALL CURENT(SIGT,JR,JT,JTU,JTOT,NEXP,NINT)
C
C     CALCULATE THE SCATTERED FLUX IN THE SOURCE DIRECTION BY
C     SUBTRACTING THE UNSCATTERED FLUX COMPONENT.
C
      F(M,IS)=F(M,IS)-F(1,IS)*DEXP(-1.*WIDTH*SIGT/U(IS))
C
      WRITE(6,912)
      WRITE(6,913)
      DO 60 I=1,NTOT
      WRITE(6,914) U(I),F(1,I),M,U(I),F(M,I)
   60 CONTINUE
C
```

```
      WRITE(6,916) JR
      WRITE(6,917) JT
      WRITE(6,918) JTU
      WRITE(6,919) JTOT
      IF(NEXP.EQ.1) THEN
        WRITE(6,921)
      ELSE IF(NEXP.EQ.2) THEN
        WRITE(6,922)
      ELSE IF(NEXP.EQ.3) THEN
        WRITE(6,923)
      END IF
C
      WRITE(6,915)
C
C     OUTPUT FORMATS
  900 FORMAT('1',2X,'PROBLEM PARAMETERS:',/)
  901 FORMAT(5X,'SLAB WIDTH      = ',F7.4,' CM.')
  902 FORMAT(5X,'SLAB WIDTH      = ',F7.4,' M.F.P.')
  903 FORMAT(5X,'NUMBER OF NODES = ',I3)
  904 FORMAT(/,5X,I2,' REFLECTED QUADRATURE DIRECTIONS')
  905 FORMAT(5X,I2,' TRANSMITTED QUADRATURE DIRECTIONS')
  906 FORMAT(5X,'UNIT FLUX INCIDENT AT ',F9.6,/)
  907 FORMAT(5X,'UNIT CURRENT INCIDENT AT ',F9.6,/)
  908 FORMAT(5X,'CONVERGENCE CRITERIA FOR ANGULAR FLUXES = ',E11.4)
  909 FORMAT(5X,'THE ANGULAR FLUX AT ALL POINTS CONVERGED TO WITHIN',E11
     @.4)
  910 FORMAT(5X,'AFTER ',I3,' ITERATIONS')
  911 FORMAT(//,5X,'NO CONVERGENCE REACHED AFTER ',I3,' ITERATIONS')
  912 FORMAT(4(/),3X,'REFLECTED ANGULAR FLUXES',17X,'TRANSMITTED ANGULAR
     @ FLUXES')
  913 FORMAT(1X,29('-'),12X,31('-'))
  914 FORMAT(1X,'F(1,',F9.6,') = ',E12.5,12X,'F(',I3,',',F9.6,') = ',E12
     @.5)
  915 FORMAT('1')
  916 FORMAT(////,5X,'THE REFLECTED CURRENT              = ',F9.6)
  917 FORMAT(5X,'THE COLLIDED TRANSMITTED CURRENT   = ',F9.6)
  918 FORMAT(5X,'THE UNCOLLIDED TRANSMITTED CURRENT = ',F9.6)
  919 FORMAT(/,5X,'THE TOTAL ESCAPING CURRENT         = ',F9.6)
  920 FORMAT(5X,'C                  = ',F7.4)
  921 FORMAT(3(/),2X,'APPROXIMATED SCATTERING KERNEL METHOD USED (LINEAR
     @ FLUX EXPANSION)')
  922 FORMAT(3(/),2X,'APPROXIMATED SCATTERING KERNEL METHOD USED (QUADRA
     @TIC FLUX EXPANSION)')
  923 FORMAT(3(/),2X,'APPROXIMATED SCATTERING KERNEL METHOD USED (CUBIC
     @FLUX EXPANSION)')
  100 CONTINUE
      RETURN
      END
C
C
C
C     SUBROUTINE TO CALCULATE ESCAPING CURRENTS
      SUBROUTINE CURENT(SIGT,JR,JT,JTU,JTOT,NEXP,NINT)
      IMPLICIT REAL*8 (A-H,O-Z)
```

```
      REAL*8 JR,JT,JTT,JTU,JTOT,NORM
      DIMENSION FF(50),UU(50)
      COMMON/B1/ F(200,50),G(200,50),Q(200,50),U(50),A(50,50)
      COMMON/B2/ M,NR,NT,IS,WIDTH,ERR1,ERR2,ERR3
C
      NR1=NR+1
      NTOT=NR+NT
C
C     CALCULATE REFLECTED CURRENT
      JR=0.
      DO 100 I=1,NR
      CALL NORMAL(U,I,1,NORM,NEXP,NINT)
      JR=JR+F(1,I)*NORM
  100 CONTINUE
C
      JR=-1.*JR
C     CALCULATE TOTAL TRANSMITTED CURRENT
      JTT=0.
      DO 200 I=NR1,NTOT
      CALL NORMAL(U,I,1,NORM,NEXP,NINT)
      JTT=JTT+F(M,I)*NORM
  200 CONTINUE
C
C     CALCULATE THE COLLIDED TRANSMITTED CURRENT
      DO 210 I=NR1,NTOT
      FF(I)=F(M,I)
  210 CONTINUE
      FF(IS)=F(M,IS)-F(1,IS)*DEXP(-1.*WIDTH*SIGT/U(IS))
C
      JT=0.
      DO 220 I=NR1,NTOT
      CALL NORMAL(U,I,1,NORM,NEXP,NINT)
      JT=JT+FF(I)*NORM
  220 CONTINUE
C
C     CALCULATE THE UNCOLLIDED TRANSMITTED CURRENT BY SUBTRACTING THE
C     COLLIDED TRANSMITTED CURRENT FROM THE TOTAL TRANSMITTED CURRENT.
C
      JTU=JTT-JT
C
      JTOT=JR+JTT
C
      RETURN
      END
```

SEMI-ANALYTICAL EVALUATION OF THE SCATTERING SOURCE TERM IN DISCRETE-ORDINATES TRANSPORT CALCULATIONS

by

JOEL MARK RISNER

B.S., Kansas State University, 1983

AN ABSTRACT OF A MASTER'S THESIS

submitted in partial fulfillment of the

requirements for the degree

MASTER OF SCIENCE

Department of Nuclear Engineering

KANSAS STATE UNIVERSITY
Manhattan, Kansas

1986

ABSTRACT

A fundamental difficulty with discrete-ordinates transport calculations is the accurate evaluation of the scattering source term for highly anisotropic problems (i.e., those problems that are characterized by anisotropic fluxes as well as by anisotropic scattering). For such problems, the conventional Legendre expansion of the differential scattering cross section often yields very inaccurate and even negative angular fluxes. Alternatively, the use of the exact cross sections for transfer from one discrete direction to another (the "exact kernel method") provides better accuracy, but suffers from an angular redistribution problem when low-order quadrature is used.

In this work, a new method for evaluating the scattering source term is proposed. This new method represents both the angular flux and the scattering cross section by piecewise polynomial expansions so that the resulting scattering source term can be integrated analytically. The integrated results can be used in a standard discrete-ordinates code with minor modification of the scattering source term calculation.

From the results of several slab albedo transport problems, it is apparent that the new method provides better accuracy than does the Legendre expansion method, and also eliminates the angular redistribution problem which limits the exact kernel method for low quadrature orders. The accuracy which can be obtained with the new method, however, depends on the degree of anisotropy in the angular flux, the number of discrete ordinates used, and the order of the piecewise polynomial expansion used to represent the angular flux. Often the simple linear approximation gives the best results for highly anisotropic problems, since this approximation is the only one guaranteed to always yield a positive source term.